Weld Pool Oscillation during Gas Tungsten Arc Welding

Weld Pool Oscillation during Gas Tungsten Arc Welding

proefschrift

ter verkrijging van de graad van doctor
aan de Technische Universiteit Delft,
op gezag van de Rector Magnificus, Prof. Drs. P.A. Schenck,
in het openbaar te verdedigen ten overstaan van een commissie
aangewezen door het College van Decanen,
op dinsdag 14 april 1992 te 16.00 uur

door

You Hong Xiao

geboren te Hubei, Volksrepubliek China
Master of Engineering

Dit proefschift is goedgekeurd door de promotor

Prof. Dr. G. den Ouden

This research work is carried out in the group Welding Technology and NDT, Laboratory of Materials Science, Department of Chemical Engineering and Materials Science, Delft University of Technology, Delft, The Netherlands.

to Yingkai
to our parents
to Qiujia

Contents

Chapter 1

General Introduction

Welding has been used as a joining method since ancient times. Today it is an indispensable procedure in nearly all manufacturing processes.

Welding processes fall into two broad classes: fusion welding and solid state welding. Fusion welding is a joining process in which the coalescence of metals is accomplished by fusion. It is much more widely used in the joining of structural materials than solid state welding. The fusion welding processes are classified as: gas welding, arc welding - including shielded metal arc welding (SMAW), gas tungsten arc welding (GTAW), plasma arc welding (PAW), gas metal arc welding (GMAW), submerged arc welding (SAW) and electroslag welding (ESW) - and high-energy beam welding.

Gas tungsten arc (GTA) welding is an arc welding process in which arc heat is produced between a nonconsumable electrode and a metal workpiece. It is normally carried out autogenously, i.e. without the addition of filler material. This process is widely used in the production of high quality components for power plant, chemical plant, nuclear plant, aerospace industry etcetera and is particularly well suited for the welding of all types of steel. Advantages of this process over other processes are:

- the ability to weld most metals and alloys, including reactive metals that form refractory oxides, such as aluminium and magnesium;
- the absence of slag and spatter, which leads to a clean weld bead surface;
- the ability to weld small workpieces and thin plate materials.

GTA welding can be carried out under constant current (conventional) and pulsed current conditions. In pulsed current GTA welding the arc current alternates between two levels. Heating and melting take place during the periods

of high current, cooling and solidification during the low current periods. Pulsed current GTA welding has several advantages over conventional GTA welding. When pulsed current is applied, the heat input to the base metal is reduced, the weld bead size is reduced, weld pool penetration is increased, grain size is reduced, weld distortion is reduced and thinner materials can be welded successfully. The latter is due to the fact that high pulses provide the high current levels needed to complete penetration in open root welding, while low pulses cool the weld pool, thus preventing melt-through at the root of the joint [1.1 - 1.4].

In recent years the trend in high productivity and high quality welding has been towards process automation. This has stimulated the increased use of robotics and associated systems. When replacing a manual welder by a robot, it is necessary to provide the control system with information about the location of the weld bead and the geometry of the weld bead. Successful implementation of weld pool process control involves three principal issues: sensing, modelling and control. In order to promote the development of automated welding systems, it is essential to be able to sense the welding process in real-time. The objectives of sensors at present are:

- seam tracking (maintaining proper location of the heat source with respect to the weld groove);
- sensing weld pool geometry (obtaining the desired joint geometry).

The first objective has been achieved in production environments, whereas work related to the second objective is much more difficult and is still in the laboratory research stage.

A particular problem occurring in the case of the GTA welding process is the difficulty of obtaining consistently complete penetration of the weld over the entire length of the weld.

Two different types of weld pool penetration should be distinguished: partial penetration and full penetration [1.5]. As depicted in Fig. 1.1a, a partially penetrated weld pool is a weld pool which fails to extend throughout the whole thickness of the metal being welded. Full penetration occurs when the weld metal completely fills the groove and is fused to the base metal throughout its total thickness as illustrated in Fig. 1.1b.

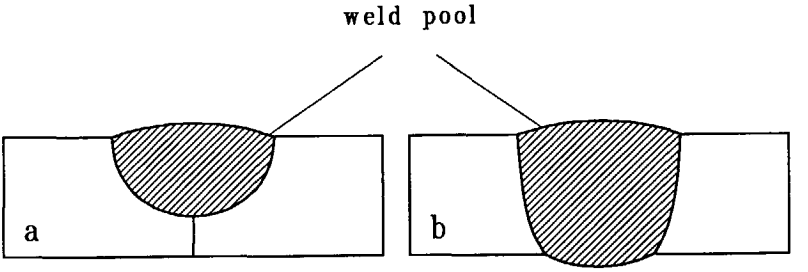

Fig. 1.1 Schematic illustration of weld pool penetration:
(a) partially penetrated weld pool;
(b) fully penetrated weld pool.

Consistent penetration is an essential property of a good weld, especially in the case of root pass welds in thin plate. Too little penetration (or lack of penetration) results in incomplete adhesion between the two parts to be welded, whereas too much penetration results in burn-through. Repair of inadequately penetrated welds is time consuming and uneconomical. This makes the measurement and in-process control of weld pool geometry, in particular of weld pool penetration, highly attractive, especially in the case of welding austenitic stainless steel where so-called cast-to-cast variation in penetration may occur. Over the last years a number of attempts has been made to measure and control the weld pool penetration. Depending on the position of the sensor with respect to the weld pool, the techniques developed to monitor the weld pool geometry in real-time can be classified into two major categories: backface sensing (sensing from the underside of the workpiece) and topface sensing (sensing on the torch side).

backface sensing

Backface sensing weld pool geometry, especially sensing weld pool penetration, can be performed by several means. For instance, by detecting the radiation from the molten weld pool which is related to the weld pool dimensions [1.6 and 1.7], by monitoring the back bead shadow motion [1.8] and by optical viewing the back bead area with an optical fiber connected to a camera [1.9]. These techniques have as drawback that they can only sense the full penetration situations and are limited in practical applications because of the fact that the back side is not always accessible.

topface sensing

Sensing the weld pool geometry on the torch side can be achieved in a number of ways. For instance, by optical viewing the weld pool [1.10], by ultrasonic measurements [1.11 - 1.13] and by analysing the surface temperature distribution and gradient [1.14 - 1.16].

The method of optical viewing on the torch side yields only information about the top side shape of the weld pool and no information about weld pool depth (penetration) can be obtained. With ultrasonic sensing some information about weld pool depth can be obtained. However, a contact probe attached to the workpiece surface is needed to move in step with the welding torch. Moreover, the surface of the workpiece is, in most cases, relatively rough, harming the contact probe and hence affecting the measurement results.

In the case of infrared detecting the surface temperature distribution, the degree of weld pool penetration can be determined indirectly. However, this technique requires an accurate description of the welding joint and does not respond well to material thickness changes.

Another way of determining weld pool penetration is to measure the arc voltage, as the arc voltage is directly related to the sagging of the weld pool when full penetration occurs in the flat position [1.17 and 1.18]. However, the change

in arc voltage in this case is not only the result of the sagging related with the full penetration, but is also the result of arc length changes due to surface roughness and the technique is unlikely to function well in other than flat welding positions.

A new attractive approach to sense the weld pool geometry, especially weld pool penetration, is to monitor the weld pool dynamics by means of optical and/or electric methods [1.19 - 1.25]. This approach is based on the phenomenon that the oscillation frequency of a weld pool when it is brought into oscillation, is related to the weld pool geometry. If the oscillation frequency can be measured during the welding process, then the weld pool geometry can be determined in real-time. The oscillation frequency can be measured optically and electrically. These two approaches are based on the principle that the arc length change due to the weld pool oscillation results in a simultaneous change in arc radiation and in arc voltage, which are both linearly proportional to the arc length. The change in the arc radiation can be observed optically, while the change in the arc voltage can be measured electrically.

outline of the thesis

The aim of this study is to obtain fundamental knowledge about the weld pool oscillation behaviour during GTA welding of mild steel and austenitic stainless steel under various conditions and to explore the possibility to use this oscillation behaviour as a means of sensing the weld pool geometry. The weld pool is excited into oscillation by short current pulses of rectangular shape and the oscillation frequency is measured by analysing the arc voltage signal, which is directly related with the weld pool oscillation. The oscillation behaviour, oscillation mode and oscillation amplitude, are also directly observed with the help of high-speed moving pictures.

This thesis is built up as follows.

In Chapter 2 the theoretical background of weld pool oscillation is given taking into account the real welding conditions.

Chapter 3 describes the experimental setup used throughout the study, including the oscillation triggering method, the sensing system and the extraction of the oscillation frequency.

The results of direct observation of weld pool oscillation with the help of high-speed moving pictures, taken of the weld pool oscillation in three different modes, are presented in Chapter 4.

The experimental investigation of weld pool oscillation was started under stationary arc conditions and the results are presented in Chapter 5. In this chapter the detectability of weld pool oscillation by sensing through-the-arc, the measurement of the weld pool oscillation frequency and the dependence of the weld pool oscillation on the welding conditions, the material properties and the oscillation modes are discussed. Special attention is given to the difference in the oscillation behaviour between a partially penetrated weld pool and a fully penetrated weld pool.

In Chapter 6, the results of experiments dealing with the oscillation behaviour of weld pools in plates of mild steel Fe 360 under travelling arc conditions are presented. The relationship between the weld pool oscillation and the formation of surface ripples is briefly discussed in this chapter as well.

The results of the oscillation behaviour obtained with austenitic stainless steel AISI 304 are presented in Chapter 7.

Finally, the possibility of detecting the weld pool geometry, width and penetration, by monitoring the arc voltage variation under more realistic welding conditions was tested and the results are presented in Chapter 8.

References

1.1 E.P. Vilkas, "Pulsed current and its application", Welding Journal, Vol.49, no.4 (1970), p. 255-262.

1.2 R.E. Leitner, G.H. McElhinney and E.L. Pruitt, "An investigation of pulsed GTA welding variables", Welding Journal, Vol.52, no.9 (1973), p. 405s-410s.

1.3 D.W. Becker, "Investigation of pulsed GTA welding parameters", Welding Journal, Vol.57, no.5 (1978), p. 134s-138s.

1.4 P. Boughton, "Penetration characteristics of pulsed TIG-welding", Welding Research International, Vol.3, no.1 (1973), p. 47-69.

1.5 American society for metals, Metal Handbook, Vol.6, 1983, p.4-12.

1.6 C.J. Smith, "Self-adaptive control of penetration in a tungsten inert gas weld", Advances in Welding Processes, Proceedings of 3rd International Conference, Harrogate, UK, 7-9 May 1974, p. 272-282.

1.7 C.J. Smith and G. Rider, "Predicting defects in welds", Advanced Welding Systems, Proceedings of 1st International Conference, 19-21 Nov. 1985, London, UK, paper 23, p. 239-260.

1.8 M. Zacksonhouse and D.E. Hardt, "Weld pool impedance identification for size measurement and control", Journal of Dynamic System, Measurement and Control, Vol.105, no.9 (1983), p. 179-184.

1.9 D. Stone, J.S. Smith and J. Lucas, "Sensor for automated weld bead penetration control", Measurement Science and Technology, Vol.1 (1990), p. 1143-1148.

1.10 A.R. Vroman and H. Brandt, "Feedback control of GTA welding using puddle width measurement", Welding Journal, Vol.55, no.9 (1976), p. 742-749.

1.11 N.M. Carlson and J.A. Johnson, "Ultrasonic sensing of weld pool penetration", Welding Journal, Vol.67, no.11 (1988), p. 239s-246s.

1.12 R. Fenn, "Monitoring and controlling welding by ultrasonic means", British Journal of NDT, Vol.31, no.2 (1989), p. 82-86.

1.13 R. Stroud, "Problems and observations whilst dynamically monitoring molten weld pools using ultrasonic", British Journal of NDT, Vol.31, (1989), p. 29-32.

1.14 S.M. Govardhan and B.A. Chin, "Monitoring GTA weld puddle geometry using measured surface temperature gradients", Proceedings of 2nd International Conference on Trends in Welding Research, Gatlinburg, Tennessee, USA, 14-18 May 1989, p. 383-386.

1.15 W. Chen and B.A. Chin, "Monitoring joint penetration using infrared sensing techniques", Welding Journal, Vol.69, no.4 (1990), p.181s-185s.

1.16 W.H. Chen, P. Banerjee and B.A. Chin, "Study of penetration variations in automated gas tungsten arc welding", Proceedings of 2nd International Conference on Trends in Welding Research, Gatlinburg, Tennessee, USA, 14-18 May 1989, p. 517-522.

1.17 D. Ainscough, "Automatic control of weld penetration", Ph.D. Dissertation, The University of Liverpool, Department of Electrical Engineering and Electronics, UK, 1987.

1.18 K. Masubuchi and D.E. Hardt, "Improvement of reliability of welding by in process sensing and control", Proceedings of Conference on Trends in Welding Research in The United States, New Orleans, Louisiana, USA, 16-18 Nov. 1981, p. 667-688.

1.19 R.J. Renwick and R.W. Richardson, "Experimental investigation of GTA weld pool oscillation", Welding Journal, Vol.62, no.2 (1983), p. 29s-35s.

1.20 C.D. Sorensen and T.W. Eagar, "Digital signal processing as a diagnostic tool for gas tungsten arc welding", Proceedings of 1st International Conference on Trends in Welding Research, Gatlinburg, Tennessee, USA, 1986, p. 467-472.

1.21 R.B. Madigan and R.J. Renwick, "Computer based control of full penetration GTA welds using pool oscillation sensing", Proceedings of 1st International Conference on Computer Technology in Welding, The Welding Institute, London, UK, 1986, p. 165-174.

1.22 R.J. Salter and R.T. Deam, "A practical front face penetration control system for TIG welding", Proceedings of 2nd International Conference on Developments in Automated and Robotic Welding, London, 17-19 Nov. 1987, p. 145-156.

1.23 R.T. Deam, "Weld pool frequency: A new way to define a weld procedure", Proceedings of 2nd International Conference on Trends in Welding Research, Gatlinburg, Tennessee, USA, 14-18 May 1989, p. 967-971.

1.24 C.D. Yoo, "Effect of weld pool conditions on pool oscillation", Ph.D. Dissertation, The Ohio State University, Department of Welding Engineering, USA, 1990.

1.25 Q. Wang, Z. Geng and S. Yin, "Real-time full-penetration control with sensor in the TIG welding of aluminum alloy", Proceedings of International Conference Joining/Welding 2000, The Hague, The Netherlands, 1-2 July 1991, p. 9-16.

Chapter 2

Modelling of Weld Pool Oscillation

2.1 Introduction

The concept of measuring weld pool geometry, especially weld pool penetration, by monitoring weld pool oscillation behaviour is based on the fact that a weld pool can be brought into natural oscillation and that the oscillation frequency of the weld pool is related to the weld pool geometry.

To measure and control the weld pool geometry by monitoring the weld pool oscillation, it is necessary to determine the relation between the oscillation frequency and the weld pool geometry in some way.

Limited attention has so far been paid to the theoretical modelling of weld pool oscillations. In 1972 Kotecki et al. suggested an oscillation model for fully penetrated weld pools under stationary arc conditions [2.1]. Later, in 1986, Sorensen and Eagar proposed an oscillation model for the partially penetrated weld pool, both under stationary arc and travelling arc conditions [2.2]. They also carried out some experiments to measure the oscillation frequency. However, an apparent difference in oscillation frequency was found to exist between the theoretical prediction and the experimental results.

Maruo and Hirata [2.3] proposed another oscillation model for partially penetrated weld pools under travelling arc conditions. According to this model the oscillation frequency would be much lower than that predicted by the model suggested by Sorensen and Eagar.

In this chapter, the liquid motion in GTA weld pools will be discussed and a model of weld pool oscillation will be given, which forms the basis of the relationship between the oscillation frequency of the weld pool on the one hand and the weld pool geometry and the physical properties of the liquid metal in the weld pool on the other hand. The equations governing the oscillation behaviour of a partially penetrated weld pool are derived in section 2.2. Using an analytical/numerical approach, the solution of these equations are obtained by considering the practical situation occurring during real welding. Section 2.3 deals with the oscillation of a fully penetrated weld pool. The various factors affecting the oscillation behaviour are discussed in section 2.4.

2.2 Partially penetrated weld pools

When a weld pool is brought into oscillation, its behaviour can be described mathematically by applying the principles of classical hydrodynamics to the liquid metal in the weld pool.

Consider the motion of the liquid metal in a circular container with diameter D and uniform depth h as shown in Fig. 2.1. The wall of the container is rigid and the free surface of the liquid metal in equilibrium is flat. It is assumed that the liquid metal is incompressible (or hard to be compressed) and inviscid, and that the motion of the liquid metal is irrotational. If, under the action of some external perturbation, the surface is moved from its equilibrium position at some point, motion will occur in the liquid metal. The motion of the liquid metal can be described by Laplace's equation [2.4]:

$$\Delta\Phi = 0 \tag{2.1}$$

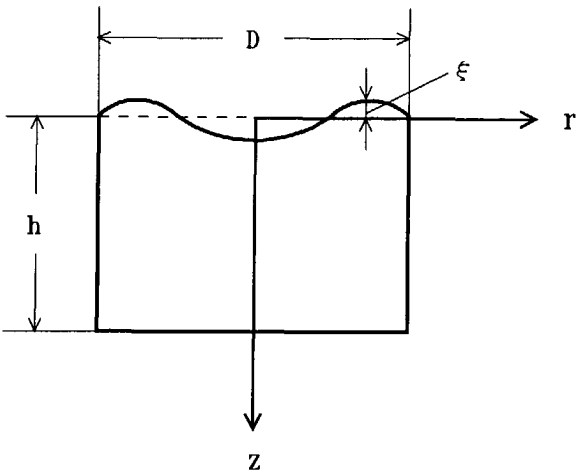

Fig. 2.1 Schematic drawing of liquid motion in a circular container with uniform depth.

where Φ is the velocity potential of the motion of the liquid metal, being a function of time and position.

Equation (2.1) can also be expressed in cylindrical co-ordinate form which leads to:

$$\frac{\partial^2\Phi}{\partial r^2} + \frac{1}{r}\frac{\partial\Phi}{\partial r} + \frac{1}{r^2}\frac{\partial^2\Phi}{\partial\theta^2} + \frac{\partial^2\Phi}{\partial z^2} = 0 \qquad (2.2)$$

The motion of the liquid in the circular container satisfies the following boundary conditions:

- the velocity of the liquid metal at the container bottom is zero:

$$\frac{\partial\Phi}{\partial z} = 0 \qquad \text{(for } z = h\text{)} \qquad (2.3)$$

- there is no motion at the container boundary:

$$\Phi = 0 \qquad (\text{at } r = \frac{D}{2}) \tag{2.4}$$

In the following the solution of equation (2.2) will be discussed for two different cases, i.e. for stationary arc conditions and for travelling arc conditions respectively.

2.2.1 Stationary arc welding

Let us first consider the case of stationary GTA welding. The arc generates a plasma jet acting on the centre of the weld pool. As a consequence of this, the liquid metal in the weld pool centre is depressed towards the weld pool bottom, whilst near the weld pool boundary the liquid metal is piled up, making the weld pool surface curved and deviating from its equilibrium position. Hence, the motion of the liquid metal in the weld pool caused by the plasma jet force is symmetrical with respect to the weld pool centre. This implies that:

$$\frac{\partial^2 \Phi}{\partial \theta^2} = 0 \tag{2.5}$$

Equation (2.2) can now be simplified to:

$$\frac{\partial^2 \Phi}{\partial r^2} + \frac{1}{r}\frac{\partial \Phi}{\partial r} + \frac{\partial^2 \Phi}{\partial z^2} = 0 \tag{2.6}$$

A solution of Laplace's equation subject to the boundary conditions (2.3) and (2.4) can be found readily using separation of variables:

$$\Phi = R(r) \cdot Z(z) \cdot T(t) \tag{2.7}$$

where R(r), Z(z) and T(t) are functions of the radial distance r from the weld pool centre, the distance z from the weld pool surface in the vertical direction and time t only. The general solution of equation (2.6) can be written as:

$$\Phi = AJ_0(kr)\left(B_1 e^{kz} + B_2 e^{-kz}\right)\cos(\omega t + \omega_0) \tag{2.8}$$

in which A, B_1, B_2, k and ω_0 are constants determined by the original conditions and the boundary conditions, J_0 is the first kind zero order Bessel function and ω is the angular frequency of the oscillation. Taking the boundary condition (2.3) into account, the following relationship between B_1 and B_2 is obtained:

$$B_1 = B_2 e^{-2kh} \tag{2.9}$$

To determine the frequency of the oscillation, the pressure balance on the weld pool surface should be considered.

If we denote the z co-ordinate of a point on the surface by ξ (ξ being the vertical displacement of the surface from its equilibrium position, see Fig. 2.1), ξ is zero in equilibrium. As ξ is very small compared with the oscillation wavelength, the pressure difference between the two sides of the surface is given by [2.5]:

$$p - p_0 = -\gamma\left(\frac{1}{r}\frac{\partial \xi}{\partial r} + \frac{\partial^2 \xi}{\partial r^2}\right) \tag{2.10}$$

with p the pressure in the liquid metal near the surface, p_0 the constant external pressure and γ the surface tension. For potential flow (or irrotational flow) p can be expressed as:

$$p = -\rho_l g\xi - \rho_l \frac{\partial \Phi}{\partial t} \tag{2.11}$$

with ρ_l the density of the liquid metal and g the gravitational constant.

Substituting equation (2.11) into equation (2.10) leads to:

$$\rho_l g\xi + \rho_l \frac{\partial \Phi}{\partial t} + p_0 - \gamma\left(\frac{1}{r}\frac{\partial \xi}{\partial r} + \frac{\partial^2 \xi}{\partial r^2}\right) = 0 \tag{2.12}$$

Differentiating equation (2.12) with respect to time t, and replacing $\partial\xi/\partial t$ by $\partial\Phi/\partial z$, the boundary condition on the surface is obtained:

$$\rho_l g\frac{\partial \Phi}{\partial z} + \rho_l \frac{\partial^2 \Phi}{\partial t^2} - \gamma \frac{\partial}{\partial z}\left(\frac{1}{r}\frac{\partial \Phi}{\partial r} + \frac{\partial^2 \Phi}{\partial r^2}\right) = 0 \quad \text{(for } z = 0\text{)} \tag{2.13}$$

By differentiating equation (2.8) with respect to r, z and t and substituting $\partial\Phi/\partial r$, $\partial^2\Phi/\partial r^2$, $\partial\Phi/\partial z$ and $\partial^2\Phi/\partial t^2$ into equation (2.13), the angular oscillation frequency ω of the weld pool is obtained as a function of weld pool geometry, surface tension and density of the liquid metal:

$$\omega^2 = \left(gk + \frac{\gamma}{\rho_l}k^3\right)\tanh(2kh) \tag{2.14}$$

The value of k is determined by the oscillation mode. To satisfy the boundary condition (2.4), it is necessary that:

$$J_0\left(k\frac{D}{2}\right) = 0 \qquad (2.15)$$

The roots of the Bessel function J_0 have to be evaluated numerically [2.6]. In principle a number of different oscillation modes may occur, corresponding with the different roots of the Bessel function. The magnitude of the high terms of the Bessel function usually decreases rapidly, so that only the first few terms are taken into account.

Considering the real situation of a partially penetrated weld pool under stationary arc conditions, it appears that one oscillation mode is dominant. This oscillation mode is illustrated in Fig. 2.2. In this figure the symbol "+" means positive surface displacement in z direction and the symbol "-" means negative surface displacement in z direction (see Fig. 2.1). The corresponding root of this mode of oscillation is $kD/2 = 5.52$ or $k = 11.04/D$.

Substituting the value of k into equation (2.14) and using the equation $f = \omega/2\pi$, the relationship between the oscillation frequency f and the weld pool geometry, surface tension and density of the liquid metal for this mode of oscillation (denoted as mode 1 to distinguish this mode from other oscillation modes to be derived later in this chapter) can be written as:

$$\text{mode 1}: \quad f^2 = \frac{1}{4\pi^2}\left(\frac{11.04}{D}g + \frac{1345.5}{D^3}\frac{\gamma}{\rho_l}\right)\tanh\left(22.08\frac{h}{D}\right) \qquad (2.16)$$

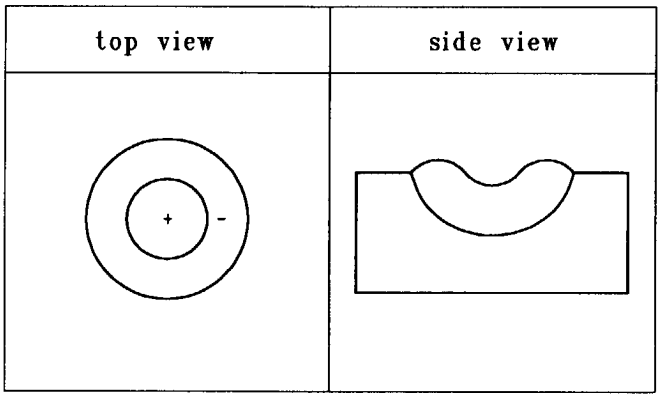

Fig. 2.2 Dominant oscillation mode (mode 1) in a partially penetrated weld pool under stationary arc conditions.

2.2.2 Travelling arc welding

In the case of travelling arc welding, the weld pool is elongated due to the fact that heat is absorbed ahead of the arc by melting of the solid metal, whereas heat is released behind the arc by solidification of the liquid metal. Thus, the arc deviates from the geometrical centre of the weld pool and the motion of the liquid metal in this case is not symmetrical with respect to the geometrical centre any more. Therefore Laplace's equation cannot be simplified as in the case of the stationary weld pool, but retains the form of equation (2.2). The general solution of equation (2.2) is:

$$\Phi = AJ_n(kr)\left(B_1 e^{kz} + B_2 e^{-kz}\right)\cos(\omega t + \omega_0)\cos(n\theta + \theta_0) \qquad (2.17)$$

where J_n is the first kind nth order Bessel function (with n = 0, 1, 2, ...), θ the angle with respect to the co-ordinate r and θ_0 a constant.

In a similar way as in the case of stationary arc welding, the relationship between the angular oscillation frequency on the one hand and the weld pool geometry and liquid metal properties on the other hand can be derived. This leads to:

$$\omega^2 = \left(gk + \frac{\gamma}{\rho_l} k^3 \right) \tanh(2kh) \tag{2.18}$$

It can be seen that equation (2.18) has the same form as equation (2.14). However, in this case the value of k is determined by:

$$J_n\left(k\frac{D_1}{2} \right) = 0 \tag{2.19}$$

where D_1 is the diameter of the equivalent circle having an area equal to the surface area of the elongated weld pool.

The amplitude of the higher order Bessel functions (J_2, J_3, J_4, ...) decays rapidly, therefore only the lower order Bessel functions (J_0 and J_1) are taken into account. Considering the real situation of a partially penetrated weld pool under travelling arc conditions, it appears that two oscillation modes are dominant. They are illustrated in Fig. 2.3. The oscillation mode depicted in Fig. 2.3a is the same as that under stationary arc conditions. The oscillation mode shown in Fig. 2.3b does not occur in the stationary weld pool and is denoted as mode 2. For mode 2 oscillation, k has the value $7.66/D_1$. This leads to the following expressions for mode 1 and mode 2 oscillation under travelling arc conditions:

$$\text{mode 1 :} \quad f^2 = \frac{1}{4\pi^2}\left(\frac{11.04}{D_1}g + \frac{1345.5}{D_1^3}\frac{\gamma}{\rho_l}\right)\tanh\left(22.08\frac{h}{D_1}\right) \tag{2.20}$$

$$\text{mode 2 :} \quad f^2 = \frac{1}{4\pi^2}\left(\frac{7.66}{D_1}g + \frac{449}{D_1^3}\frac{\gamma}{\rho_l}\right)\tanh\left(15.32\frac{h}{D_1}\right) \tag{2.21}$$

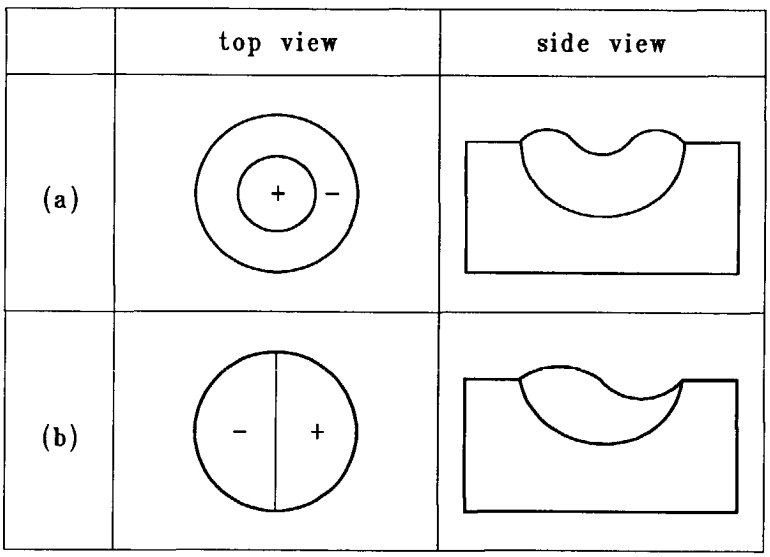

Fig. 2.3 Dominant oscillation modes (mode 1 and mode 2) in a partially penetrated weld pool under travelling arc conditions.

2.3 Fully penetrated weld pools

An oscillation model of fully penetrated weld pools under stationary arc conditions has been proposed by Kotecki et al. [2.1]. In this model, the fully penetrated weld pool is regarded as a stretched membrane. The motion of the weld pool then satisfies the following two-dimensional wave equation [2.7]:

$$\frac{\partial^2 \Phi}{\partial t^2} = \frac{\Gamma}{m} \Delta \Phi \tag{2.22}$$

In the case of stationary arc welding, the arc is located in the centre of the weld pool. Therefore, the motion in the weld pool is symmetrical with respect to the arc. In this case the liquid motion of the weld pool can be described in cylindrical co-ordinates:

$$\frac{\partial^2 \Phi}{\partial t^2} = \frac{\Gamma}{m}\left(\frac{\partial^2 \Phi}{\partial r^2} + \frac{1}{r}\frac{\partial \Phi}{\partial r}\right) \tag{2.23}$$

under the boundary condition:

$$\Phi = 0 \qquad \left(\text{for } r = \frac{D}{2}\right) \tag{2.24}$$

where Γ is the surface energy and m the mass of the liquid metal in the weld pool. The solution of equation (2.23) is:

$$\Phi = A J_0(kr)\cos\left(k\left(\frac{\Gamma}{m}\right)^{1/2} t + C\right) \tag{2.25}$$

with A and C constants depending on the original conditions.

For harmonic oscillation, the following relation must be satisfied:

$$k\left(\frac{\Gamma}{m}\right)^{1/2}T = 2\pi \tag{2.26}$$

or:

$$T = \frac{2\pi}{k}\left(\frac{\Gamma}{m}\right)^{-1/2} \tag{2.27}$$

in which T is the period of the oscillation.

Hence, the oscillation frequency of the fully penetrated weld pool can be written as:

$$f = \frac{1}{T} = \frac{k}{2\pi}\left(\frac{\Gamma}{m}\right)^{1/2} \tag{2.28}$$

To assess the value of k, the boundary condition expressed by equation (2.24) should be considered. For equation (2.25) to satisfy the boundary condition of equation (2.24), it is necessary that:

$$J_0\left(k\frac{D}{2}\right) = 0 \tag{2.29}$$

Considering the real situation of a fully penetrated weld pool and the roots of the Bessel function J_0, it appears that a fully penetrated weld pool oscillates in a mode having a corresponding k value of 4.81/D. This mode is illustrated in Fig. 2.4 and is denoted as mode 3.

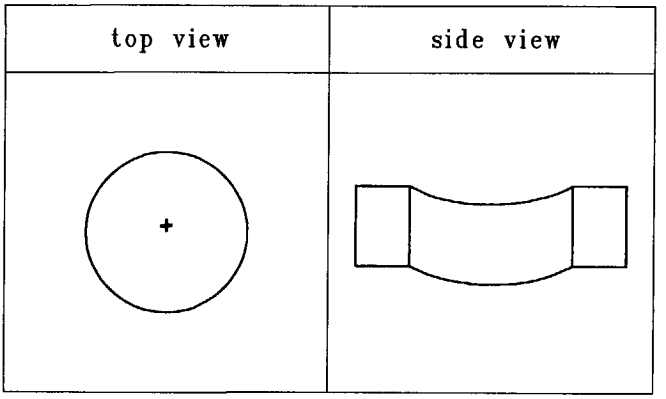

Fig. 2.4 Dominant oscillation mode (mode 3) in a fully penetrated weld pool.

For a fully penetrated weld pool in a plate of thickness H, the surface energy Γ and the mass of the weld pool m are given by:

$$\Gamma = 2\pi\left(\frac{D}{2}\right)^2\gamma \tag{2.30}$$

and:

$$m = \pi\left(\frac{D}{2}\right)^2 H\rho_l \tag{2.31}$$

Combination of equations (2.28), (2.30) and (2.31) and substituting 4.81/D for k leads to the following expression for the oscillation frequency of a fully penetrated weld pool as a function of surface tension γ, density of the liquid metal ρ_l and weld pool geometry:

$$\text{mode 3 :} \qquad f = 1.08\left(\frac{\gamma}{H\rho_l}\right)^{1/2} D^{-1} \tag{2.32}$$

This equation describes the influence of weld pool geometry and material properties on the oscillation frequency. Equation (2.32) shows that the oscillation frequency decreases with increasing weld pool diameter and plate thickness due to the increase of mass in the weld pool.

Although equation (2.32) is derived for stationary arc conditions, it is expected that this equation will also be adequate for a fully penetrated weld pool under travelling arc conditions. In that case, D in equation (2.32) should be taken as the equivalent diameter of the elongated weld pool.

2.4 Discussion of the oscillation modes

2.4.1 Influence of the depth/width ratio h/D on the oscillation frequency of partially penetrated weld pools

In equations (2.20) and (2.21), the weld pool depth h enters the development of oscillation only through the factor tanh(2kh), i.e. tanh(22.08 h/D) for mode 1 and tanh(15.32 h/D) for mode 2. In practical GTA welding (either under stationary arc conditions or under travelling arc conditions), the ratio of h/D is generally larger than 0.2. In that case, the value of tanh(22.08 h/D) is 0.9997, whereas the value of tanh(15.32 h/D) is 0.9956. Thus, for both oscillation modes the factor tanh(2kh) can be regarded as 1 with an error in oscillation frequency 0.03% for mode 1 and 0.44% for mode 2. This implies that the oscillation is virtually independent of the weld pool depth. However, at decreasing weld pool depth h (shallow and wide weld pool), the depth will start to play a role in the oscillation behaviour.

When neglecting the term tanh(2kh), equations (2.20) and (2.21) become:

$$\text{mode 1 :} \quad f^2 = \frac{1}{4\pi^2 D_1}\left(11.04g + \frac{1345.5}{D_1^2}\frac{\gamma}{\rho_l}\right) \tag{2.33}$$

$$\text{mode 2 :} \quad f^2 = \frac{1}{4\pi^2 D_1}\left(7.66g + \frac{449}{D_1^2}\frac{\gamma}{\rho_l}\right) \tag{2.34}$$

2.4.2 Evaluation of the gravitational force in oscillation

In equations (2.33) and (2.34), the two terms on the right hand side correspond to two different reaction forces acting on the displaced surface. The first term depends on g and represents the tendency of the liquid metal, which is piled up in the wave crests, to level off under the action of gravity. The second term represents the effect of surface tension, which tends to straighten out the curvature of the surface. To evaluate the role played by the two forces in the development of the oscillation in more detail, some estimating calculations were carried out. The results are given below.

Denote $f_{g,\gamma}$ as the oscillation frequency without neglecting the contribution of the gravitational force and f_γ as the frequency after neglecting the term of the gravitational force in equations (2.33) and (2.34). The relative error ε in the oscillation frequency can now be written as:

$$\varepsilon = \frac{f_{g,\gamma} - f_\gamma}{f_{g,\gamma}} \tag{2.35}$$

Taking for g the value of 9.8 m/s^2 and for γ/ρ_l the value of $1.25 \cdot 10^{-4}$ m^3/s^2, the relative error ε can then be expressed as a function of weld pool diameter D_1 by the following equations:

$$\text{mode 1 :} \qquad \varepsilon_1 = 1 - \sqrt{\frac{16.82}{1.08D_1^2 + 16.82}} \tag{2.36}$$

$$\text{mode 2 :} \qquad \varepsilon_2 = 1 - \sqrt{\frac{623.8}{0.75D_1^2 + 623.8}} \tag{2.37}$$

These two equations show that the relative error ε in oscillation frequency is a function of weld pool diameter for both modes of oscillation. Figure 2.5 shows the relationship between the relative error and the weld pool diameter for both modes of oscillation. It can be seen that for a weld pool with diameter smaller than 10 mm, the relative error is smaller than 3% for mode 1 oscillation and smaller than 6% for mode 2 oscillation. Generally speaking, the weld pool diameter in GTA welding is rarely larger than 10 mm. Therefore, the term representing the gravitational force in equations (2.33) and (2.34) can be neglected, resulting in the simplified equations:

$$\text{mode 1 :} \qquad f = 5.84\left(\frac{\gamma}{\rho_l}\right)^{1/2} D_1^{-3/2} \tag{2.38}$$

$$\text{mode 2 :} \qquad f = 3.37\left(\frac{\gamma}{\rho_l}\right)^{1/2} D_1^{-3/2} \tag{2.39}$$

Equations (3.38) and (3.39) indicate that the oscillation frequency of a partially penetrated weld pool, either in mode 1 or in mode 2, increases with increasing surface tension and decreases with increasing liquid metal density and weld pool diameter.

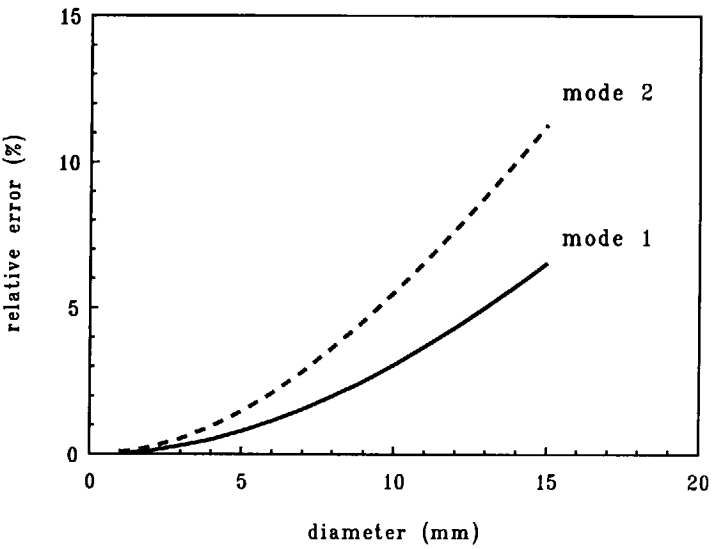

Fig. 2.5 Relative error in oscillation frequency as a function of weld pool diameter when neglecting the gravitational force.

2.4.3 Evaluation of the oscillation frequency of the three oscillation modes

In addition to the properties of the liquid metal and the weld pool geometry, the oscillation mode plays also an important role in the oscillation frequency. In order to visualise the differences in oscillation frequency between the three oscillation modes, the oscillation frequency is plotted as a function of weld pool diameter for the three oscillation modes for the case of iron in Fig. 2.6. In this

figure the lines represent the three oscillation modes as expressed by equations (2.38), (2.39) and (2.32) respectively, taking the values of surface tension and density of liquid metal equal to those of iron as given in Table 2.1 and the plate thickness as 4 mm for mode 3. It can be seen from this figure that the oscillation frequency differs considerably for the three oscillation modes. If weld pool oscillation transfers from one oscillation mode to another oscillation mode, a significant change in oscillation frequency can be observed. This is especially of importance in the case of the transition from partial penetration (mode 1 or mode 2) to full penetration (mode 3). This transition forms the basis of control of weld pool penetration by monitoring the weld pool oscillation frequency. In this respect it should be noticed that the frequency difference between mode 1 and mode 3 is much larger than that between mode 2 and mode 3 and that the oscillation frequency of fully penetrated weld pools decreases with increasing plate thickness.

Table 2.1 Physical properties of some liquid metals at the melting temperature [2.8]

metal	surface tension γ (N/m)	density ρ_l (kg/m^3)	γ/ρ_l (Nm^2/kg)
Fe	1.872	$7.03 \cdot 10^3$	$2.66 \cdot 10^{-4}$
Al	0.914	$2.38 \cdot 10^3$	$3.84 \cdot 10^{-4}$
Cu	1.303	$8.00 \cdot 10^3$	$1.63 \cdot 10^{-4}$

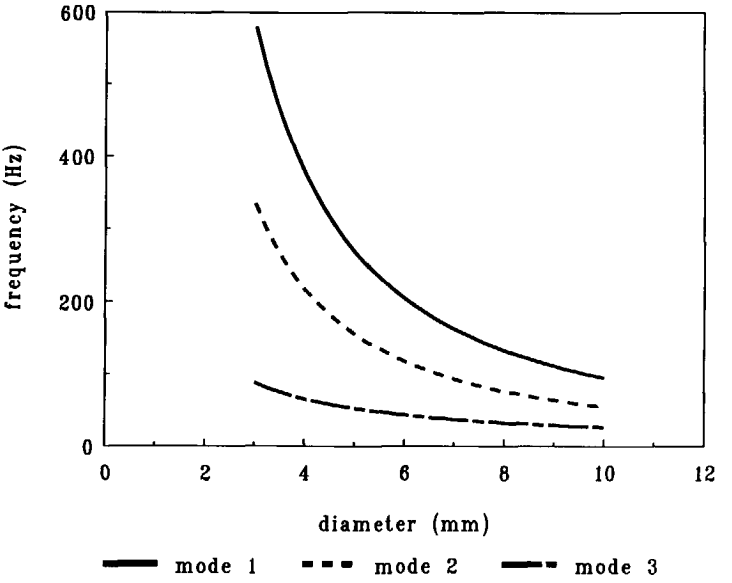

Fig. 2.6 Oscillation frequency as a function of weld pool diameter for the three oscillation modes in iron.

2.4.4 Influence of weld pool geometry, surface tension and density on the oscillation frequency

The factors influencing the oscillation frequency, i.e. surface tension, density and weld pool size as discussed above are summarised in Fig. 2.7. In this figure the oscillation frequency of three typical materials, namely iron, copper and aluminium, is plotted as a function of the weld pool diameter in case of mode 1. As can be seen in this figure, the oscillation frequency of aluminium is the highest compared with that of the other two materials for a given weld pool diameter. This is due to its relatively high γ/ρ_l ratio (see Table 2.1). In the case of full penetration, the oscillation frequency decreases with increasing plate thickness as shown in Fig. 2.8, in which the oscillation frequency of mode 3 oscillation (full penetration) is plotted as a function of the plate thickness for a weld pool diameter of 6 mm.

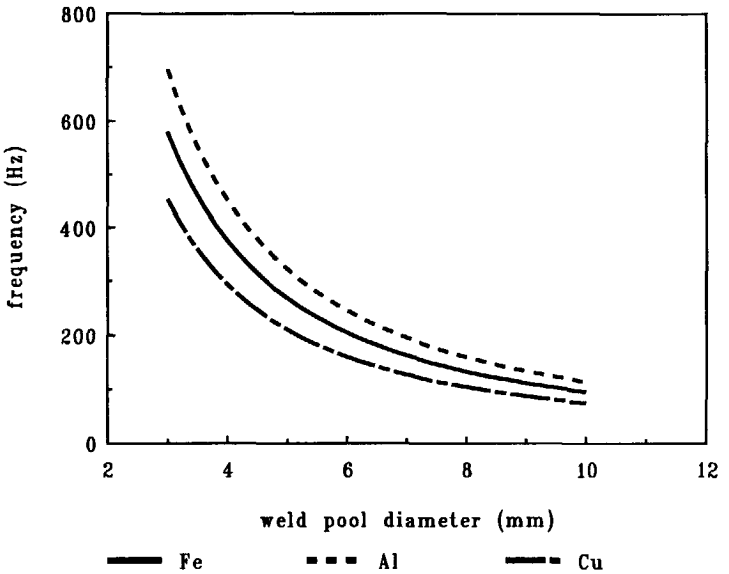

Fig. 2.7 Oscillation frequency of mode 1 oscillation as a function of weld pool diameter for three different materials.

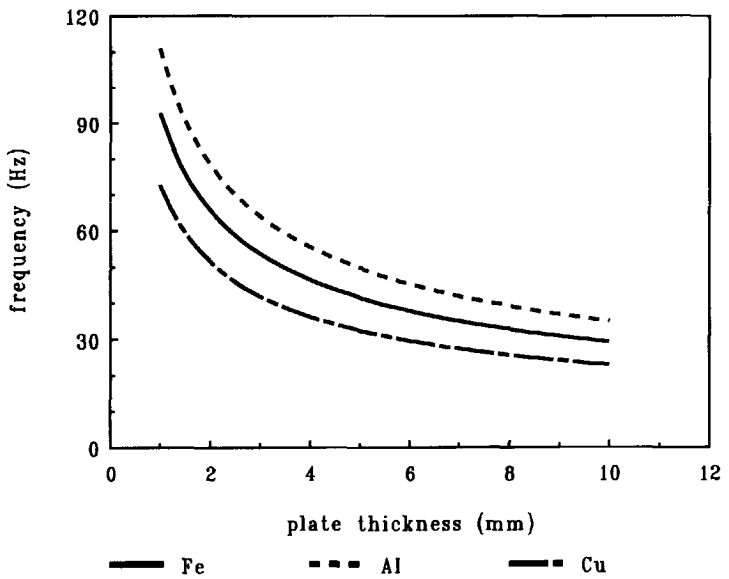

Fig. 2.8 Influence of plate thickness on the oscillation frequency in case of full penetration for a weld pool diameter of 6 mm.

2.5 Conclusions

In this chapter a model of weld pool oscillation is presented with special reference to the practical welding situation, providing the theoretical basis for controlling weld pool geometry by monitoring weld pool oscillation. It is shown that a partially penetrated weld pool in case of stationary arc conditions oscillates in a specific mode - mode 1, whilst a partially penetrated weld pool under travelling arc conditions can oscillate in one of two modes - mode 1 and mode 2. A fully penetrated weld pool will oscillate in another mode - mode 3, characterised by a much lower oscillation frequency than that of partially penetrated weld pools.

It appears that the oscillation frequency of the partially penetrated weld pool, both in the case of mode 1 oscillation and mode 2 oscillation, decreases with increasing weld pool size and drops rapidly when transition to full penetration occurs. If the oscillation frequency can be measured accurately, the weld pool size and the transition from partial penetration to full penetration and vice versa can be determined. This would make it possible to control weld pool geometry, especially penetration, by monitoring the weld pool oscillation frequency.

References

2.1 D.J. Kotecki, D.L. Cheever and D.G. Howden, "Mechanism of ripple formation during weld solidification", Welding Journal, Vol.51, no.8 (1972), p. 386s-391s.

2.2 C.D. Sorensen and T.W. Eagar, "Digital signal processing as a diagnostic tool for gas tungsten arc welding", Proceedings of 1st International Conference on Trends in Welding Research, Gatlinburg, Tennessee, USA, 1986, p. 467-472.

2.3 H. Maruo and Y. Hirata, "Study on Pulsed TIG Arc Welding", Technology Reports of The Osaka University, Vol.37, no.1872 (1987), p. 51-63.

2.4 L.D. Laudan and E.M. Lifshitz, Fluid Mechanics, 2nd edition, New York, 1987, p. 18.

2.5 L.D. Laudan and E.M. Lifshitz, Fluid Mechanics, 2nd edition, New York, 1987, p. 244-245.

2.6 M. Abramowitz and T.A. Stegun, (editor) Handbook of Mathematical Functions, New York, p. 390-392.

2.7 C.R. Wylie, Advanced Engineering Mathematics, New York, 1960, p. 347-348.

2.8 T. Iida and R.I.L. Guthrie, The Physical Properties of Liquid Metals, Clarendon Press, Oxford, 1988.

Chapter 3

Triggering and Measuring of Weld Pool Oscillation

3.1 Triggering of weld pool oscillation

3.1.1 Triggering method

To monitor weld pool oscillation behaviour, the weld pool should be brought into oscillation in a proper way. Oscillations of the weld pool can be triggered by mechanical vibrations, by the impact of droplets entering the weld pool (occurring in the case of gas metal arc (GMA) welding), by gas bubbling and by a sudden change in arc current. For GTA welding, the most convenient triggering method is to change the arc current rapidly. This method has been used throughout the present study.

The principle of triggering the weld pool by a sudden change in arc current is based on the phenomenon that the arc creates a stream of gas, the so-called plasma jet, travelling from the electrode towards the workpiece. The impingement of the plasma jet on the weld pool tends to depress the centre of the weld pool [3.1], hence providing stimulating energy to the oscillation system (weld pool). The arc pressure p, generated by the plasma jet, is found to be proportional to the square of the arc current I [3.2], i.e.

$$p \propto I^2 \tag{3.1}$$

Considering the weld pool as a dynamic system, the weld pool is exposed to a pulsed pressure on its surface when pulsed current is applied. During the pressure pulse, the weld pool surface in the centre is depressed, until a pressure balance is built up between the external pressure (arc pressure) and the internal pressure (surface tension force and gravitational force). The situation is schematically given in Fig. 3.1. The work performed by the arc pressure is converted into the dynamic system in the form of kinetic and potential energy. After the pressure pulse is released, the weld pool surface tends to move back to its equilibrium position, which leads to the oscillation of the weld pool surface. By choosing a proper waveform for the current pulse, the weld pool will be depressed periodically during the peak current (high pressure) followed by oscillation after the peak current is shut off, due to the action of the surface tension force and the gravitational force.

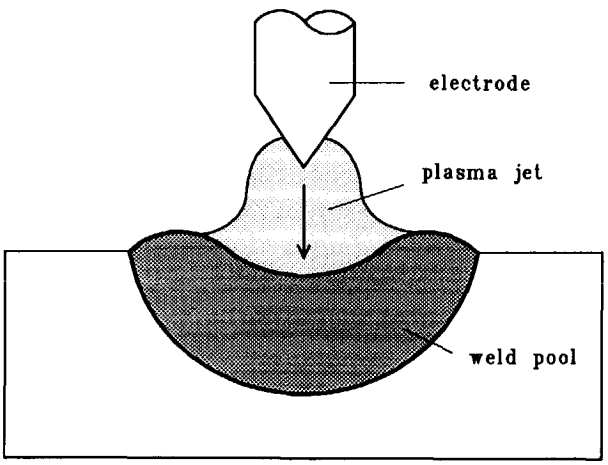

Fig. 3.1 Schematic illustration of weld pool surface depression due to plasma jet force.

3.1.2 Current pulse waveform

As mentioned above, weld pools can be excited into oscillation by a pressure pulse acting on the weld pool. The pressure pulse can be provided by a current pulse of various waveforms, for instance by a sinusoidal wave, a triangular wave, a square wave and a short current pulse of rectangular shape.

There are two important considerations in selecting an input current waveform. In the first place the stimulating energy of the pulse should be high enough to generate oscillation in the weld pool which can be observed. Secondly, the pulse width should be so small that the weld pool can oscillate freely for a sufficiently long time, so that the signals can be sampled and further analysed.

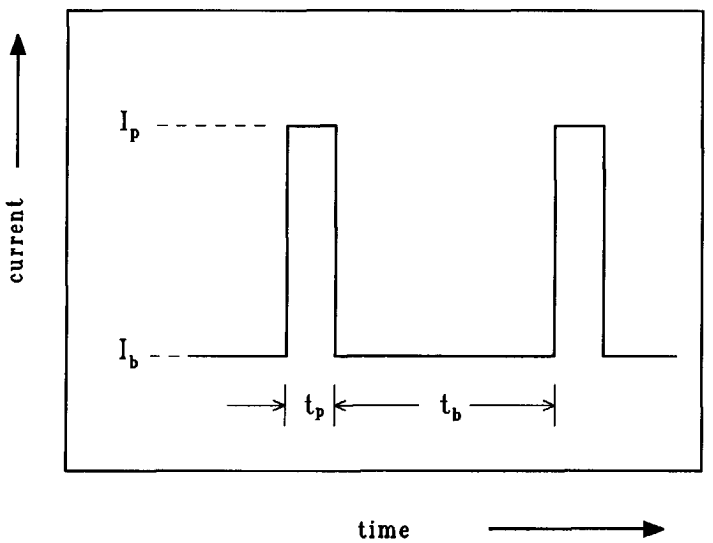

Fig. 3.2 Current pulse of rectangular shape:
I_p - peak current; I_b - base current;
t_p - peak current duration; t_b - base current duration.

On the basis of these considerations a choice was made for short current pulses of rectangular shape as shown schematically in Fig. 3.2. These current pulses can provide sufficient stimulating energy and leave the weld pool to oscillate under free state conditions for a sufficiently long time. The parameters of the current waveform, i.e. peak current, peak current duration, base current and base current duration, can be adjusted separately. Throughout this study, the weld pools were triggered by short current pulses of rectangular shape.

3.2 Measurement of the oscillation frequency

An appropriate way to measure the oscillation frequency is to monitor the arc voltage variation. This approach is very convenient and easy to be applied in an automation system.

Using the arc as a sensor (sensing through-the-arc) has been applied for many years in arc length control, and is recently also used in seam tracking during automatic GTA welding. Sensing through-the-arc has the following advantages compared with other sensing systems:

- there is no need for external equipment, such as ultrasonic probes, optical fibers etcetera, with the associated concern for their reliability in the harsh environment of the welding arc;
- its costs are relatively low;
- it can be universally applied.

To explain the principle of sensing weld pool oscillations by monitoring the arc voltage signals, it is necessary to briefly consider the characteristics of the welding arc.

The welding arc can be divided into three distinct regions: the arc column, the anode fall region and the cathode fall region. The situation is shown schematically in Fig. 3.3. The total arc voltage V can be considered as the sum of the voltage drop over the anode fall region V_a, the voltage drop over the cathode fall region V_c and the voltage drop over the arc column LE (with L the arc length

and E the electric field strength in the arc column) [3.2], or:

$$V = V_a + V_c + LE \tag{3.2}$$

For constant arc current the sensitivity of the arc voltage to arc length change can be obtained by differentiating equation (3.2) with respect to arc length L. Because V_a and V_c are virtually independent of arc length L, the following expression can be obtained:

$$\frac{dV}{dL} = E \tag{3.3}$$

Equation (3.3) indicates that the sensitivity of detecting the arc length change by measuring the arc voltage variation depends on the strength of the electric field in the arc column E. The value of E is different in different shielding gas and decreases slightly with increasing arc length. For argon, E has a value between 0.5 V/mm and 1 V/mm, while in the case of helium, the value of E varies from 1 V/mm to 4 V/mm [3.3].

In Fig. 3.4 the arc voltage is given as a function of arc current for three different values of arc length. This figure shows that the arc voltage rises slowly with increasing arc current and that the voltage-current characteristic shifts upwards with increasing arc length.

When oscillation occurs in a weld pool, the arc length changes in a periodic way simultaneously with the motion of the weld pool surface, which results in a periodic variation in arc voltage. Thus, the oscillation frequency can be measured by monitoring the arc voltage variation.

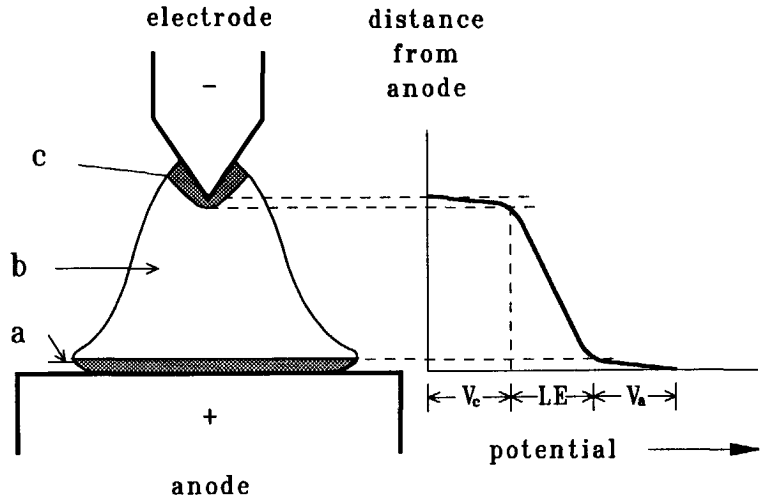

Fig. 3.3 Schematic illustration of arc and arc voltage distribution: a - anode fall region; b - arc plasma (arc column); c - cathode fall region.

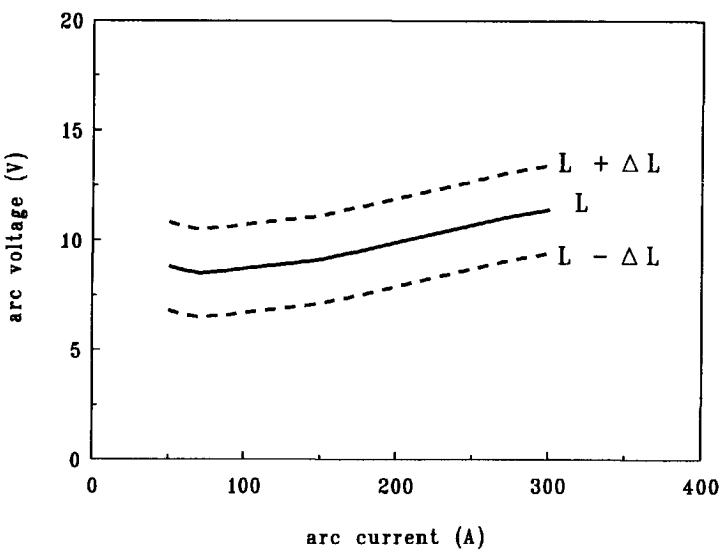

Fig. 3.4 Arc voltage as a function of arc current for three different values of arc length.

3.3 Experimental setup

To study weld pool oscillation behaviour, an experimental setup was built as shown in Fig. 3.5. It consists of a three-phase full-wave rectified switched-mode welding machine (power supply) with a vertical voltage-current characteristic (Philips PZ 2351) provided with a pulse generator and a commercially available GTA welding torch, a welding monitor, a RC filter, an oscilloscope and a transient waveform recorder or a computer data acquisition system. Unless otherwise stated, a 2% thoriated tungsten electrode with diameter 2.4 mm and tip angle 60^0 was used at straight polarity (electrode negative). The pulse generator can produce current pulses of rectangular shape with a frequency ranging from 0.1 Hz to 100 Hz and with a maximum peak current of 400 A. The peak current I_p, base current I_b, peak current duration t_p and base current duration t_b (see Fig. 3.2) can be controlled digitally and can be adjusted separately in steps of 1 A in current level, 10 ms in pulse period and 1% in duty cycle.

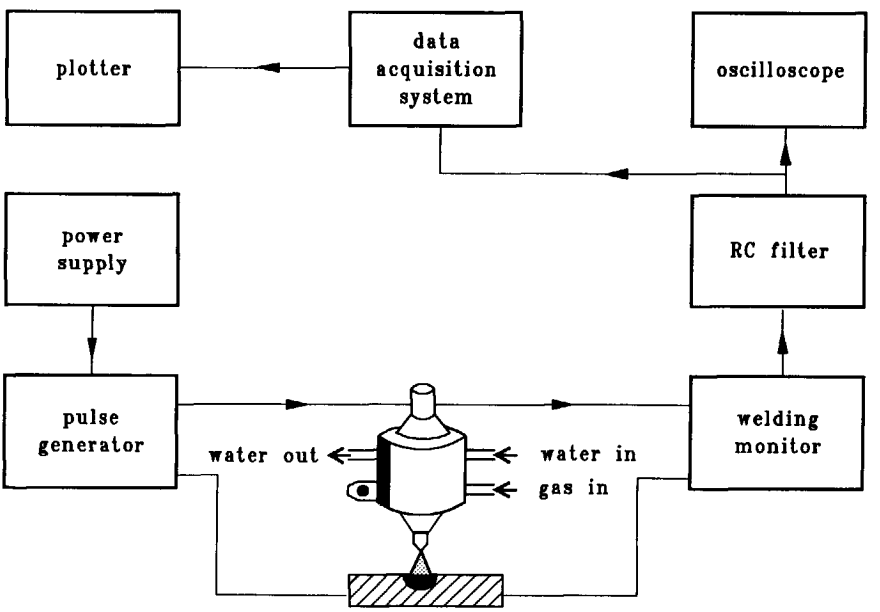

Fig. 3.5 Experimental setup.

3.3.1 Data acquisition

The arc voltage signals were taken from the welding process at the two terminals: the electrode and the workpiece. The signals were passed through a welding monitor, an electronic unit which serves as a complete galvanic separation between the welding setup and the measuring devices and provides a first stage filtering of high-frequency noise (above 10 kHz).

To avoid the obscuring effect of the high-frequency noise originating from the power source, a low-pass filter (RC filter) with a slope of 6 dB/octave was added to the system before the transient waveform recorder or the data acquisition system. The cut-off frequency was set to be 600 Hz (the noise frequency from the power supply was measured to be 1200 Hz and the highest input frequency was estimated to be about 400 Hz).

The voltage signals were collected by a transient waveform recorder and later in the study by a computer based data acquisition system. The signals were sampled and stored during welding and subsequently plotted or analysed after welding for calculating the frequency and amplitude of the oscillation.

transient waveform recorder

The transient waveform recorder (Biomation mode 805) is capable to collect the signals with input voltage ranging from 100 mV to 50 V with a resolution of 8 bits, meaning that the amplitude resolution is 0.4% of the full scale amplitude. The full scale of the voltage input was set to ± 1 V, hence a resolution of 4 mV could be obtained. The sampling speed of the transient recorder is up to 5 MHz. A digital-to-analog converter, built in the transient recorder, is capable to smooth the digital data stored in the memory by a low-pass filter after the converter, making the output appear to be a somewhat continuous trace rather than a series of points. The arc voltage oscillation frequency was determined after welding from the plots registered by the waveform recorder by measuring the average time interval between two oscillation peaks in each period of a current pulse.

data acquisition system

In the data acquisition system, an IBM-XT compatible Olivetti PC, fitted with a Tecmar Labmaster board A/D convertor. The analog I/O board had 16 single-ended channels for A/D input and 2 channels for D/A output. Two A/D channels were used to collect the arc current signal and the arc voltage signal from the low-pass frequency filter respectively. To eliminate the influence of high-frequency signals produced during ignition of the arc on the stability of the measuring system, an isolating transformer (type MCB reguvolt D100) was used. The Olivetti PC was protected from HF-disturbance at the main inlet and at all the connections to the welding equipment by the transformer.

The oscillation frequency of the weld pool was extracted by applying a Fast-Fourier-Transform (FFT) program to process the collected voltage signal. For extraction of the oscillation frequency using the FFT program, the number of data points is required to be a power of two. The accuracy of the FFT result is related to the sampling speed f_s and the number of data points N and is given by:

$$\Delta f = \frac{f_s}{N} \tag{3.4}$$

With increasing the data points N, the frequency resolution increases (Δf decreases) for a given sampling speed. Taking this into account, each measurement was chosen to consist of a number of cycles, each cycle having a cycle length N of 1024 data points. Further increasing the cycle length N for a given sampling speed will cost resolution in time. The total recording time depends on the memory size of the computer and the sampling speed. In the present study, the sensing system can collect data up to 543 kB with a resolution of 12 bits. The full voltage scale was set to ± 10 V, which means that a resolution of 2.4 mV (0.024% of the full scale) can be reached.

3.3.2 Sampling speed

A suitable sampling speed is of great importance to extract the desired information from the process studied. Generally speaking, it is desirable to choose a high sampling speed to reduce the difference between an analogue signal and its sampled counterpart. However, a high sampling speed implies high demands on the performance of the computer and its A/D converter and short total data acquisition time for a given computer memory size.

The absolute minimum sampling speed is given by the sampling theorem [3.4] which implies that the sampling speed must be at least twice the highest input frequency of the system to be measured. The meaning of this is better understood if one regards Fig. 3.6 in which A is the real signal and B is the sampled signal of A recorded with a sampling speed lower than twice the frequency of A. Due to the fact that the sampling interval is longer than half the period of the signal A, the sampled signal B does not provide sufficient information about the original signal A. If instead the sampling interval would be a little shorter than half the period of A, the sampled signal would contain somewhat more information about A, but it would still be difficult to relate signal B with signal A.

In principle, the higher the sampling speed, the more accurate the measurement. Usually, the sampling speed in real measurements is taken to be 5 ~ 10 times higher than the highest frequency of the system to be measured. In this study, a sampling speed of 2 kHz was chosen in case the transient waveform recorder was used, allowing a 1 second acquisition period, while when the computer data acquisition system was used a sampling speed of 1 kHz was chosen, permitting a acquisition of raw data recording of approximately 132 seconds duration.

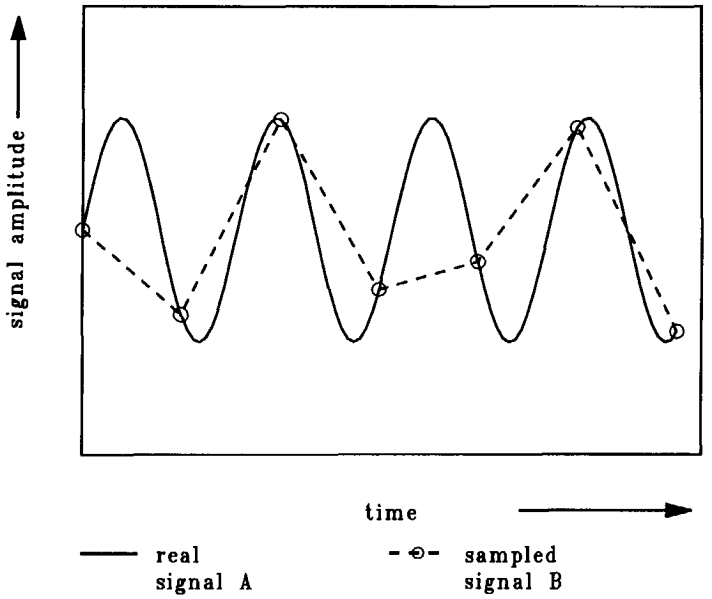

Fig. 3.6 Illustration of the influence of sampling speed on the recording result.

References

3.1 E. Friedman, "Analysis of weld puddle distortion and its effect on penetration", Welding Journal, Vol.57. no.6 (1978), p. 161s-166s.

3.2 G.E. Cook, F.M. Wellos and P.C. Levick, "Arc pressure control in GTA welding", Proceedings of 3rd International Conference on Modeling and Control of Casting and Welding Processes, Santa Barbara, California, USA, 12-17 Jan. 1986, p. 33-48.

3.3 J.P. Zijp and G. den Ouden, "Effect of shielding gas composition on heat transfer during GTA welding", Proceedings of International Conference on Advances in Joining and Cutting Processes, The Welding Institute, Harrogate, UK, 1989, p. 24-32.

3.4 J.S. Bendat and A.G. Piersol, Random Data: Analysis and Measurement Procedures, John Wiley & Sons, Inc. New York, 1971, p. 95.

Chapter 4

Direct Observation of Weld Pool Oscillation

4.1 Introduction

It has been demonstrated in Chapter 2 that weld pools can be brought into oscillation and that different oscillation modes may occur depending on the welding conditions.

This chapter deals with the direct observation of weld pool oscillation by means of high-speed filming under various welding conditions. The film results presented in this chapter confirm the existence of the oscillation modes predicted and also confirm the reliability of the method of sensing the weld pool oscillation by monitoring the voltage variation, as described in Chapter 3.

4.2 Experimental procedure

Weld pools were produced in 10 mm thick (partial penetration) and 4 mm thick (full penetration) plates of mild steel Fe 360 by means of GTA welding, using helium as shielding gas under stationary arc conditions and under travelling arc conditions. In case of full penetration, argon was used as backing gas to prevent oxidation of the bottom side of the weld pool.

The weld pools were triggered into oscillation by short arc current pulses and high-speed films were made of the weld pool oscillations using a HIMAC camera of the type 16HB-400. Filming was carried out from the side and was started after the welding process reached a steady state. The situation is sketched in Fig. 4.1.

Two half-grey optical filters were put in front of the camera lens to minimise the influence of arc radiation. The camera speed increased to about 2000 frames/second after 0.5 seconds of operation. A pulsating red light within the camera provided markers on the film at a rate of 100 markers per second. Five high intensity lamps were used to illuminate the objective area (weld pool). The films produced during welding were later analysed using a professional editing machine (Analector) with the capacity to analyse the film frame by frame and to view the film at various speeds.

Four films were successfully produced under the conditions listed in Table 4.1.

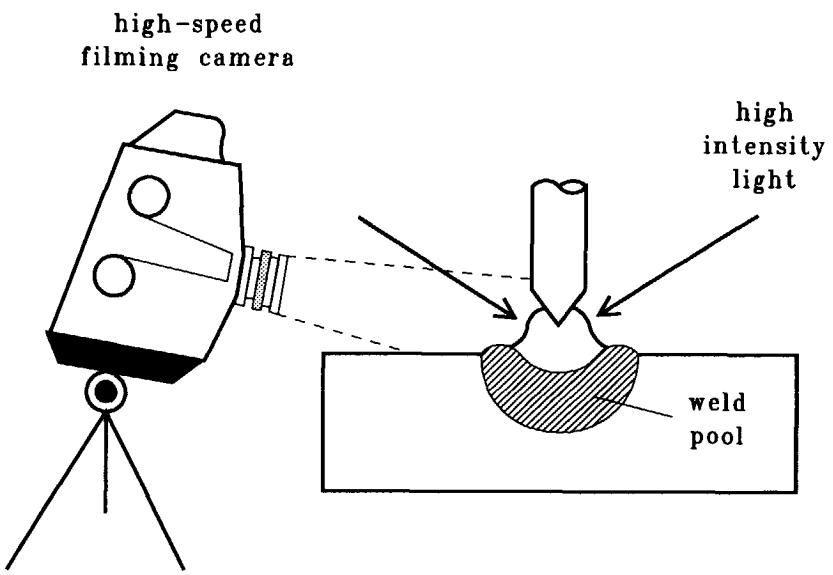

Fig. 4.1 Schematic drawing of high-speed filming setup.

Table 4.1 Welding parameters used during the production of high-speed films

	film 1	film 2	film 3	film 4
peak current (A)	300	300	300	300
base current (A)	100	100	100	55
pulse frequency (Hz)	5	5	5	5
peak current duration (ms)	6	6	10	6
arc length (mm)	2	1.5	1.5	1.5
travel speed (cm/min)	0	6.4	9.4	6.4
plate thickness (mm)	10	10	10	4

4.3 Results and discussion

4.3.1 Observation of weld pool oscillation

The oscillation of the weld pool, generated by arc current pulses, was observed by following the periodical change of the surface profile and the arc shape, and by following the reflections of the hot tungsten electrode in the weld pool. Film analysis clearly shows that three different modes of oscillation occur under the welding conditions used. It appears that characteristic differences in oscillation behaviour exist between the different modes. In the following the results obtained for each oscillation mode will be discussed separately.

mode 1 oscillation

Film 1 and film 2 were taken of weld pools under stationary arc conditions and under travelling arc conditions respectively. The films show that in both cases the weld pool surface is gradually depressed during the pressure pulse (peak current) and starts to oscillate after the pressure is released. It appears that, in the case of stationary arc welding, the surface depression does not increase further after a certain time before the end of the pressure pulse, while in the case of travelling arc welding the depression continues to increase until the pressure is released.

In the case of stationary arc welding the arc is located exactly above the centre of the weld pool. During the period of high arc pressure, the weld pool surface is symmetrically depressed and the liquid metal is pushed in radial direction. With increasing surface depression, the surface tension force increases. When the arc pressure force is balanced by the surface tension force, an equilibrium state is achieved and the weld pool surface is not depressed any further. This leads to the surface shape as shown in Fig. 4.2. After the peak current is shut off, the weld pool will start to oscillate in mode 1.

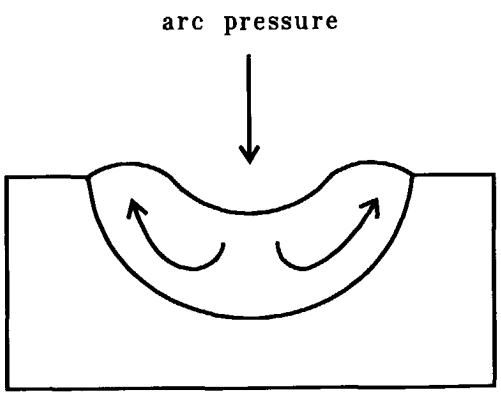

Fig. 4.2 Illustration of weld pool surface depression under stationary arc conditions.

In the case of travelling arc welding, the weld pool is elongated and the arc has an asymmetrical position with respect to the weld pool centre. Since the duration of the pressure pulse was relatively short (6 ms in the case of film 2), the depression of the weld pool surface remains small and the liquid metal in the weld pool is pushed predominantly in radial direction as indicated in Fig. 4.3a. As the travel speed was relatively low, the surface depression was found to remain about symmetrical with respect to the arc. Consequently, mode 1 oscillation resulted after the pressure was taken away.

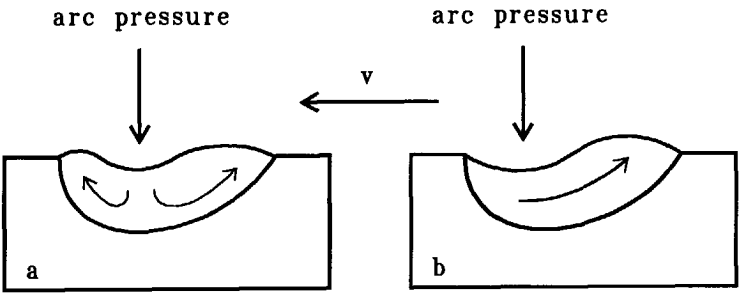

Fig. 4.3 Illustration of weld pool surface depression under travelling arc conditions:
a) - short peak current duration;
b) - long peak current duration.

In both cases, the up-and-down motion of the weld pool surface could be observed clearly before the oscillation was damped out. The number of visible oscillations between two subsequent current pulses was 22 and 9 in the case of the stationary arc and in the case of the travelling arc respectively. The oscillation reached its highest amplitude (about 1.9 mm in the case of the stationary arc and about 1.4 mm in the case of the travelling arc) immediately after the peak current was shut off, after which the oscillation amplitude damped out. The average time interval between two successive oscillations was about 8 ms both in the case of stationary arc welding and in the case of travelling arc welding.

The progression of the surface depression during the pressure pulse and the subsequent oscillation immediately after the pressure pulse are sketched in Fig. 4.4 and Fig. 4.5 for the stationary arc and the travelling arc respectively.

mode 2 oscillation

It was shown in Chapter 2 that in the case of travelling arc welding, a partially penetrated weld pool may oscillate in one of two oscillation modes: mode 1 characterised by a relatively high oscillation frequency and mode 2 characterised by a lower oscillation frequency with respect to mode 1 for a given weld pool size.

It was also shown that the occurrence of mode 2 oscillation in the case of the partially penetrated weld pool is a direct consequence of the asymmetrical location of the arc with respect to the weld pool. Due to this asymmetrical situation, a pressure difference develops between the front part and the rear part of the weld pool.

When the pressure pulse duration is short, the surface depression is still more or less symmetrical in shape. With increasing pressure pulse duration, the weld pool surface below the arc will be pushed down over a larger area and a large amount of liquid metal will be driven from the front part to the rear part [4.1], resulting in the weld pool surface shape shown in Fig. 4.3b. This front-to-back flow has also been observed by Mills [4.2]. The surface shape shown in Fig. 4.3b will eventually lead to the generation of mode 2 oscillation.

Due to the application of a longer peak current duration and a higher travel speed in the case of film 3 compared with those applied in the case of film 2 (see Table 4.1), mode 2 oscillation was found to occur. Analysis of film 3 shows that as long as the high pressure acts on the weld pool surface, the depression increases continuously and the weld pool surface transfers gradually from a symmetrical shape to an asymmetrical shape as illustrated in Fig. 4.6. The liquid metal is piled up in the rear part of the weld pool which results in the weld pool being in an

unstable state. This unstable state forces the liquid metal in the rear part of the weld pool to flow back to the front part of the weld pool after the pressure difference disappears, eventually leading to mode 2 oscillation. The front-to-back motion (and vice versa) associated with mode 2 oscillation, was clearly observed on the film (see lower part of Fig. 4.6).

The maximal oscillation amplitude of mode 2 (as recorded on film 3) was found to be about 1.1 mm, which is somewhat smaller than that of mode 1 (as recorded on film 1 and film 2) at the same peak current. The average time interval between two successive oscillations was about 17 ms.

mode 3 oscillation

In the case of film 4, welding was carried out on thin plate (4 mm thick). Under the welding conditions applied (see Table 4.1) full penetration was achieved and the weld pool oscillated in a completely different mode compared with those observed in the other films. It appears that in this case the whole weld pool surface was depressed below the workpiece surface during the pressure pulse and the weld pool surface moved in phase after the pressure pulse was released. The observed up-and-down movement of the liquid metal is consistent with the theoretical prediction for mode 3 oscillation and is much slower than that of mode 1 oscillation.

The maximal oscillation amplitude, the displacement of the weld pool surface above the workpiece surface, was measured to be about 1 mm. The average time interval between two successive oscillations in this case was evaluated to be about 26 ms. When the weld pool surface moved below the workpiece surface only the outer weld pool boundary could be distinguished. The course of events occurring in the case of this mode of oscillation is schematically illustrated in Fig. 4.7.

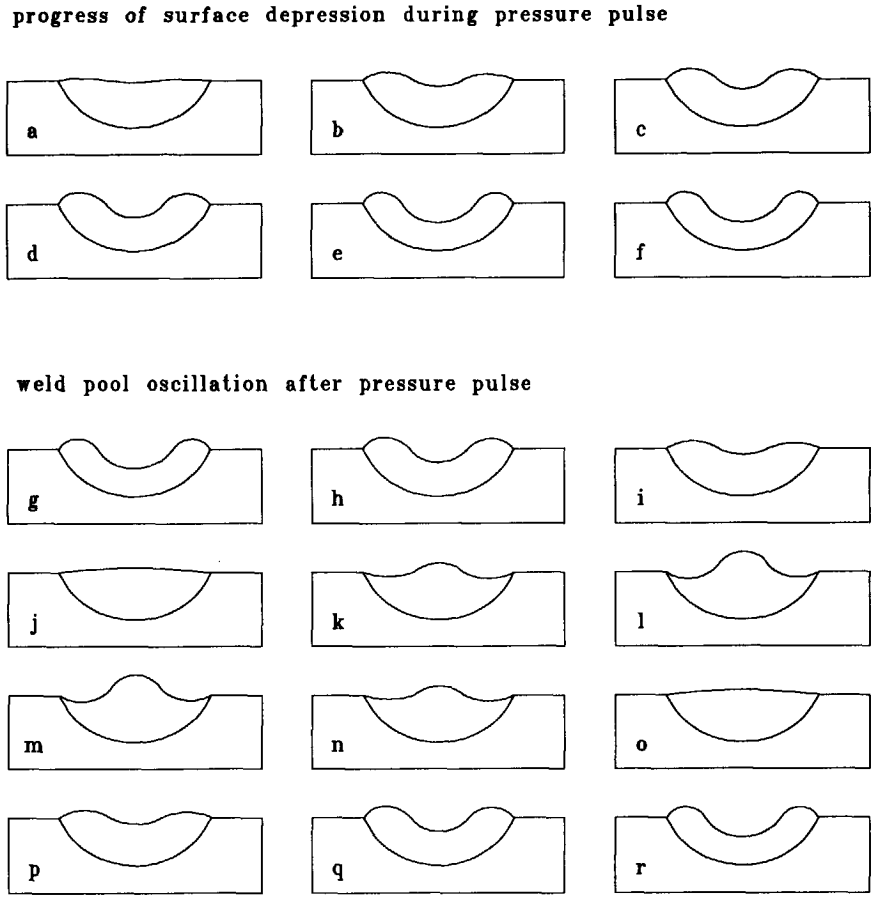

Fig. 4.4 Schematic drawing of observed weld pool surface movement in the case of mode 1 oscillation (stationary arc welding) based on the analysis of film 1.

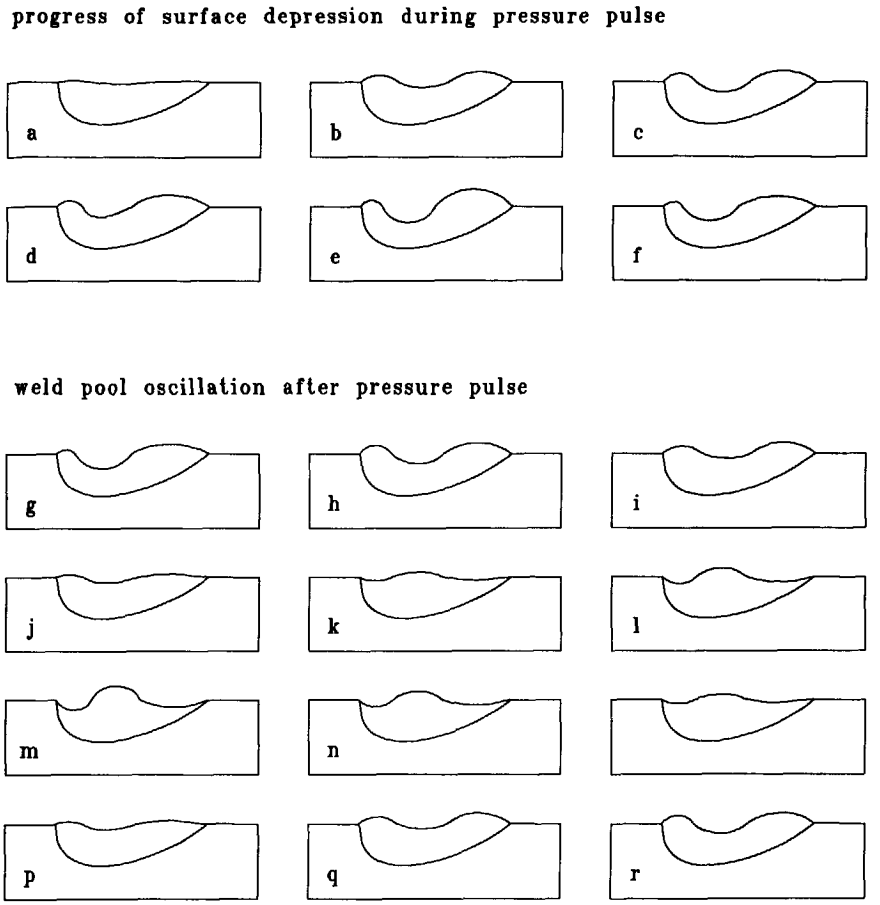

Fig. 4.5 Schematic drawing of observed weld pool surface movement in the case of mode 1 oscillation (travelling arc welding) based on the analysis of film 2.

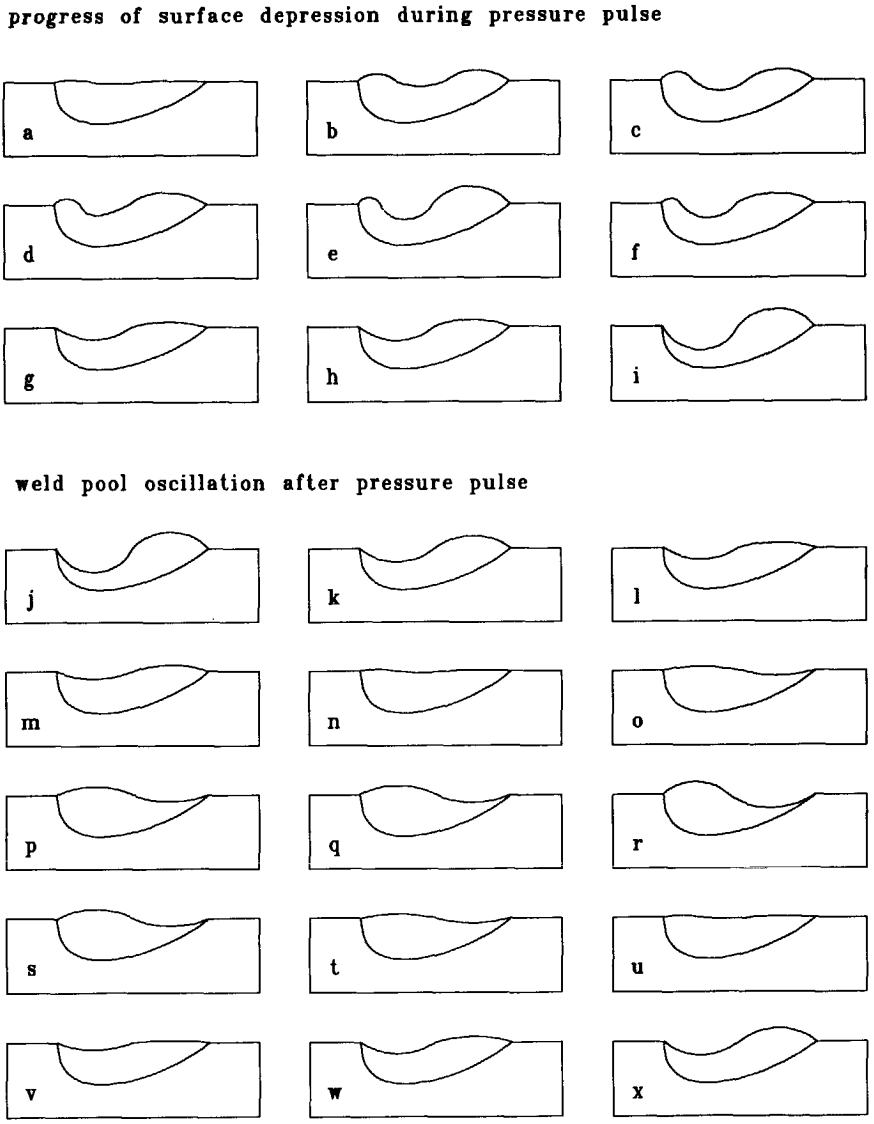

Fig. 4.6 Schematic drawing of observed weld pool surface movement in the case of mode 2 oscillation (travelling arc welding) based on the analysis of film 3.

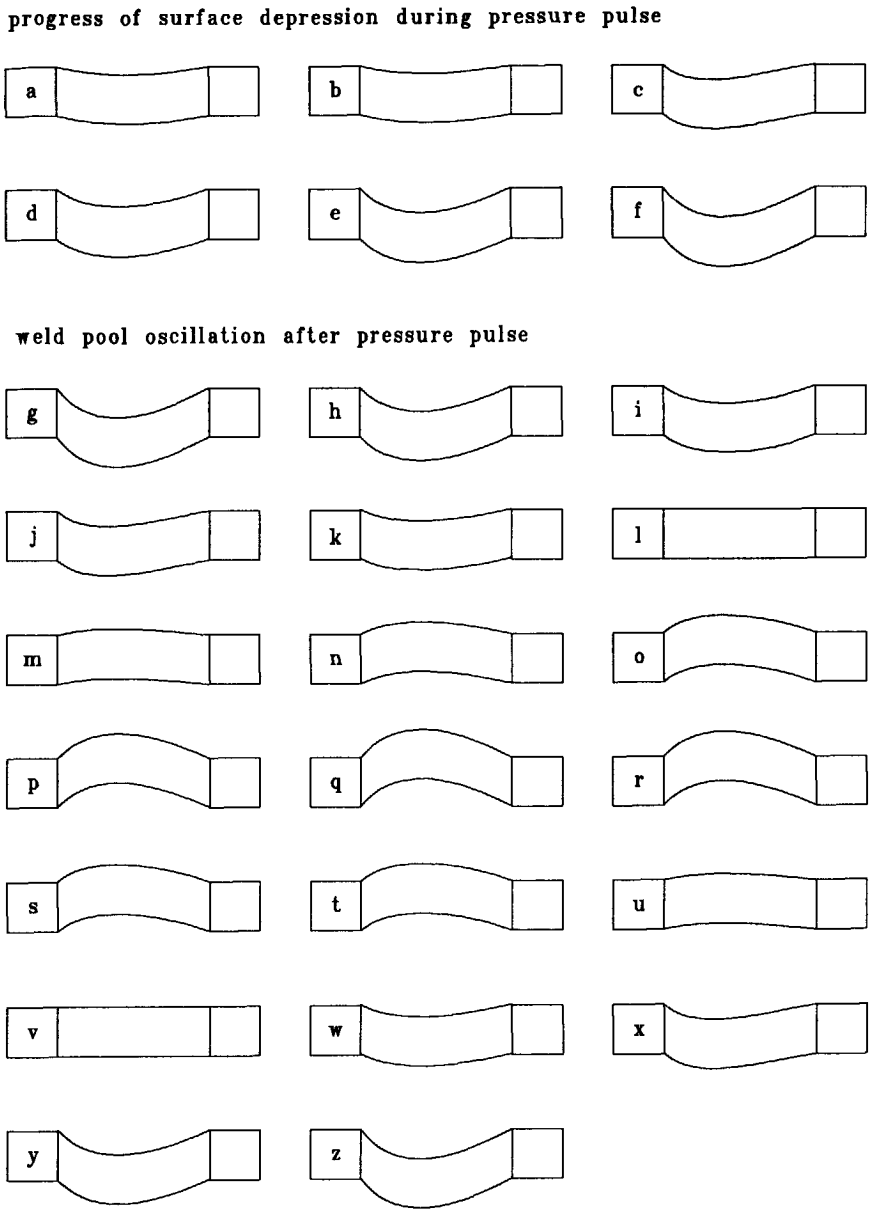

Fig. 4.7 Schematic drawing of observed weld pool surface movement in the case of mode 3 oscillation (travelling arc welding) based on the analysis of film 4.

damping of the oscillation

As was shown in the foregoing, the oscillation of the weld pool damps out as it progresses in all cases. To sensing the weld pool geometry by monitoring weld pool oscillation it is interesting to know how fast the oscillation will damp out. To obtain a better insight into the damping behaviour of the different oscillation modes, the oscillation amplitude, as obtained from the film analysis, is plotted as a function of time in Fig. 4.8. The accuracy of the amplitude measurement was about ± 0.1 mm. As can be seen from this figure, the oscillation amplitude decreases with time in all cases. It appears that the oscillation amplitude of mode 1 oscillation under travelling arc conditions decays faster than that under stationary arc conditions, and that the lower mode damps faster than the higher modes, i.e. mode 1 damps faster than mode 2, whereas mode 2 damps faster than mode 3.

The damping of the oscillation amplitude is caused by the energy losses of the oscillation: loss of kinetic energy due to solidification of the liquid weld metal at the boundary of the weld pool and dissipation of energy due to the viscosity of the liquid metal.

The damping due to solidification of the liquid weld metal increases with increasing travel speed, while the damping caused by the viscosity of the liquid metal increases with increasing oscillation frequency. Considering the causes of damping as mentioned above, it can be understood that mode 1 decays faster than mode 2, in turn mode 2 decays faster than mode 3. It should also be expected that for the same mode of oscillation the amplitude under travelling arc conditions damps more rapidly than that under stationary arc conditions, which is in agreement with the observations.

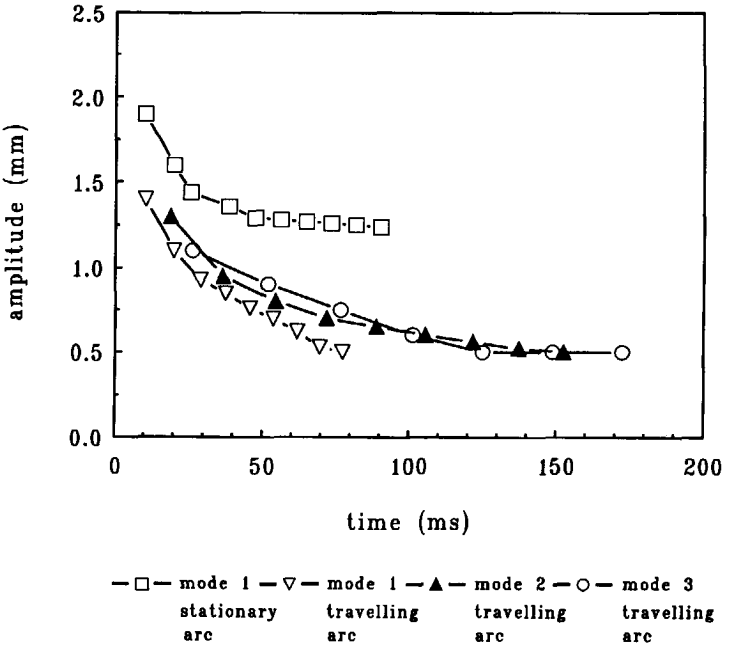

Fig. 4.8 Damping of oscillation amplitude measured from film frames.

4.3.2 Evaluation of arc voltage variation measurement

In Chapter 3 a method was described which can be used to measure the oscillation frequency and the oscillation amplitude of the weld pool. This method is based on measuring the variation of the arc voltage accompanying the oscillation.

Attempts were made to check the reliability of this measuring method by comparing the results of high-speed filming with the arc voltage measurement which were obtained simultaneously with the high-speed films during the welding process.

It appears that the film observations are in excellent agreement with the results of the arc voltage measurement as illustrated in Fig. 4.9. In this figure, the time interval between two successive oscillations as obtained by arc voltage measurement and by film analysis is plotted as a function of the number of oscillations. It can be seen in this figure that the time interval between two successive oscillations is significantly different for the three different modes of oscillation and that this interval decreases slightly as the oscillation progresses. The average time intervals obtained from the two measurements are listed in Table 4.2. The accuracy in the case of the arc voltage measurement is ± 0.25 ms (a value corresponding to ± 0.1 mm on recorder paper) and ± 0.5 ms in the case of the high-speed filming (± 1 frame). Taking this error into account, it can be concluded that the oscillation frequency of weld pools can indeed be measured accurately by monitoring the arc voltage variation.

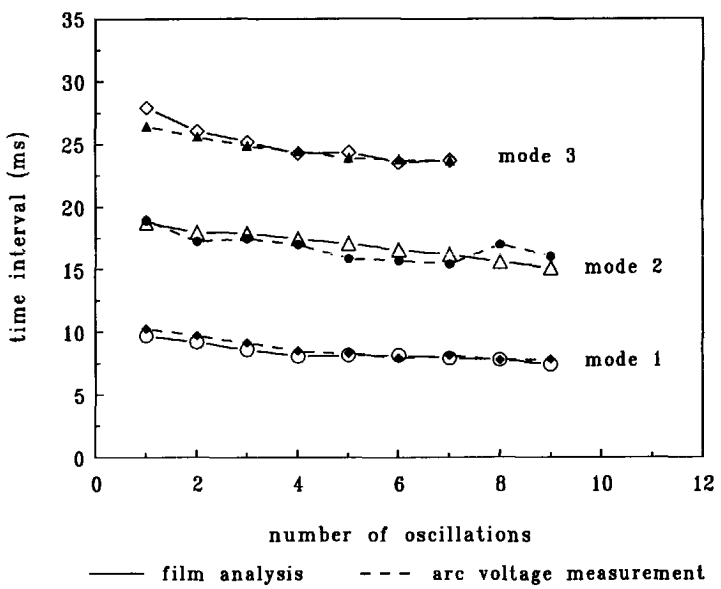

Fig. 4.9 Time interval between two successive oscillations, obtained by arc voltage measurement and by film analysis, as a function of the number of oscillations.

Table 4.2 Average time interval between two successive oscillations obtained by arc voltage measurement and by film analysis

oscillation mode	average time interval between two successive oscillations (ms)	
	arc voltage measurement	film analysis
mode 1	8.3	8.6
mode 2	16.7	16.9
mode 3	25.0	24.7

4.4 Conclusions

Weld pool oscillation was directly observed by means of high-speed filming. Based on the analysis of the films obtained, the following conclusions can be drawn.

- During GTA welding, weld pools can be set into oscillation by applying short arc current pulses.
- In the case of the partially penetrated weld pool two different oscillation modes can occur, which are characterised by a significant difference in oscillation behaviour.
- The oscillation of the fully penetrated weld pool is governed by an oscillation mode, which differs significantly from those occurring in the partially penetrated weld pool.
- The damping of the oscillation depends on the welding conditions and differs for the different oscillation modes.
- The frequency of the weld pool oscillation can be accurately measured by monitoring the arc voltage variation.

References

4.1 E. Dumps, "The pressure of the arc acting on the weld pool", Proceedings of International Conference on Arc Physics and Weld Pool Behaviours, London, UK, 1979, p. 259-266.

4.2 G.S. Mills, "Arc/weld pool interactions and their effect on GTA weld penetration", Proceedings of International Conference on Arc Physics and Weld Pool Behaviours, London, UK. 1979, p. 279-284.

Chapter 5

Oscillation Behaviour of Stationary Weld Pools

5.1 Introduction

This chapter deals with the oscillation behaviour of both partially penetrated weld pools and fully penetrated weld pools during stationary GTA welding of mild steel Fe 360 and austenitic stainless steel AISI 304. The oscillation frequency and oscillation amplitude of the weld pools were measured by monitoring the arc voltage variation after triggering the weld pool into oscillation by short arc current pulses.

Experiments were carried out to determine the detectability of the weld pool oscillation by the method used and to assess the influence of welding conditions on the oscillation behaviour. On the basis of the results obtained relations are established between the geometry of the weld pool and the oscillation frequency. Furthermore, a comparison is made between the experimental results and the results predicted by theory.

5.2 Experimental procedure

Weld pools of different size were produced in plates of mild steel Fe 360 and austenitic stainless steel AISI 304 by GTA welding under stationary arc conditions, i.e. at zero travel speed. The welding conditions used are listed in Table 5.1. The size of the weld pool was varied by gradually increasing the arc time at constant arc current and by varying the arc current level.

Table 5.1 Welding conditions used in the stationary arc experiments

peak current	100 - 300 A
peak current duration	2 - 10 ms
base current	50 - 150 A
pulse frequency	5 - 25 Hz
arc length	1 - 5 mm
polarity	electrode negative
electrode	2% thoriated tungsten
electrode diameter	1.6, 2.4, 3.2 mm
electrode tip angle	30^0, 60^0, 90^0
shielding gas	argon; 10 l/min
	helium; 24 l/min

Partially penetrated weld pools were produced in plates of 4 mm and 10 mm thickness, fully penetrated weld pools in plates of 4 mm thickness. The analysed chemical composition of both steels is given in Table 5.2.

Table 5.2 Chemical composition of steels used (wt%)

steel	C	Si	Mn	P	S	O	N	Cr	Ni
Fe 360	0.080	0.06	0.44	0.105	0.30	0.017	0.090	0.060	0.075
AISI 304	0.065	0.28	1.83	0.029	0.017	0.015	0.024	18.02	9.590

Before welding the workpieces were mechanically ground to remove the oxide layer from the surface, followed by chemical degreasing.

The weld pools were triggered into oscillation by short current pulses and the oscillation frequency and oscillation amplitude were measured by monitoring the arc voltage variation (see Chapter 3).

The geometry of the weld pool was determined from the cross-section of the spot weld obtained after solidification of the weld pool. The solidified spot weld was carefully sectioned at its centre and the cross-section was then ground, polished and etched. After chemical etching, the weld pool diameter and depth were measured using an optical microscope at 10 times magnification. A correction was made for the small increase in weld pool size, occurring directly after the arc was shut off, due to the thermal inertia of the workpiece.

5.3 Results and discussion

5.3.1 Preliminary experiments

To evaluate the measuring technique employed, a series of preliminary experiments was carried out with mild steel Fe 360 plates.

A typical example of arc voltage variation due to weld pool oscillation in the case of both partial penetration and full penetration with helium as shielding gas and argon as backing gas in the case of full penetration is given in Fig. 5.1. As can be seen in this figure, the voltage variation is more or less sinusoidal in shape with a maximal amplitude (peak to peak) of about 100 mV for a partially penetrated weld pool (see Fig. 5.1a) and with a maximal amplitude of about 400 mV for the fully penetrated weld pool (see Fig. 5.1b).

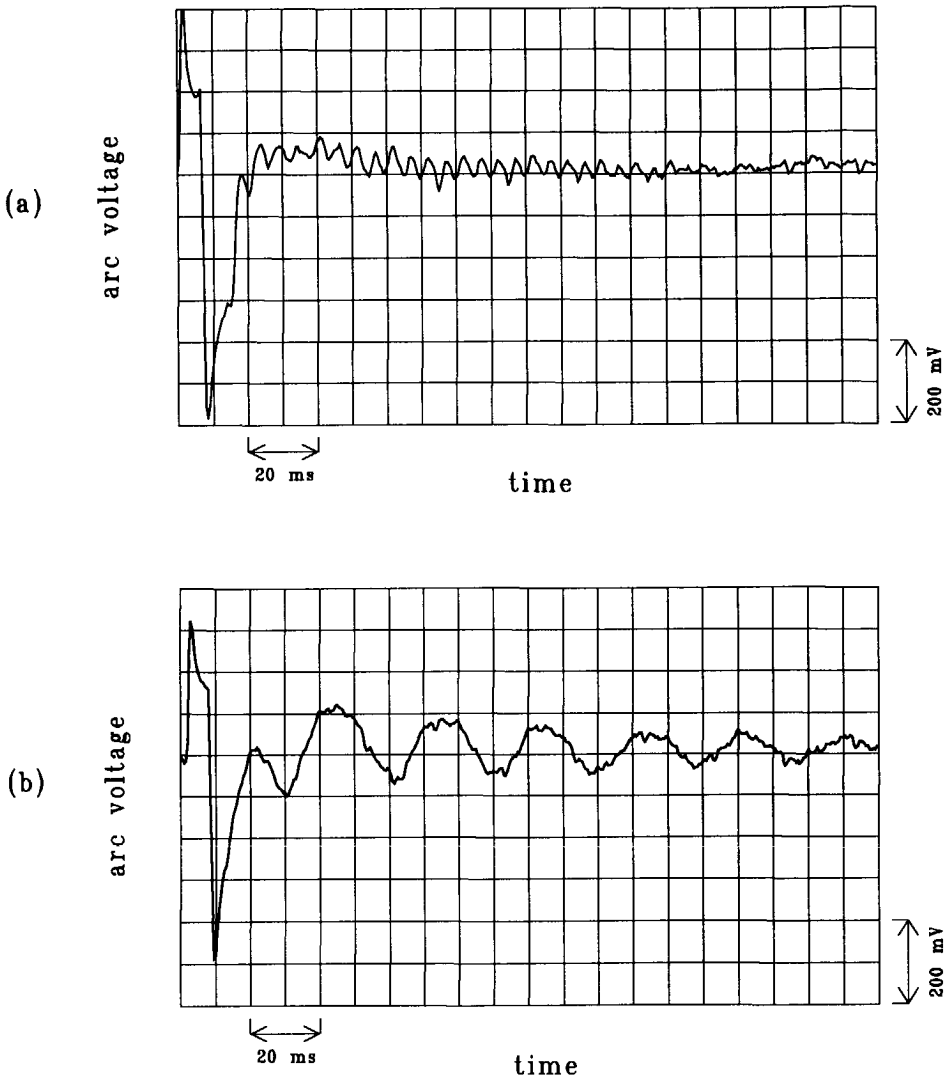

Fig. 5.1 Arc voltage variation due to weld pool oscillation (peak current 250 A, base current 50 A, pulse frequency 5 Hz, peak current duration 6 ms, with helium as shielding gas and with argon as backing gas):
(a) partial penetration; (b) full penetration.

The oscillation amplitude of the weld pool surface can be derived from the arc voltage amplitude with the help of the equation:

$$\frac{dV}{dL} = E \qquad \text{or:} \qquad dL = \frac{dV}{E} \tag{5.1}$$

which was derived in Chapter 3. In this equation V is the arc voltage, L the arc length and E the electric field strength in the arc column.

Taking for E the value of 2 V/mm [5.1], the oscillation amplitude is estimated to have a value of about 0.05 mm and 0.2 mm for the partially penetrated weld pool and for the fully penetrated weld pool respectively. It should be noted that in the case of partial penetration, the actual oscillation amplitude of the weld pool is probably somewhat higher than the value obtained from the arc voltage variation, due to the fact that the voltage variation does not reflect the largest distance between the electrode and the weld pool surface, but the average distance as observed by high-speed filming.

5.3.2 Detectability of weld pool oscillation

Although the input current is rectified by the power supply, it may be expected that still small fluctuations in the current level occur. These fluctuations in arc current will result in corresponding fluctuations in arc voltage, which in turn influence the sensitivity of the measurement of the weld pool oscillation. To assess the detectability of weld pool oscillations by monitoring the arc voltage variation, the voltage fluctuations were evaluated by measuring the voltage variation of an arc between the electrode and a 10 mm thick tungsten plate (no weld pool) under conditions of constant arc current (150 A) and constant arc length (1.5 mm) with argon and helium as shielding gas respectively. In this way it was possible to determine the smallest detectable amplitude of the weld pool

oscillation, which can be detected with the measuring system. The maximal magnitude of the arc voltage fluctuations was measured to be about 50 mV and 60 mV in argon and in helium respectively.

Using equation (5.1) and taking for E the value of 1 V/mm and 2 V/mm for argon shielding and helium shielding respectively [5.1], the fluctuation in arc length corresponding to the voltage fluctuation was estimated to be about 0.05 mm for argon and about 0.03 mm for helium. This implies that oscillations with an amplitude larger than 0.05 mm in argon, and with an amplitude larger than 0.03 mm in helium can in principle be detected by monitoring the arc voltage variation. The actual detectable oscillation amplitude is somewhat larger than the value evaluated by the arc voltage measurement as observed by high-speed filming.

5.3.3 Influence of welding conditions on oscillation amplitude

To be able to detect the weld pool oscillation, its amplitude should be sufficiently high (larger than 0.05 mm in argon and larger than 0.03 mm in helium, see previous section). It is to be expected that the oscillation amplitude depends on the welding conditions, especially on arc length, pulse parameters and the shielding gas used. In order to evaluate the influence of these parameters on the oscillation amplitude, a series of experiments was carried under various welding conditions with mild steel Fe 360.

influence of arc length

The results of experiments carried out with different arc length show that the oscillation amplitude decreases with increasing arc length. This can be understood by realising that the shorter the arc length, the higher the arc current density and, hence, the higher the arc pressure on the weld pool centre, which in turn

leads to a stronger triggering force. As a result, the oscillation amplitude of the weld pool is higher and easier to be detected.

The arc length above which the variation of arc voltage becomes undetectable, was measured to be 3 mm in argon and 5 mm in helium for a peak current of 300 A. When the arc length was increased above 5 mm in helium, the arc itself became less stable, making the measurement increasingly difficult. Thus, it appears that the detectability of weld pool oscillation by means of arc voltage sensing when using helium as shielding gas is also limited in practice by the arc stability itself and that short arc length is preferred for obtaining reliable arc voltage signals.

influence of pulse parameters

The arc voltage variation due to weld pool oscillation shown in Fig. 5.1 was obtained with a peak current of 250 A. To investigate the effect of peak current on the oscillation amplitude, the oscillation amplitude was measured for a number of weld pools at different peak current levels (from 100 A to 300 A). It was found that the amplitude of the arc voltage variation increases with increasing peak current for both argon shielding and helium shielding. To get detectable arc voltage signals, the minimal peak current (stimulating energy) required to trigger a weld pool was found to increase with increasing arc length. This is in agreement with the results presented above.

It was also found that the oscillation amplitude increases with increasing peak current duration. When the peak current duration is longer than a certain value, the oscillation amplitude does not increase any further at a given peak current. This can be explained by considering the surface depression process in more detail (see Fig. 5.2).

The depression of the weld pool surface, which develops during the arc current pulse, is a direct consequence of the work performed by the plasma jet force against the surface tension force: the plasma jet force tends to push down the

molten metal at the centre of the weld pool, causing the molten metal to pile up near the boundary of the weld pool (liquid metal is incompressible and obeys the mass conservation law). In reaction, the surface tension force tends to straighten the curved surface, keeping the surface in an energy state as low as possible. With increasing surface curvature, the surface tension force increases until the two counteracting forces, the plasma jet force and the surface tension force, become equal. Thus, the weld pool surface reaches its equilibrium state with a depression depth h_0, which is in fact the maximal oscillation amplitude at the given peak current (arc pressure). The value of h_0 was found to increase with increasing arc current and weld pool diameter [5.2 and 5.3]. Since increasing the peak current leads to an increase of the strength of the plasma jet, the depth of the surface depression also increases with increasing peak current. This means that the arc voltage variation, which is directly related to the oscillation amplitude, increases with increasing peak current.

As described above, it appears that a certain time t_c is required to depress the weld pool surface from its equilibrium position to its maximal depression depth h_0 under a given arc pressure. If $t_p < t_c$, the oscillation amplitude will increase continuously with increasing t_p. If $t_p > t_c$, further increasing t_p will have no influence any more on the oscillation.

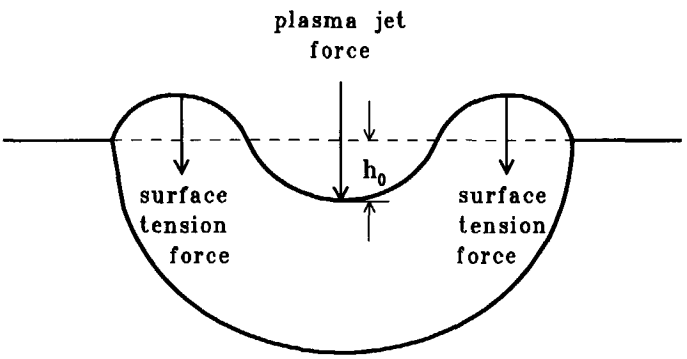

Fig. 5.2 Illustration of pressure balance on the weld pool surface.

influence of shielding gas

The amplitude of the weld pool oscillation is not only sensitive to the arc length, but is also very sensitive to the shielding gas used because the arc pressure acting on the weld pool and the electric field strength E depend on the shielding gas used.

To test the influence of the shielding gas on the oscillation amplitude, two series of experiments were carried out with argon and helium as shielding gas respectively, using peak currents of 150 A and 250 A, a variable peak current duration and an arc length of 1.5 mm.

The results of these experiments show that the magnitude of the arc voltage for a given arc length is strongly dependent on the shielding gas used. The average arc voltage was measured to be 10-11 V in the case of argon shielding and 14-16 V in the case of helium shielding. Furthermore, it was found that the amplitude of the arc voltage variation due to the weld pool oscillation in helium shielding gas is much higher than that in argon shielding gas under the same peak current. As an illustration of this, some of the results obtained with peak current 250 A on 4 mm thick plate are presented in Fig. 5.3. The arc voltage variation for partial penetration and full penetration in the case of argon are presented in Fig. 5.3a and Fig. 5.3b respectively and, the arc voltage variation for partial penetration and full penetration in the case of helium are presented in Fig. 5.3c and Fig. 5.3d. As can be seen in this figure that the arc voltage variation in helium shielding is about 4 times higher than that in argon shielding both for partial penetration and for full penetration. This is due to the higher value of the electric field strength E in helium shielding compared with that in argon shielding. The higher arc voltage variation in helium compared with that in argon implies that using helium as shielding gas is more sensitive to detect the weld pool oscillation by monitoring the arc voltage variation than using argon as shielding gas.

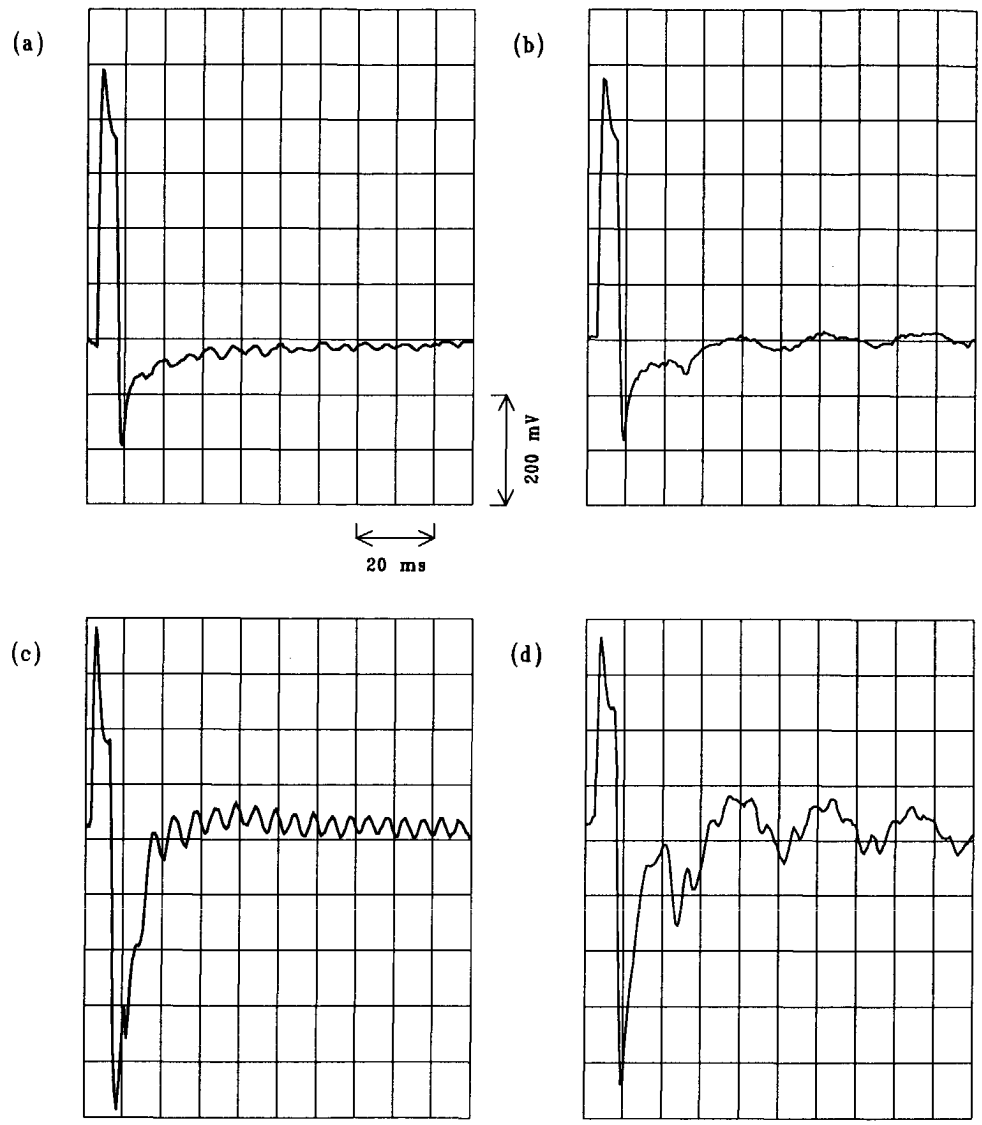

Fig. 5.3 Arc voltage variation due to weld pool oscillation (peak current 250 A, base current 70 A in argon and 50 A in helium, pulse frequency 10 Hz, peak current duration 5 ms):
(a) partial penetration weld pool in argon;
(b) full penetration weld pool in argon;
(c) partial penetration weld pool in helium;
(d) full penetration weld pool in helium.

influence of electrode geometry

In addition to the influence of the shielding gas used, the geometry of the electrode, diameter and tip angle also plays a role in the arc pressure distribution. It appears that the smaller the electrode tip angle, the higher the pressure generated by the arc at the same arc current [5.4]. In addition, a smaller electrode tip angle results in the arc being conical or bell shaped [5.5] in cross-section with a small anode spot. Thus, it may be expected that the electrode geometry will influence the oscillation behaviour of the weld pool and, hence, the results of the measurement.

To test this, a number of experiments was carried out with electrodes of different diameters (1.6, 2.4 and 3.2 mm) and different tip angles (30^0, 60^0 and 90^0). The results of these experiments indicate that the smaller the electrode diameter the higher the oscillation amplitude. This is due to the fact that with decreasing electrode diameter the arc pressure concentrates increasingly at the weld pool centre. Furthermore, the results of the experiments show that the smaller the electrode tip angle, the higher the oscillation amplitude. This is because in the case of smaller electrode tip angles the arc exerts a higher pressure on the weld pool, which leads to a higher oscillation amplitude.

Summarising the influence of welding parameters on the oscillation amplitude, it can be stated that there is an optimum condition under which good measurements can be performed. In the case of short arc length, reliable measurements are possible with both argon and helium as shielding gas. With increasing arc length, higher peak current is required to get a detectable oscillation amplitude, whereas helium should be used as shielding gas.

5.3.4 Influence of weld pool geometry on oscillation frequency

To investigate the influence of weld pool geometry on the oscillation frequency, a large number of experiments was performed with mild steel Fe 360 and austenitic stainless steel AISI 304 using argon as shielding gas. The welding conditions used are listed in Table 5.1.

partially penetrated weld pools

In the case of partial penetration, the oscillation frequency of weld pools, as obtained from the arc voltage variation, was found to decrease with increasing weld pool diameter. This is clearly illustrated in Fig. 5.4, in which the oscillation frequency of partially penetrated weld pools in mild steel Fe 360 is plotted as a function of the weld pool diameter. For instance, the oscillation frequency is 330 Hz for a weld pool 3.7 mm in diameter and decreases to 80 Hz for a weld pool 9.9 mm in diameter. Similar results were obtained in the case of austenitic stainless steel AISI 304 as shown in Fig. 5.5. It should be noted that the oscillation frequency in the case of mild steel Fe 360 is somewhat lower than that in the case of austenitic stainless steel AISI 304 for a given weld pool diameter. This difference in oscillation frequency is directly related to the difference in physical properties of both materials and will be explained later.

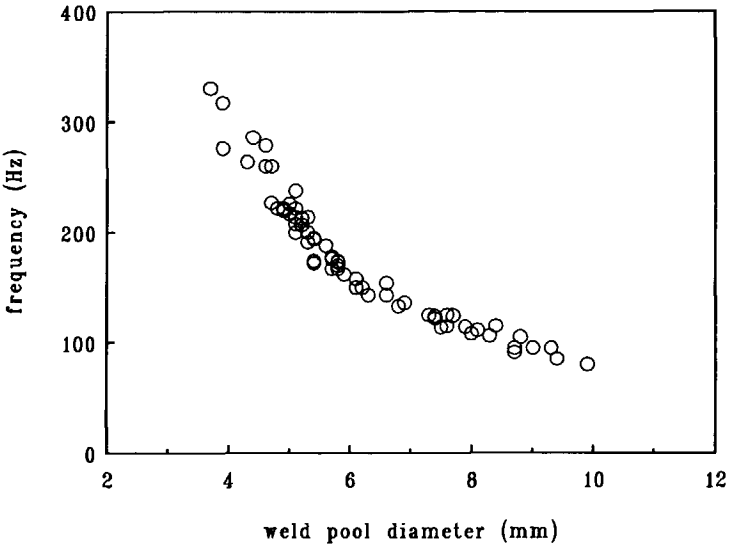

Fig. 5.4 Oscillation frequency of partially penetrated weld pool under stationary arc conditions as a function of weld pool diameter (mild steel Fe 360).

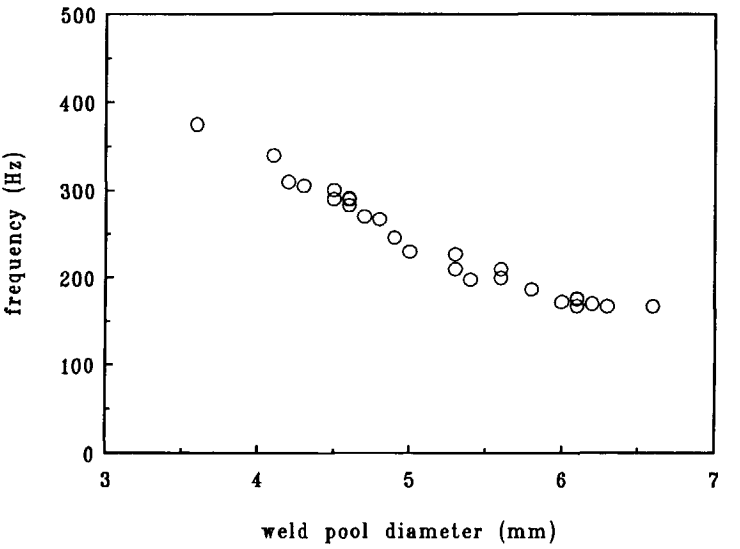

Fig. 5.5 Oscillation frequency of partially penetrated weld pool under stationary arc conditions as a function of weld pool diameter (austenitic steel AISI 304).

In Chapter 2 a model was developed for the oscillation of a partially penetrated weld pool. According to this model the oscillation frequency f and the weld pool diameter D are related by the equation:

$$f = 5.84\left(\frac{\gamma}{\rho_l}\right)^{1/2} D^{-3/2} \qquad (5.2)$$

with γ the surface tension of the liquid metal, ρ_l the density of the liquid metal and D the weld pool diameter.

To test the validity of this model, the measured values of the oscillation frequency were plotted as a function of $D^{-3/2}$. The results are shown in Fig. 5.6 and Fig. 5.7 for mild steel Fe 360 and for austenitic stainless steel AISI 304 respectively. The straight lines in these figures represent equation (5.2), taking for γ and ρ_l the values listed in Table 5.3. The figures show that the measured oscillation frequency tends to be somewhat higher than the calculated frequency, especially in the case of austenitic stainless steel. This deviation might well be due to the uncertainty in the value of γ (presumably, the actual value of γ is somewhat higher than the value used in the present case).

Table 5.3 Physical properties used for the calculation of the oscillation frequency

material	surface tension γ (N/m)	density of liquid ρ_l (kg/m^3)	density of solid ρ_s (kg/m^3)
steel Fe 360	1.0 [5.3]	$7.0 \cdot 10^3$ [5.7]	$7.8 \cdot 10^3$ [5.8]
steel AISI 304	1.2 [5.6]	$7.5 \cdot 10^3$ [5.9]	$7.8 \cdot 10^3$ [5.10]

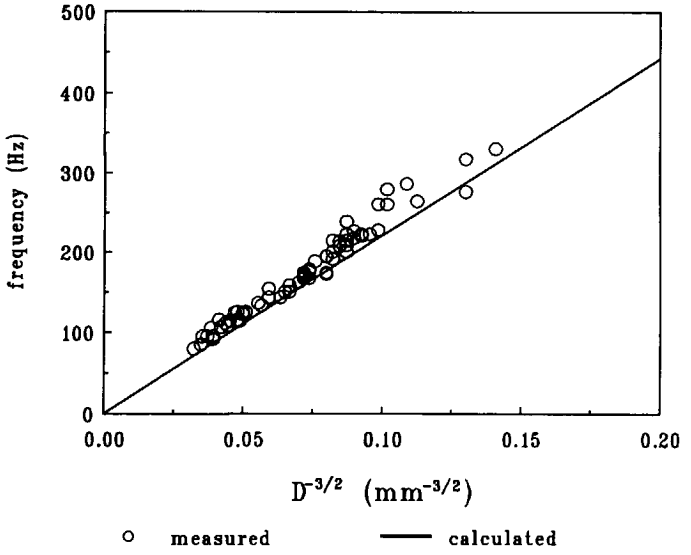

Fig. 5.6 Oscillation frequency of partially penetrated weld pool under stationary arc conditions as a function of $D^{-3/2}$ (mild steel Fe 360).

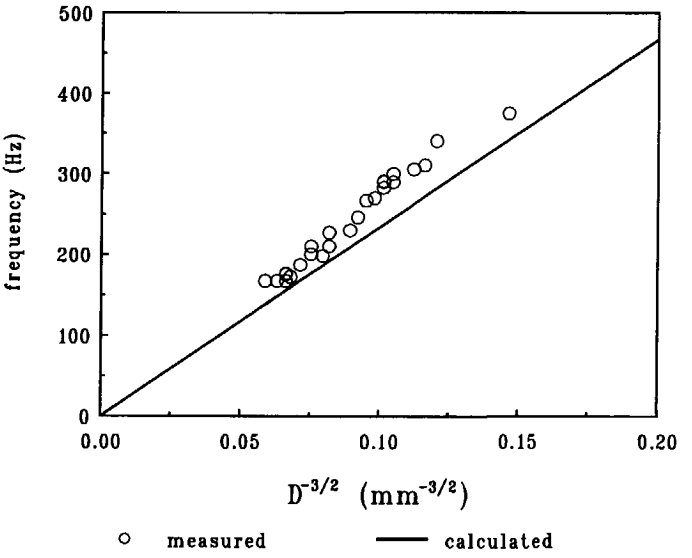

Fig. 5.7 Oscillation frequency of partially penetrated weld pool under stationary arc conditions as a function of $D^{-3/2}$ (austenitic steel AISI 304).

Taking this uncertainty into account it can be concluded that there is good agreement between experiment and theory. Apparently, the oscillation frequency of the partially penetrated weld pool is adequately described by equation (5.2). The higher oscillation frequency observed in the case of austenitic stainless steel AISI 304 compared with that observed in the case of mild steel Fe 360 arises from the higher surface tension of austenitic stainless steel AISI 304 with respect to that of mild steel Fe 360 (see Table 5.3).

It was suggested by Renwick and Richardson [5.11] that the oscillation frequency of the partially penetrated weld pool is not only dependent on the diameter of the weld pool, but also on its depth. The results of the present work do not support this view and clearly show that the oscillation frequency of the partially penetrated weld pool is independent of weld pool depth, at least under the experimental conditions used. These findings prove that neglecting the term tanh(2kh), as discussed in Chapter 2, is justified in the present case. This is understandable because the present experiments were carried out under conditions of a relatively deep weld pool (high depth/width ratio). It is expected, however, that with decreasing depth/width ratio, the depth of the weld pool will start to play a role in the oscillation behaviour.

fully penetrated weld pools

The situation of the fully penetrated weld pool is essentially different from that of the partially penetrated weld pool (see Fig. 1.1). Whereas the liquid weld metal in the partially penetrated weld pool is backed by a solid bottom, this is not the case in the fully penetrated weld pool. In fact, the liquid weld metal in the fully penetrated weld pool has an extra degree of freedom (normal to the surface of the weld pool) and it is evident that this extra degree of freedom will influence the oscillation behaviour.

To obtain a better understanding of the oscillation behaviour of fully penetrated weld pools, a series of experiments with fully penetrated weld pools was carried out. It was found that when full penetration is achieved, two

oscillation modes can be observed. These oscillation modes can best be dealt with in terms of D_b, the bottom diameter of the fully penetrated weld pool.

In Fig. 5.8 the measured oscillation frequency of a fully penetrated weld pool in mild steel Fe 360 is plotted as a function of the bottom diameter D_b. It appears that at relatively small values of D_b the weld pool still oscillates in the partial penetration mode (mode 1) having a high frequency (f ~ 150 Hz). At a certain value of D_b a transition occurs to a different mode (mode 3), having a much larger amplitude and a much lower frequency (f ~ 30 Hz) than that of the partial penetration mode. Similar results were obtained with austenitic stainless steel AISI 304 as shown in Fig. 5.9. The transition between the two modes occurs rather abruptly at D_b ~ 4.9 mm both for mild steel Fe 360 and for austenitic stainless steel AISI 304, a value corresponding to about 1.2 times the plate thickness (4 mm in the present case) or to 0.8 for the ratio D_b/D_t (D_t is the top diameter of the weld pool). This is in accordance with the results obtained by Yoo [5.12]. This transition is of considerable interest, as it may be used as a tool for in-process control of weld pool penetration. This point will be discussed in more detail in Chapter 8.

As was been shown in Chapter 2, a fully penetrated weld pool may oscillate as a stretched membrane. In that case the relation between the oscillation frequency and the weld pool diameter is given by:

$$f = 1.08\left(\frac{\gamma}{H\rho_l}\right)^{1/2} D_2^{-1} \tag{5.3}$$

with H the plate thickness, γ the surface tension of the liquid metal, ρ_l the density of the liquid metal and D_2 the diameter of the cylinder whose volume is equal to the volume of the real weld pool.

Although this equation refers to a stationary weld pool of cylindrical shape (fusion boundary normal to the plate surface or $D_b/D_t = 1$), it is assumed that the equation remains essentially valid for the case of the more realistic stationary weld pool, having a shape close to a tapered cylinder as exposed by cross-sections of the solidified weld beads.

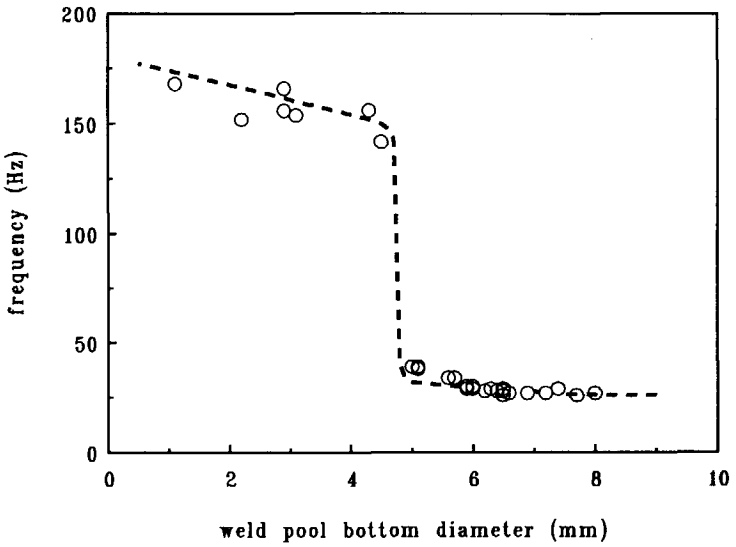

Fig. 5.8 Oscillation frequency of fully penetrated weld pool under stationary arc conditions as a function of the diameter of the bottom surface (mild steel Fe 360).

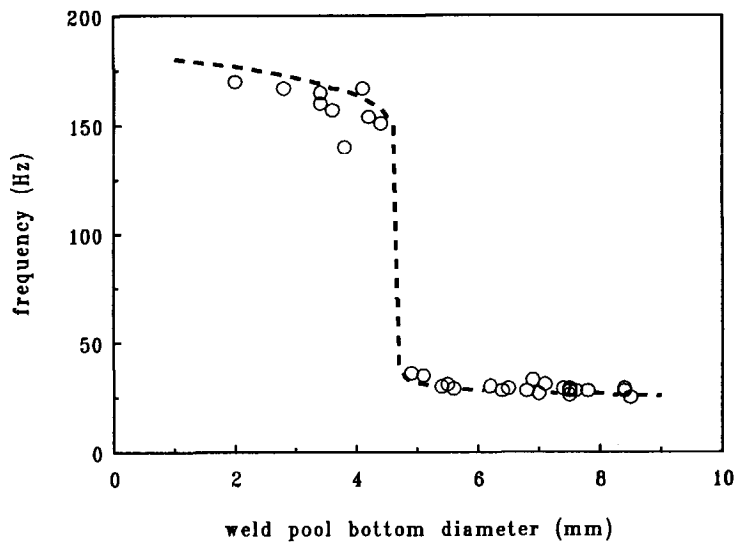

Fig. 5.9 Oscillation frequency of fully penetrated weld pool under stationary arc conditions as a function of the diameter of the bottom surface (austenitic stainless steel AISI 304).

According to the law of mass conservation, the mass of the liquid metal in the weld pool must be equal to the mass of the solid metal before melting. This can be expressed as:

$$m = \frac{\pi}{4} D^2 H \rho_l = \frac{\pi}{4} D_2^2 H \rho_s \tag{5.4}$$

in which H is the plate thickness, ρ_s the density of the solid plate material and D_2 is the diameter of the cylinder having a volume equal to the volume of the tapered weld pool. The value of D_2 is related to the top diameter D_t and the bottom diameter D_b of the tapered weld pool according to the equation:

$$D_2^2 = \frac{1}{3}\left(D_t^2 + D_t D_b + D_b^2\right) \tag{5.5}$$

By replacing ρ_l by ρ_s and D by D_2 in equation (5.3) the following expression for the oscillation frequency is obtained:

$$f = 1.08 \left(\frac{\gamma}{H \rho_s} \right)^{1/2} D_2^{-1} \tag{5.6}$$

To test the validity of the stretched membrane model for the situation of real weld pool oscillation, the measured values of the oscillation frequency are plotted as a function of D_2 in Fig. 5.10 and in Fig. 5.11 for mild steel Fe 360 and for austenitic stainless steel AISI 304 respectively. The straight lines in these figures represent equation (5.6), taking H the value of 4 mm and γ and ρ_s the values as listed in Table 5.3. It appears that, although considerable scatter occurs, there is a reasonable agreement between calculation and experiment for welds having a D_b larger than about 5 mm ($D_b/D_t > 0.8$). Thus, it seems justified to describe the

fully penetrated weld pool to a first approximation in terms of a stretched membrane as long as D_b is larger than 5 mm. The deviation between the experimental results and the theoretical prediction occurring for relatively small weld pool size (in the present case, when $D_b/D_t < 0.8$, or when $D_b < 5$ mm) can be easily understood when realising that mode 3 oscillation represents the oscillation of a stretched membrane having a dimension in the plate thickness direction small compared with its dimensions in the other two directions.

Although the results presented in this chapter refer to the situation of the stationary GTA weld pool, they offer a basic understanding of the weld pool oscillation behaviour in general. In the following chapters the oscillation behaviour of the GTA weld pool in the case of a travelling arc will be discussed.

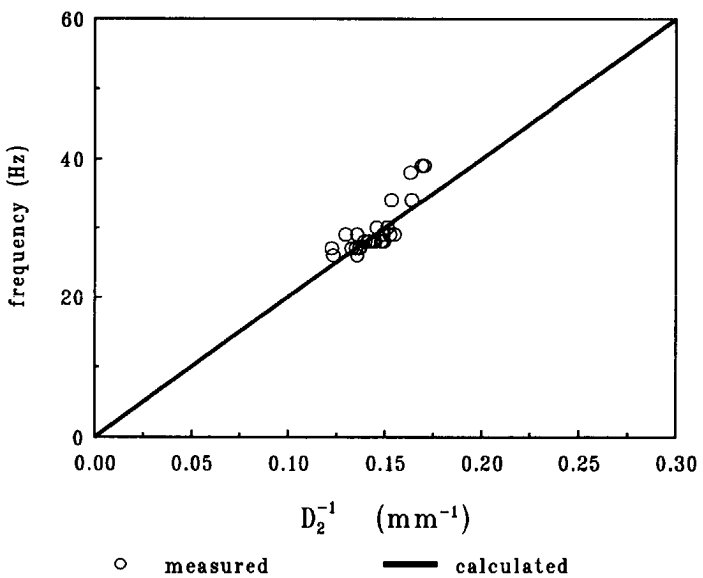

Fig. 5.10 Oscillation frequency of fully penetrated weld pool under stationary arc conditions as a function of D_2^{-1} (mild steel Fe 360).

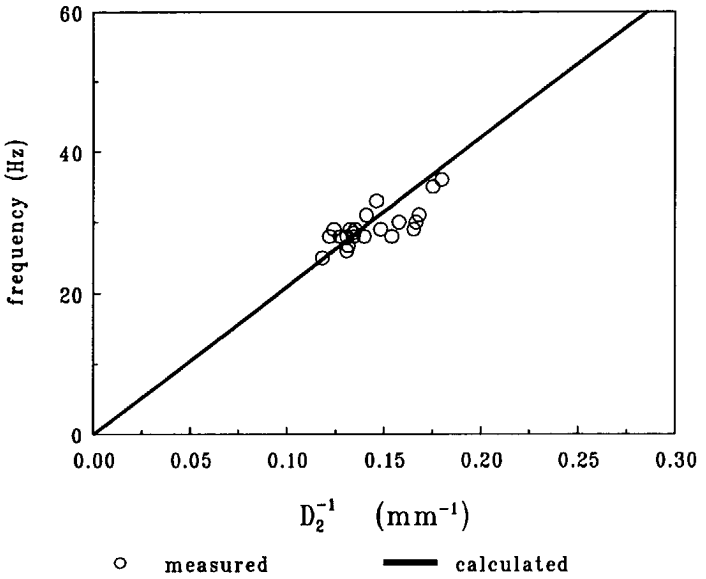

Fig. 5.11 Oscillation frequency of fully penetrated weld pool under stationary arc conditions as a function of D_2^{-1} (austenitic stainless steel AISI 304).

5.4 Conclusions

The results presented in this chapter lead to the following conclusions.

- The oscillation amplitude and frequency of stationary GTA weld pools, both in mild steel Fe 360 and in austenitic stainless steel AISI 304, can be accurately measured during welding by monitoring the arc voltage variation after triggering the weld pool by an arc current pulse.
- The detectability of the oscillation amplitude was found to be ~ 0.05 mm in argon and ~ 0.03 mm in helium.
- The oscillation amplitude increases with increasing peak current, increasing peak current duration, decreasing arc length, decreasing electrode diameter and decreasing electrode tip angle.
- In the case of partial penetration the oscillation frequency lies in the range between 100 and 400 Hz and decreases with the diameter D of the weld pool as $D^{-3/2}$.
- In the case of full penetration two different situations can occur:
  - when the bottom diameter of the weld pool is relatively small the weld pool behaves as a partial penetration weld pool and oscillates in the partial penetration mode (mode 1);
  - when the bottom diameter is relatively large the weld pool oscillates in a different mode characterised by an oscillation frequency which lies in the range between 25 and 40 Hz and decreases with the diameter of the weld pool as D^{-1} (mode 3).
- The observed oscillation behaviour of both the partially penetrated weld pool and the fully penetrated weld pool can be satisfactorily explained in terms of classical hydrodynamics, taking into account the pressure balance on the weld pool surface.
- An abrupt transition occurs between the two modes of oscillation. This transition may be used for in-process control of weld pool penetration.

References

5.1 J.P. Zijp and G. den Ouden, "Effect of shielding gas composition on heat transfer during GTA welding", Proceedings of International Conference Advances in Joining and Cutting Processes, The Welding Institute, Harrogate, UK, 1989, p. 24-32.

5.2 B.J. Bradstreet, "Effect of surface tension and metal flow on weld bead formation", Welding Journal, Vol.47. no.7 (1968), p. 314s-322s.

5.3 E. Friedman, "Analysis of weld puddle distortion and its effect on penetration", Welding Journal, Vol.57, no.6 (1978), p. 161s-166s.

5.4 M.L. Lin and T.W. Eagar, "Pressures produced by gas tungsten arcs", Metallurgical Transactions, Vol.17B, (1986), p. 601-607.

5.5 S.S. Glickstein, "Basic study of the welding process", Proceedings of Conference on Trends in Welding Research in The United States, New Orleans, USA, 16-18 Nov. 1981, p. 3-51.

5.6 J. Wen and C.D. Lundin, "Surface tension of 304 stainless steel under welding conditions", Welding Journal, Vol.65, no.5 (1986), p. 138s.

5.7 T. Iida and R.J.L. Guthrie, The Physical Properties of Liquid Metals, Clarendon Press, Oxford, UK, 1988.

5.8 American Society for Metals, Metal Handbook, 9th edition, Vol.1, 1976, p. 145.

5.9 U.M. Ahmad and L.E. Murr, "Surface free energy of nickel and stainless steel at temperature above the melting point", Journal of Materials Science, Vol.11, (1976), p. 224-230.

5.10 American Society for Metals, Metal Handbook, 9th edition, Vol.3, 1976, p. 34.

5.11 R.J. Renwick and R.W. Richardson, "Experimental investigation of GTA weld pool oscillation", Welding Journal, Vol.62, no.2 (1983), p. 29s-35s.

5.12 C.D. Yoo, "Effect of weld pool conditions on pool oscillation", Ph.D. Dissertation, The Ohio State University, Department of Welding Engineering, USA, 1990.

Chapter 6

Weld Pool Oscillation during GTA Welding of Mild Steel

6.1 Introduction

It was shown in Chapter 5 that the oscillation frequency and oscillation amplitude of a stationary GTA weld pool, excited into oscillation by short current pulses, can be measured by monitoring the arc voltage. It appears that the oscillation behaviour of a partially penetrated weld pool differs significantly from that of a fully penetrated weld pool. More specifically, it was found that the oscillation frequency of the partially penetrated weld pool is considerably higher than that of the fully penetrated weld pool, whereas the reverse is the case for the oscillation amplitude. The transition between the two modes of oscillation occurs rather abruptly at a specific degree of penetration (in the present case when the bottom diameter of the weld pool is about 1.2 times the plate thickness). It is expected that these characteristics can be used as a possible tool for in-process control of weld geometry, in particular penetration.

The feasibility of such in-process control is especially important in the case of practical GTA welding using a travelling arc. For this reason it is interesting to find out whether the weld pool in the case of travelling arc welding behaves in a similar way as in the case of stationary arc welding. As during travelling arc welding the arc moves with respect to the workpiece, the welding arc moves away from the geometrical centre of the weld pool towards the front edge of the weld pool, which results in an asymmetrical position of the arc with respect to the weld pool. Thus, it is evident that the oscillation behaviour of the weld pool in the case

of travelling arc welding is considerably more complex than that in the case of stationary arc welding.

This chapter deals with the oscillation behaviour of weld pools in the case of travelling arc welding of mild steel Fe 360. The influence of welding parameters on the oscillation behaviour of partially penetrated weld pools was investigated under various welding conditions. Also the relationship between the weld pool oscillation and the formation of surface ripples on the weld bead was studied. Special attention was given to the different oscillation modes which may occur in travelling weld pools and to the transition from partial penetration to full penetration.

6.2 Experimental procedure

Weld pools were produced by GTA welding in 10 mm thick (partial penetration) and 4 mm thick (partial penetration and full penetration) plates of mild steel Fe 360. The preparation of the test plates is described in section 5.2. The chemical composition of the plate material is given in Table 5.2. Welding was conducted using helium or argon as shielding gas under various welding conditions. During welding, the torch was fixed while the test plate moved with respect to the welding torch. The travel speed could be adjusted continuously from 0 to 50 cm/min.

The weld pool was excited into oscillation by means of short arc current pulses and the oscillation frequency and oscillation amplitude were measured by monitoring the arc voltage variation as described in detail in sections 3.1 and 3.2.

Information about the geometry of the weld pool was obtained after welding from the cross-section of the solidified weld bead (see section 5.2).

6.3 Results and discussion

6.3.1 Oscillation behaviour of partially penetrated weld pools

A large number of experiments was carried out to investigate the oscillation behaviour of partially penetrated weld pools under travelling arc conditions. As in travelling arc welding the arc deviates from the geometrical centre of the weld pool where the oscillation amplitude is maximum, it is to be expected that the detectability of the weld pool oscillation by monitoring the arc voltage variation under travelling arc conditions will become smaller compared with that under stationary arc conditions.

To obtain detectable signals of weld pool oscillation (sufficiently high oscillation amplitude), a higher peak current or a longer peak current duration is therefore required to trigger the weld pool in the case of travelling arc welding than in the case of stationary arc welding. It was found, however, that with increasing peak current duration t_p, the oscillation frequency decreases abruptly at a certain value of t_p, whereas the weld pool geometry remains virtually unchanged, as shown in Fig. 6.1. This large change in oscillation frequency is believed to be caused by a transition in oscillation mode, i.e. the transition from mode 1 to mode 2, as predicted by theory (see Chapter 2) and confirmed experimentally by direct observation (see Chapter 4).

The appearance of mode 2 oscillation in a partially penetrated weld pool will reduce the difference in oscillation frequency when the weld pool transfers from partial penetration to full penetration as discussed in Chapter 2. Thus, mode 2 oscillation should be precluded if the weld pool penetration is to be controlled by monitoring the oscillation frequency of the weld pool. Moreover, mode 2 oscillation in most cases may result in a highly irregular, unacceptable weld bead such as the so-called humping bead.

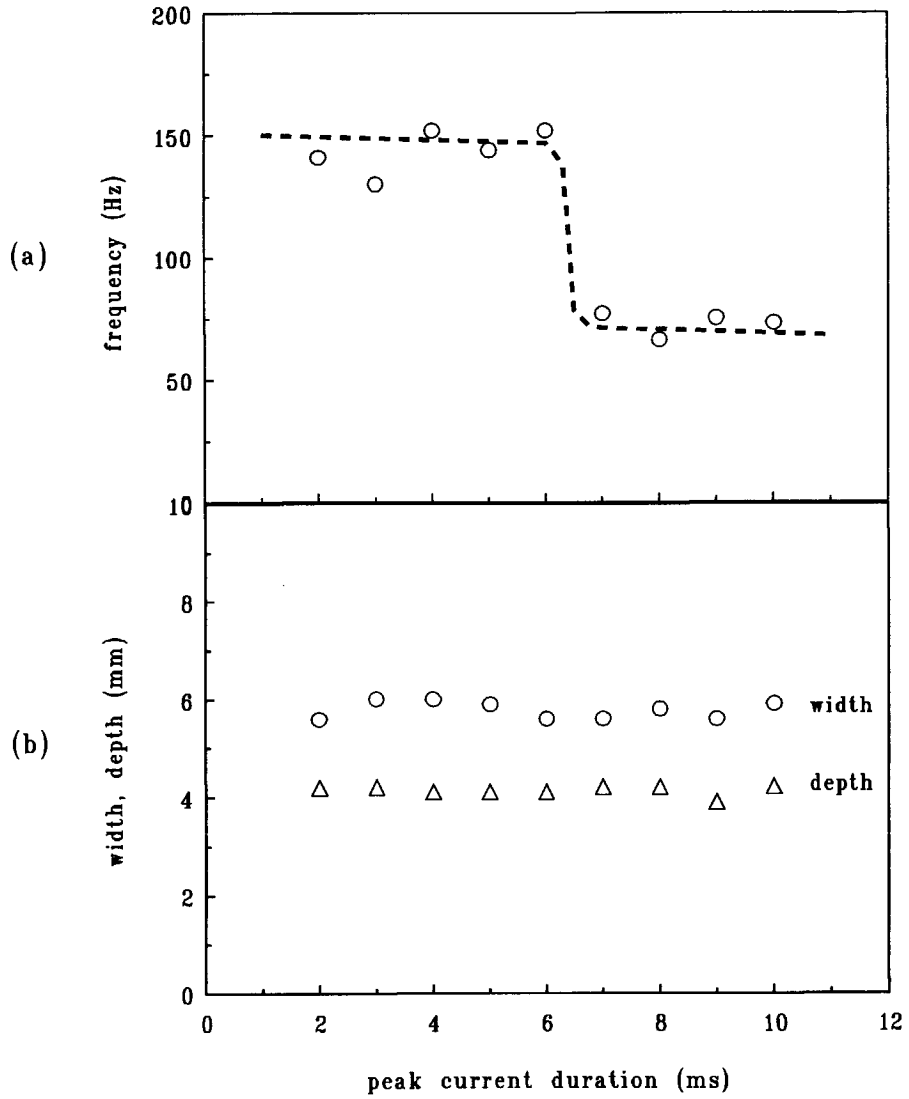

Fig. 6.1 Oscillation frequency and weld pool geometry as a function of peak current duration under travelling arc conditions:
(a) oscillation frequency; (b) weld pool width and depth.

To be able to avoid the occurrence of mode 2 oscillation, it is essential to know under which conditions mode 2 oscillation may occur. It has been shown by means of high-speed filming that the decisive factor, determining the oscillation behaviour of the weld pool, is the pressure pulse duration, i.e. the peak current duration t_p. In fact, it is expected that the oscillation behaviour can be characterised by a critical peak current duration t_{pc} defined as follows: when $t_p < t_{pc}$ the weld pool will oscillate in mode 1, when $t_p > t_{pc}$ mode 2 oscillation will occur.

It was also shown by means of high-speed filming that the occurrence of mode 2 oscillation is the result of front-to-back flow of the liquid metal in the weld pool. Considering the driving force of the front-to-back flow of the liquid metal, it is evident that the value of t_{pc} depends on the peak current and also on other welding parameters. In order to find out under what experimental conditions which of the two oscillation modes is generated by the current pulse, t_{pc} was measured as a function of peak current, travel speed and arc length with helium and argon as shielding gas. This was done by measuring the oscillation frequency as a function of peak current duration. In order to eliminate possible effects of weld pool geometry variations on the oscillation frequency, the heat input was kept as constant as possible throughout the measurements by adapting the level of the effective arc current to the value of the travel speed and keeping the effective arc current constant during each series of measurements.

influence of peak current

Since the weld pools were brought into oscillation by short current pulses, the peak current is a key factor in determining the weld pool oscillation behaviour. To evaluate the influence of peak current on the oscillation behaviour, five series of experiments were performed under the conditions given in Table 6.1. The influence of peak current on t_{pc} is shown in Fig. 6.2. It can be seen in this figure that the critical peak current duration t_{pc} decreases with increasing peak current. This is

understandable, since the higher the peak current the higher the arc pressure acting on the weld pool as explained in the foregoing. The higher peak current results in a higher pressure gradient across the surface of the weld pool, driving the liquid metal to flow more rapidly from the front to the rear of the weld pool. Consequently, the time needed for the weld pool surface to change from the shape depicted in Fig. 4.3a to the shape depicted in Fig. 4.3b is shorter, implying that t_{pc} is shorter.

Table 6.1 Welding conditions used in testing the effect of peak current on critical peak current duration

peak current	250 - 350 A
effective current	127 A
arc length	1.5 mm
travel speed	10 cm/min
shielding gas	helium; 24 l/min

The force generated by the arc acting on the weld pool was measured as a function of arc current by Lin and Eagar [6.1]. Their results are presented in Fig. 6.3 and indicate that the arc force increases with increasing arc current, which is entirely consistent with the observed tendency that the value of t_{pc} decreases with increasing peak current.

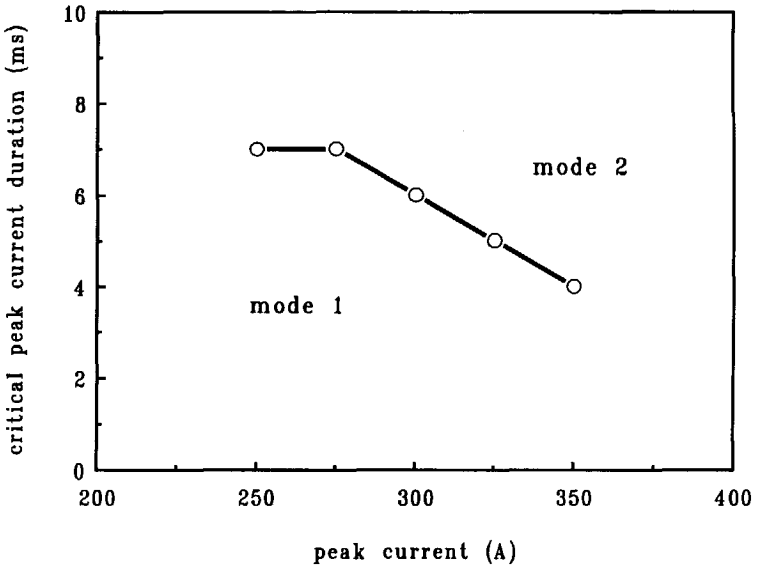

Fig. 6.2 Influence of peak current on critical peak current duration (arc length 1.5 mm, travel speed 10 cm/min and helium as shielding gas).

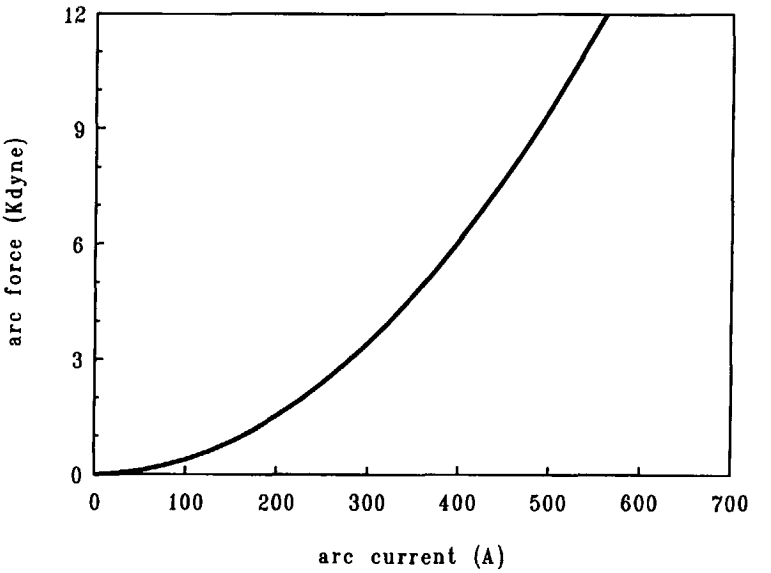

Fig. 6.3 The force generated by the arc acting on the weld pool as a function of arc current [6.1].

influence of travel speed

Travel speed is of great importance in practical welding and is a sensitive factor with respect to the value of the critical peak current duration t_{pc}. To evaluate the influence of travel speed on t_{pc}, five different values of travel speed were applied in a series of experiments under the conditions listed in Table 6.2. To keep the weld pool width unchanged, the effective current was in all cases adjusted to the travel speed. The results of the experiments are presented in Fig. 6.4. The figure shows that the value of t_{pc} decreases with increasing travel speed and that in the case where travel speed is sufficiently low, mode 2 oscillation is precluded, even at relatively long peak current duration.

Table 6.2 Welding conditions used in testing the effect of travel speed on critical peak current duration

peak current	300 A
effective current	89 - 136 A
arc length	1.5 mm
travel speed	5 - 15 cm/min
shielding gas	helium; 24 l/min

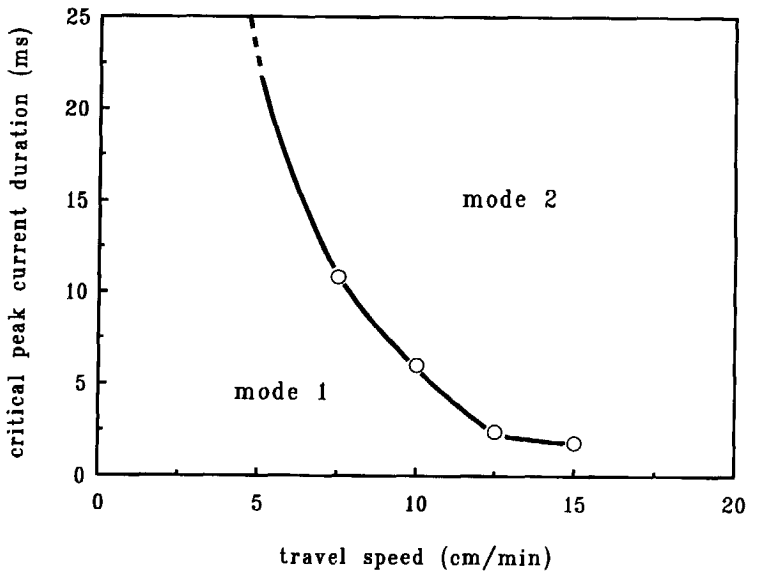

Fig. 6.4 Influence of travel speed on critical peak current duration (peak current 300 A, arc length 1.5 mm and helium as shielding gas).

The influence of travel speed on the value of t_{pc} can be explained by evaluating the effect of travel speed on weld pool geometry, more specifically the position of the arc with respect to the weld pool. Figure 6.5 schematically shows the top view of an elongated weld pool under travelling arc conditions. The weld pool parameters indicated in this figure can be evaluated by Rosenthal's three-dimensional heat flow equation for a point heat source [6.2]:

$$T - T_0 = \frac{Q}{2\pi k_s R} e^{-\frac{v (R - x)}{2\alpha}} \qquad (6.1)$$

in which T is the actual temperature, T_0 the temperature before welding, Q the heat input to the workpiece, R the radial distance from the origin O, x the distance from the origin in the direction opposite to the direction of arc travelling, v the travel speed, k_s the thermal conductivity of the solid material and α the thermal diffusivity of the solid material.

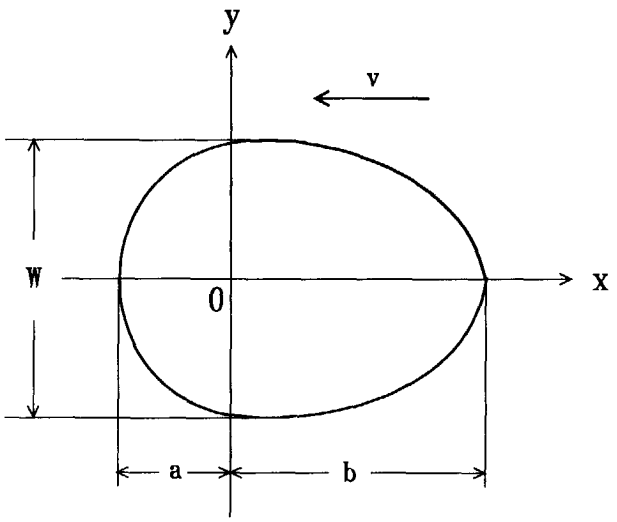

Fig. 6.5 Schematic illustration of weld pool parameters.

For a distributed heat source under travelling arc conditions, Eagar and Tsai [6.3] modified equation (6.1) to:

$$T - T_0 = \int_0^t dt'' \frac{Q}{\pi\rho_s(4\pi\alpha)^{1/2}} \frac{t''^{-1/2}}{2\alpha t'' + \sigma^2} e^{\left(-\frac{w^2 + y^2 + 2wvt'' + v^2t''^2}{4\alpha t'' + 2\sigma^2} - \frac{z^2}{4\alpha t''}\right)} \qquad (6.2)$$

In this equation ρ_s is the density of the solid material, σ the distribution parameter of the heat source and, $w = x - vt$ (with x the distance from the origin in travelling direction), $t'' = t - t'$ (with t' a specific time related to the location of

the moving heat source) and y the distance from the origin in the direction vertical to arc travelling.

The distribution parameter σ was found to be a function of arc current and arc length. It increases with arc current and arc length and ranges from 1.6 mm to 4 mm for an arc length between 2 mm and 9 mm [6.4]. In the present case the arc length was 1.5 mm, and the value of σ was taken to be 1.5 mm.

With the help of equation (6.2) the influence of travel speed on weld pool geometry was determined by substituting T_m (melting temperature of the material) for T into the equation, taking for ρ_s and α the values given in Table 6.3, for σ the value of 1.5 mm and for Q the value required for obtaining a fixed weld pool width of 6.5 mm. The results of the calculation are shown in Fig. 6.6. In this figure the value of (b-a)/2 represents the deviation of the arc from the geometrical centre of the weld pool (see Fig. 6.5). It can be seen from this figure that with increasing travel speed, the weld pool will become increasingly elongated and the arc will deviate further away from the geometrical centre of the weld pool. Consequently, the pressure difference between the two parts of the weld pool, front and rear, becomes higher. This increasing pressure difference promotes the front-to-back flow, leading to mode 2 oscillation. It appears from Fig. 6.4 and Fig. 6.6 that, when (b-a)/2 is smaller than about 0.3 mm, mode 2 oscillation can be prevented.

Table 6.3 Physical properties of mild steel Fe 360 [6.5]

melting temperature T_m (K)	density of solid* ρ_s (kg/m^3)	thermal conductivity* k_s (J/m.s.K)	specific heat* C_s (J/kg.K)	thermal diffusivity* α (m^2/s)
1800	$7.9 \cdot 10^3$	41	662	$7.8 \cdot 10^{-6}$

*) at 500 ^{0}C

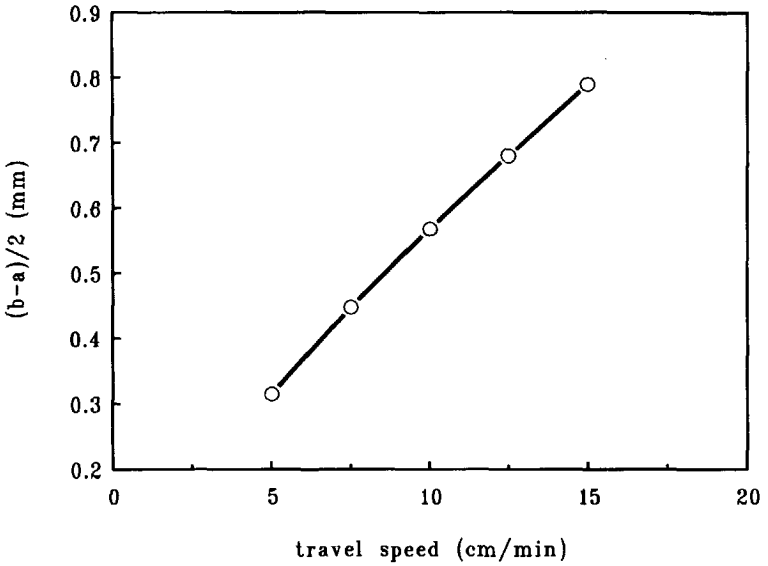

Fig. 6.6 Influence of travel speed on weld pool parameters calculated using equation (6.2) for a weld pool width of 6.5 mm.

Note that the calculation of the weld pool geometry was based on the assumption that the thermal properties of the material are constant and that no melting and solidification occur. When taking the heat of fusion into account, as in the real welding process, the overall position of the weld pool will shift in the direction opposite to that of arc travelling [6.6], since heat is absorbed ahead of the moving heat source to melt the solid metal, while heat is released behind the moving heat source as solidification of the liquid metal takes place. Because of this, the arc position will deviate even more from the geometrical centre.

influence of arc length

It is expected that the distribution of the arc pressure depends on the arc length. To obtain insight into the influence of arc length on the critical peak

current duration t_{pc}, a series of experiments was carried out with five different arc lengths. The other welding parameters used are listed in Table 6.4. The results of these experiments are presented in Fig. 6.7 and show that with increasing arc length, the value of t_{pc} decreases. This is consistent with the results obtained by Savage et al. [6.7] and Yamauchi et al. [6.8] who found that the travel speed limit to avoid the occurrence of humping decreases with increasing arc length.

The influence of arc length on the value of t_{pc} can again be explained in terms of the position of the arc with respect to the weld pool. Figure 6.8 shows the effect of the distribution parameter σ on the arc position. The data plotted in this figure were calculated using equation (6.2) by substituting different values of the distribution parameter, which is proportional to the arc length, for a weld pool width of 6.5 mm. The figure shows that the larger the distribution parameter, the more the arc deviates from the geometrical centre, encouraging the weld pool to oscillate in mode 2. In addition, it was found that with increasing arc length the weld pool becomes slightly wider, resulting in a deeper surface depression [6.9], which also stimulates mode 2 oscillation.

Table 6.4 Welding conditions used in testing the influence of arc length on critical peak current duration

peak current	300 A
base current	109 - 115 A
arc length	1, 1.5, 2, 2.5, 3 mm
travel speed	10 cm/min
shielding gas	helium; 24 l/min

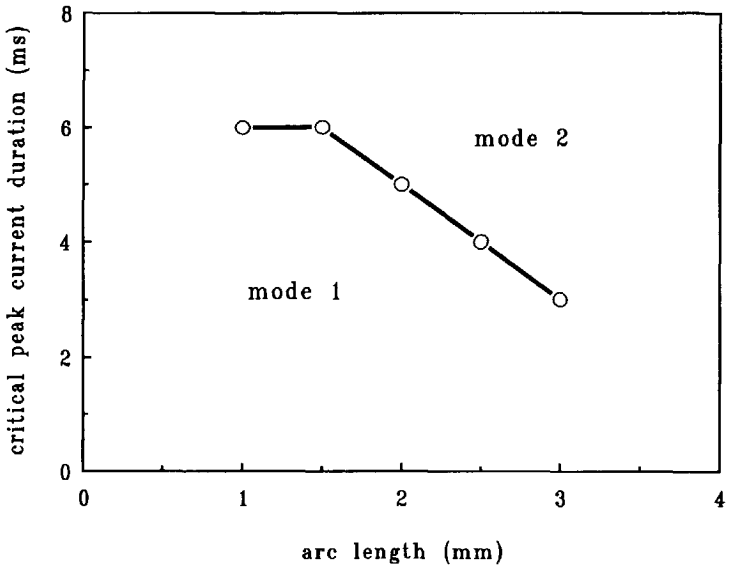

Fig. 6.7 Influence of arc length on critical peak current duration (peak current 300 A, travel speed 10 cm/min and helium as shielding gas).

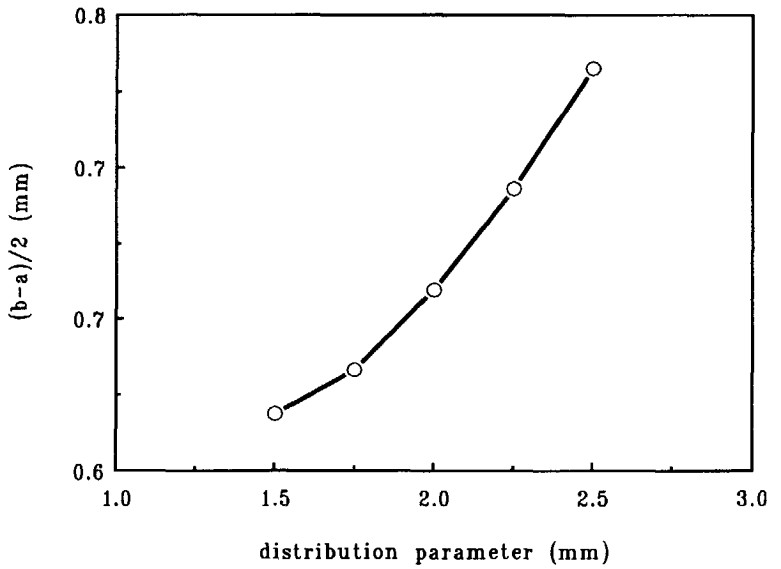

Fig. 6.8 Influence of distribution parameter on weld pool parameters calculated using equation (6.2) for a weld pool width of 6.5 mm.

influence of shielding gas

The most widely used shielding gases in GTA welding are argon and helium. To evaluate the influence of shielding gas on the oscillation behaviour of the weld pool, two series of experiments were carried out with argon and helium as shielding gas respectively, using the welding parameters given in Table 6.5. It was found that the value of t_{pc} in the case of helium shielding is much higher than that in the case of argon shielding as shown in Fig. 6.9. In addition, it was found that the oscillation frequency of mode 1 oscillation in both cases is about the same for a given weld pool width, while in the case of mode 2 oscillation the oscillation frequency in helium shielding is higher than that in argon shielding as can be seen in Fig. 6.10. The observed differences in oscillation behaviour in argon and in helium are believed to be due to the difference in weld pool shape. Specifically the length/width ratio of the weld pool is of importance in this respect.

Table 6.5 Welding conditions used in testing the influence of shielding gas on critical peak current duration

peak current	250 - 350 A
effective current	127 A in helium
	150 A in argon
arc length	1.5 mm
travel speed	10 cm/min
shielding gas	helium; 24 l/min
	argon; 10 l/min

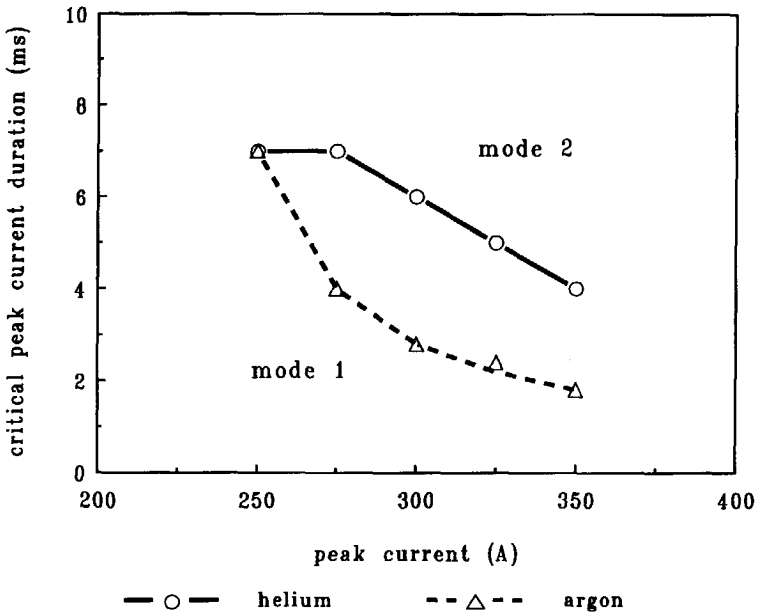

Fig. 6.9 Influence of shielding gas on critical peak current duration (travel speed 10 cm/min, arc length 1.5 mm).

It is possible to evaluate the b/W ratio (see Fig. 6.5) of a weld pool by analysing the surface ripples of the weld bead after welding, since the surface ripples represent the profile of the rear part of the weld pool during welding. Examination of photographs of surface ripples taken of two weld beads obtained in argon and in helium respectively, reveals that the b/W ratio of the weld produced in argon is larger than that obtained in helium, implying that for a given weld pool width, the weld pool in argon is longer than that in helium.

In the case of the symmetrical mode 1 oscillation, the wavelength of the oscillation is mainly determined by the weld pool width. Therefore, the oscillation frequency is scarcely influenced by the increase in weld pool length and no difference in frequency will occur between oscillation in argon and in helium for a given weld pool width (see Fig. 6.10a).

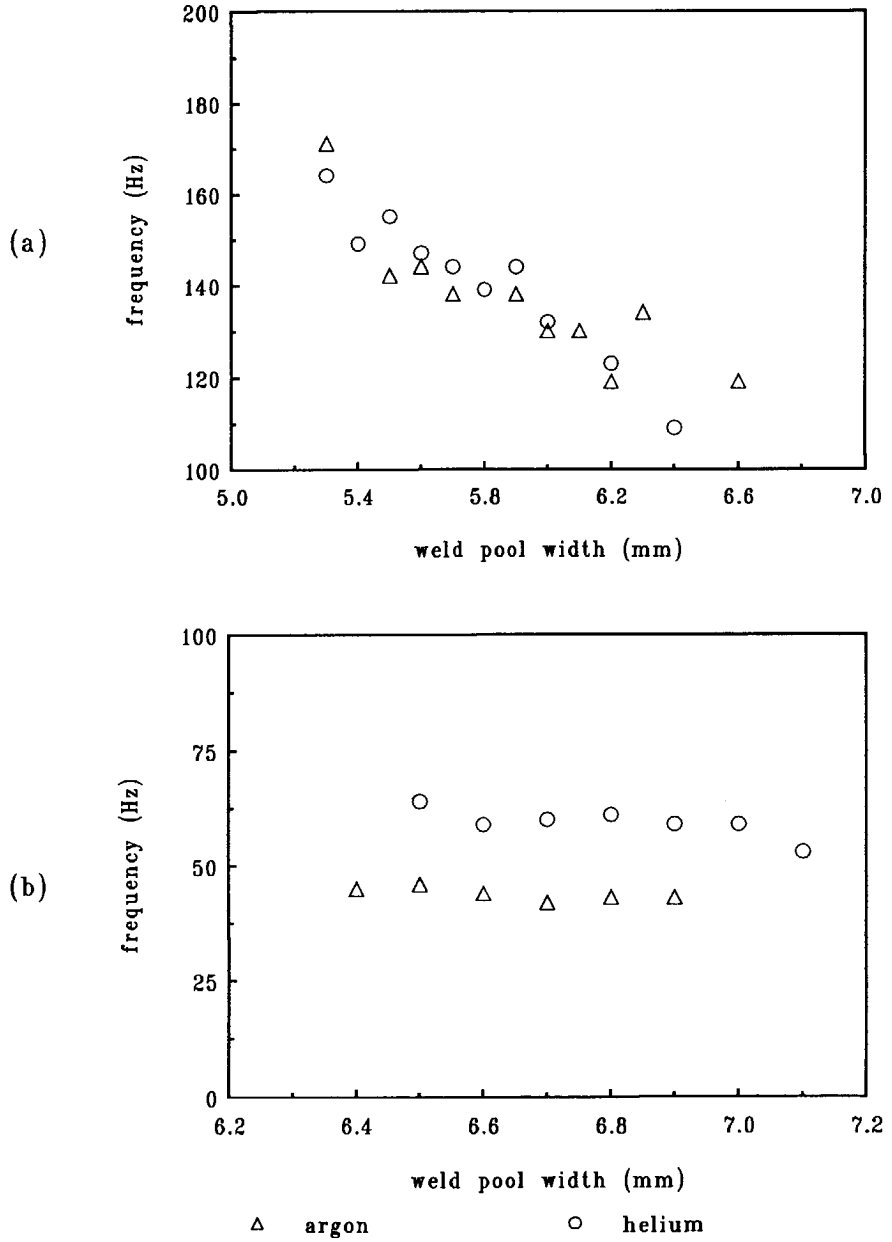

Fig. 6.10 Oscillation frequency as a function of weld pool width under travelling arc conditions:
(a) mode 1 oscillation; (b) mode 2 oscillation.

In the case of mode 2 oscillation, however, the oscillation frequency depends strongly on the length of the weld pool, since this kind of oscillation is in fact a front-to-back motion of the liquid metal and vice versa. As the oscillation frequency decreases with increasing weld pool length, it must be expected that the oscillation frequency in helium is higher than that in argon, which is in accordance with observation (see Fig. 6.10b). The finding that the frequency of mode 2 oscillation decreases with increasing travel speed as shown in Fig. 6.11, again supports this point, since with increasing travel speed the weld pool becomes more elongated and the b/W ratio increase.

On the basis of the results described in the foregoing, it is possible to define the conditions under which mode 1 oscillation and mode 2 oscillation will occur in a weld pool during travelling arc welding. These conditions are in fact given by the experimental data presented in Figs. 6.2, 6.4, 6.7 and 6.9. Generally speaking, it appears that mode 1 oscillation is favoured by the use of short peak current duration, short arc length, low travel speed and helium as shielding gas.

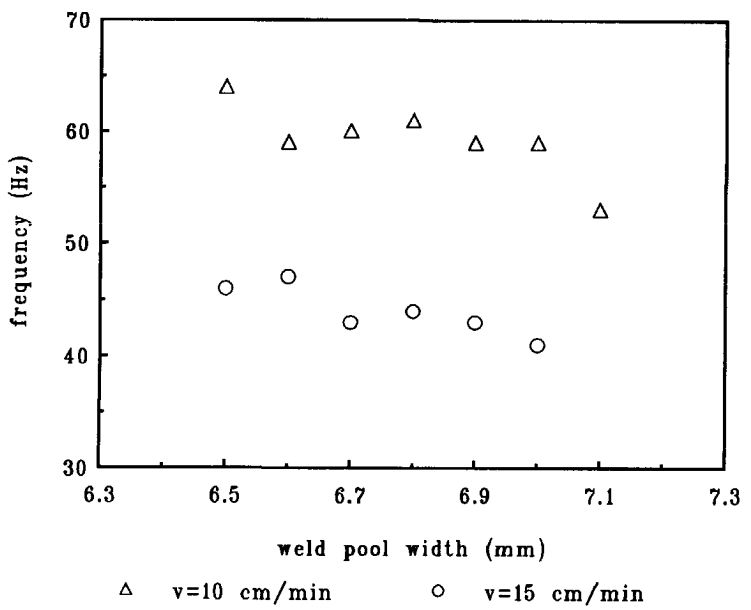

Fig. 6.11 Oscillation frequency of mode 2 oscillation as a function of weld pool width for different travel speeds (peak current 300 A, arc length 1.5 mm and helium as shielding gas).

influence of weld pool geometry on oscillation frequency

In the foregoing it was shown that in the case of partial penetration the weld pool under travelling arc conditions can oscillate in one of two modes (mode 1 and mode 2), depending on the welding conditions. A model of these modes was developed in Chapter 2. According to this model the oscillation frequency of the two oscillation modes can be expressed by the equations:

$$\text{mode 1 :} \qquad f = 5.84\left(\frac{\gamma}{\rho_l}\right)^{1/2} D_1^{-3/2} \tag{6.3}$$

$$\text{mode 2 :} \qquad f = 3.37\left(\frac{\gamma}{\rho_l}\right)^{1/2} D_1^{-3/2} \tag{6.4}$$

with γ the surface tension of the liquid metal, ρ_l the density of the liquid metal and D_1 the diameter of the circle having a surface area equal to the surface area of the elongated weld pool.

To test the validity of equations (6.3) and (6.4) in the case of travelling arc welding, the measured oscillation frequency is plotted as a function of $D_1^{-3/2}$ for the two oscillation modes in Fig. 6.12, taking for D_1 the average weld bead width as measured after welding. The straight lines in the figure represent equations (6.3) and (6.4) respectively, taking for γ and ρ_l the values of 1 N/m and $7 \cdot 10^3$ kg/m^3 (see Table 5.3). It can be seen that the measured points fall into two definite groups, one close to the line representing mode 1 and the other close to the line representing mode 2. Although the experimental points are characterised by considerable scatter, probably due to the difference between the average weld bead width over the entire weld length and the local weld pool width at which the oscillation frequency was measured, the results presented in Fig. 6.12 clearly show that the experimental results are consistent with theory. The fact that the

experimental points lie somewhat below the straight lines predicted by theory, can be understood by realising that in the case of travelling arc welding the weld pool is elongated in the travelling direction so that the equivalent diameter D_1 must in fact be somewhat larger than the average width of the weld pool. It is evident that when the equivalent diameter of the weld pool was used in Fig. 6.12 instead of the average weld bead width, the experimental data would move slightly to the left, i.e. closer to the theoretical lines, especially in the case of mode 2 oscillation.

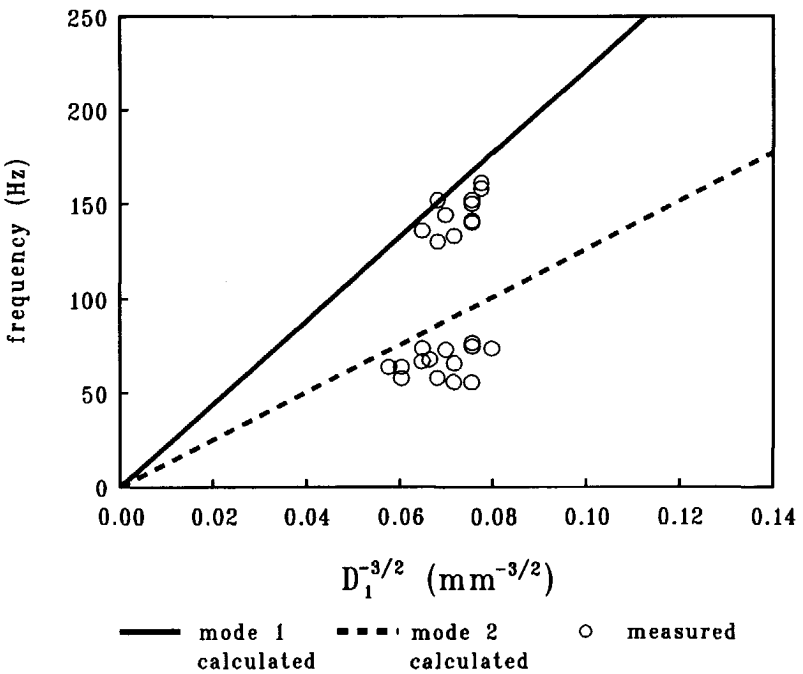

Fig. 6.12 Comparison of measured oscillation frequency with theoretical prediction in the case of partially penetrated weld pools under travelling arc conditions.

Although strictly speaking, equations (6.3) and (6.4) are only valid for a circular weld pool, the results presented in Fig. 6.12 show that these equations can also be used for an approximate description of the situation of the elongated weld pool as occurring during travelling arc welding.

6.3.2 Oscillation behaviour of fully penetrated weld pools

Experiments were also carried out to investigate the oscillation behaviour of fully penetrated weld pools. In these experiments the oscillation frequency was measured under the welding conditions listed in Table 6.6. Some of the results are presented in Fig. 6.13. This figure shows that the oscillation frequency of the fully penetrated weld pool is relatively low (in the present case between 40 and 70 Hz) and decreases slowly with increasing weld pool size.

Table 6.6 Welding conditions used in full penetration experiments

peak current	250, 300 A
peak current duration	2.4 - 4 ms
base current	30 - 70 A
pulse frequency	10, 12.5 Hz
arc length	1.5 mm
travel speed	10 cm/min
shielding gas	helium; 24 l/min

It was shown in Chapter 5 that in the case of stationary gas tungsten arc welding the oscillation behaviour of a fully penetrated weld pool differs significantly from that of a partially penetrated weld pool. In fact, it was found that fully penetrated weld pools oscillate in a mode (mode 3) which is principally different from that of partially penetrated weld pools.

For this mode of oscillation the following equation was derived:

$$\text{mode 3}: \qquad f = 1.08\left(\frac{\gamma}{H\rho_s}\right)^{1/2} D_2^{-1} \tag{6.5}$$

with γ the surface tension of the liquid metal, ρ_s the density of the solid metal, H the plate thickness and D_2 the diameter of the equivalent cylinder having a volume equal to the volume of the fully penetrated weld pool. For a tapered weld pool as examined from the cross-section the value of D_2 in this case can be approached by the relation:

$$D_2^2 = \frac{1}{3}\left(W_t^2 + W_t W_b + W_b^2\right) \tag{6.6}$$

with W_t and W_b the width of the top surface and the bottom surface of the fully penetrated weld pool respectively.

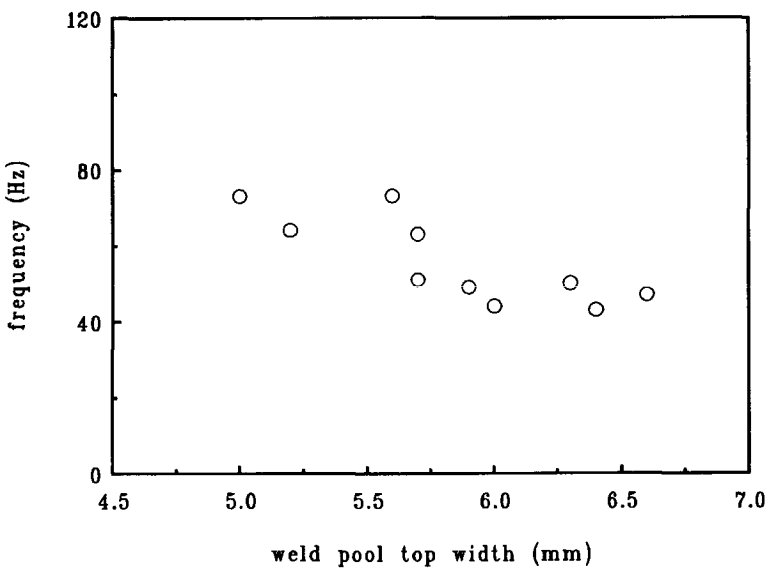

Fig. 6.13 Oscillation frequency of the fully penetrated weld pool under travelling arc conditions as a function of weld pool top width.

It must be noted that equation (6.5) was developed for stationary fully penetrated weld pools. To find out whether this equation is also valid for the case of travelling arc welding, the measured oscillation frequency was plotted as a function of D_2^{-1}. The results are shown in Fig. 6.14. The straight line in this figure represents equation (6.5) taking for γ and ρ_s the values listed in Table 5.3 and for H a value of 4 mm. It can be seen that only for relatively large values of D_2 (large weld pool) reasonable agreement exists between the calculation and the experiment and that the difference between the experimental data and the theoretical prediction increases with decreasing value of D_2. This is not surprising since the smaller the weld pool (the smaller the value of D_2), the more its shape will deviate from a cylinder.

The fact that the measured oscillation frequency is somewhat higher than that calculated is partly due to the fact that the real mass in the weld pool is smaller than the mass calculated since the weld pool is smaller than a tapered cylinder as can be seen in Fig. 6.15, especially when W_b is small. It also suggests that the real mass taking part in the oscillation is smaller than the total mass of the weld pool, due to the tapered weld pool shape.

It is to be expected that the representation of the oscillation behaviour of the fully penetrated weld pool by equation (6.5) will also become less accurate with increasing travel speed, since with increasing travel speed the top surface of the weld pool will shift with respect to the bottom surface of the weld pool and, consequently, the bulk motion of the weld pool will be more and more off the vertical direction.

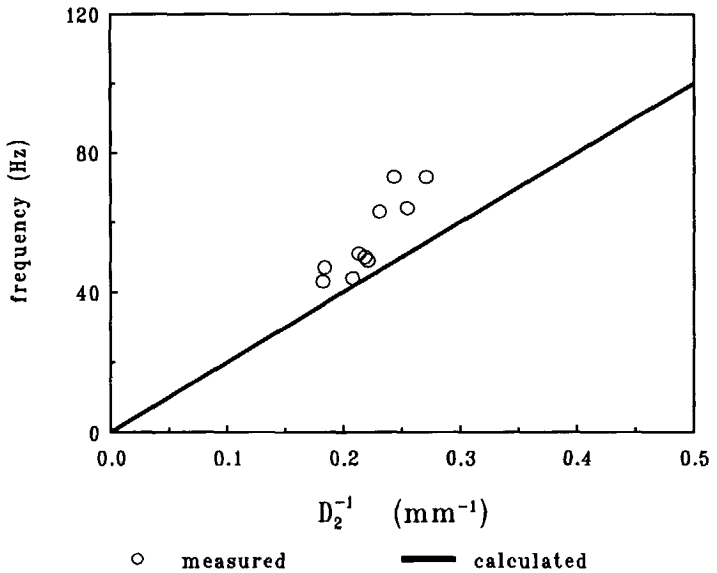

Fig. 6.14 Comparison of measured oscillation frequency with theoretical prediction in the case of fully penetrated weld pools under travelling arc conditions.

6.3.3 Transition from partial penetration to full penetration

On the basis of the results presented above, it may be expected that the transition from partial penetration to full penetration will give rise to an abrupt change in oscillation behaviour. It is believed that this transition can be used for in-process control of weld penetration. Especially, the transition from mode 1 oscillation to mode 3 oscillation is of importance in this respect.

In order to study the transition from partial penetration to full penetration in more detail, welding experiments were carried out in 4 mm thick plates. In these experiments the weld pool size was gradually increased (from partial penetration to full penetration) by increasing the base current in small steps,

leaving the other welding parameters unchanged. To prevent the generation of mode 2 oscillation in the case of partial penetration, the welding parameters were chosen in such a way that only mode 1 type oscillation could occur (see above). The welding conditions used are given in Table 6.7.

Table 6.7 Welding conditions used in the transition experiments

peak current	300 A
peak current duration	2.4 ms
base current	30 - 65 A
pulse frequency	12.5 Hz
arc length	1.5 mm
travel speed	10 cm/min
shielding gas	helium; 24 l/min
backing gas	argon; 5 l/min

It was found that during the growth of the weld pool, the oscillation frequency at first decreases gradually from 336 to 204 Hz in the range of partial penetration, then drops abruptly after reaching a certain degree of penetration and finally decreases slowly again from 100 to 37 Hz in the range of full penetration. These results are consistent with the results obtained earlier and described in the previous two sections. They also agree with the results obtained by Madigan et al. [6.10], who found that the oscillation frequency of partially penetrated weld pools ranges from 400 to 150 Hz and that of fully penetrated weld pools from 188 to 38 Hz.

As an illustration of the results obtained, the weld pool geometry and the corresponding oscillation frequency near the transition are given as a function of base current in Fig. 6.15. The weld pool geometry (weld pool profile) was obtained from the cross-section of the weld beads after welding.

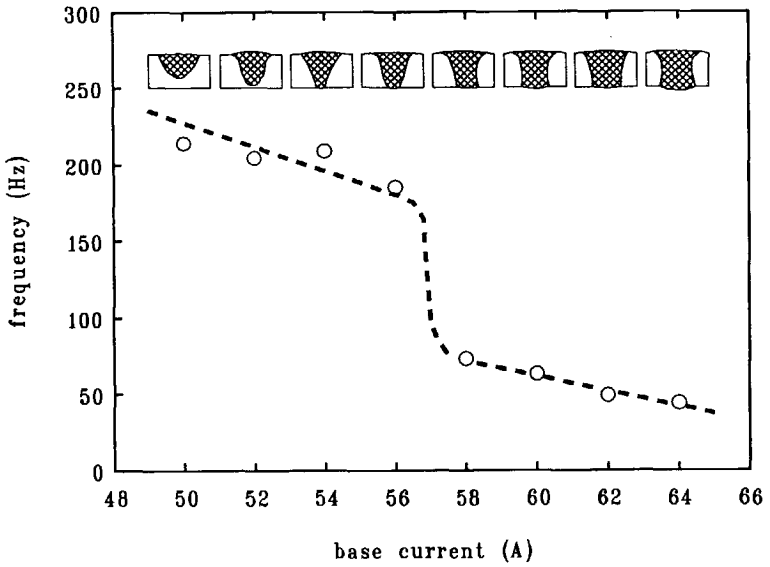

Fig. 6.15 Oscillation frequency and weld pool geometry as a function of base current (peak current 300 A, travel speed 10 cm/min, arc length 1.5 mm and helium as shielding gas).

When considering Fig. 6.15 in more detail, it appears that the drop in oscillation frequency does not exactly coincide with the transition from partial penetration to full penetration. This is illustrated even more clearly in Fig. 6.16, in which the oscillation frequency of the fully penetrated weld pool is plotted as a function of the width W_b of the bottom surface of the weld pool. Figure 6.16 shows that at relatively small value of W_b, the weld pool still oscillates in oscillation mode 1 (high frequency, low amplitude). At a certain value of W_b a transition of oscillation mode occurs (from mode 1 to mode 3). The transition between the two oscillation modes occurs abruptly at W_b ~ 2 mm, which corresponds to a value of 0.5 for the ratio W_b/W_t.

To explain why the transition of oscillation mode occurs at a non-zero value of W_b (~ 2 mm), the motion of the liquid metal in the weld pool should be considered. During the high pressure (peak current) action of the arc on the partially penetrated weld pool, the flow of the liquid weld pool is radially

symmetric with respect to the axis of the arc (see Fig. 6.17a). The flow of the liquid metal in a fully penetrated weld pool with a relatively large W_b is predominantly an axial flow, which can occur since there is no longer any solid material at the bottom to support the weld pool (Fig. 6.17b). In the situation depicted in Fig. 6.17c, the weld pool is fully penetrated but W_b is still very small and the flow of the liquid metal is partly radial, partly axial. In this case the solid bottom of the central part of the weld pool has disappeared and the liquid can move in vertical direction, whereas in the outer part of the weld pool the liquid is still backed by the solid material and is forced to flow sideways. Which kind of flow is dominant in the weld pool depends on the value of W_b. When W_b is very small, the flow in the weld pool is predominantly radial and the weld pool oscillates in mode 1. With increasing W_b, the contribution of the axial flow increases. When W_b has reached a certain value, the axial flow will become dominant and the weld pool oscillation transfers from mode 1 to mode 3.

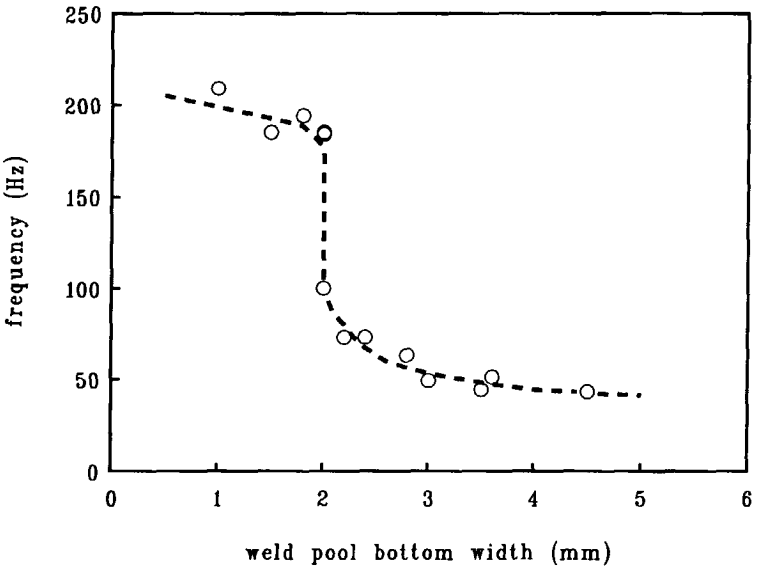

Fig. 6.16 Oscillation frequency of fully penetrated weld pool under travelling arc conditions as a function of the weld pool bottom width.

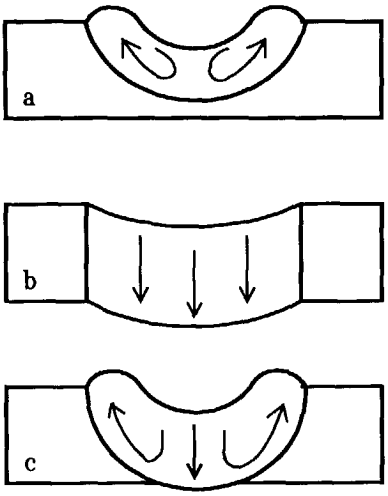

Fig. 6.17 Schematic illustration of liquid motion in weld pools of different geometry.

6.3.4 Relationship between weld pool oscillation and solidification ripples

In a number of studies [6.11 - 6.16] attention was focused on the formation of surface ripples on the weld bead in GTA welding under stationary arc conditions and travelling arc conditions. In case of travelling arc welding a correlation was found to exist between the surface ripples and internal discontinuities such as banding of solute elements, porosity and crystal defects [6.11]. This implies that the surface ripples affect the mechanical and physical properties of the weld to some extent.

Several causes of ripple formation have been proposed. For instance, it was proposed by Cheever and Howden [6.12] that the formation of surface ripples in stationary arc welding is caused by an instability in heat flow. D'Annessa [6.13] concluded that the formation of surface ripples is associated with the fluctuation in growth rate in combination with surface tension effects. According to Garland

and Davies [6.14] the changes in arc characteristics of the cyclic current supply are responsible for the formation of the surface ripples. The most reasonable explanation of surface ripple formation, however, was offered by Kotecki, Cheever and Howden [6.15]. These authors suggested that weld pool oscillation due to the physical force of the arc plasma is the cause of surface ripple formation and this was confirmed by high-speed films which were made to trace the surface movement [6.16].

In order to obtain insight into the relationship between weld pool oscillation and the surface ripples, some experiments were performed under various welding conditions. The principle of the experiments is based on the fact that in travelling arc welding solidification occurs while the weld pool is oscillating. The changes in surface displacement due to oscillation are frozen in and therefore appear as surface ripples. Each oscillation leaves one ripple on the surface of the solidified weld bead. Meanwhile each oscillation also gives one peak in the arc voltage signal and this can be measured by monitoring the arc voltage variation. By comparing the observed surface ripple pattern with the measured arc voltage pattern, it is possible to establish a relationship between ripple formation and weld pool oscillation.

In line with this, experiments were performed with 2 mm thick mild steel plate. To make comparison possible with a non-oscillation reference situation, welding experiments were carried out with and without arc current pulses. The welding conditions used are given in Table 6.8. Under these conditions full penetration occurs, characterised by a relatively low oscillation frequency and resulting in ripples on the surface which can easily be counted. In addition, a relatively high travel speed was applied to obtain a relatively large distance between the ripples, so that individual ripples could be easily distinguished.

Figures 6.18 and 6.19 show the arc current variation and the arc voltage variation collected under pulsed arc current conditions and under constant arc current conditions respectively. Figures 6.20 and 6.21 are the photographs taken of the back side surface of the two corresponding weld beads after welding.

Table 6.8 Welding conditions used in the surface ripple formation experiments

peak current	200 A
peak current duration	4 ms
base current	65 A
pulse frequency	10 Hz
effective current	75 A
arc length	1 mm
travel speed	18.6 cm/min
shielding gas	helium; 30 l/min
backing gas	argon; 5 l/mm

It can be seen from these figures that when pulsed arc current is applied, the arc voltage varies regularly (see Fig. 6.18) and at the same time regular ripples are formed on the weld bead surface (see Fig. 6.20), indicating that weld pool oscillation occurs during welding. The oscillation frequency in arc voltage is measured to be ~ 49 Hz. The average distance between two surface ripples is estimated to be ~ 0.065 mm, corresponding to a ripple formation frequency of ~ 48 Hz.

When constant arc current is applied, there is no indication of oscillation of the weld pool (see Fig. 6.19) and also no regular ripples are present on the weld bead surface (see Fig. 6.21).

Considering the situation in more detail, it appears that an exact correlation exists between the weld pool oscillation and the surface ripples, indicating that the formation of surface ripples is directly due to weld pool oscillation.

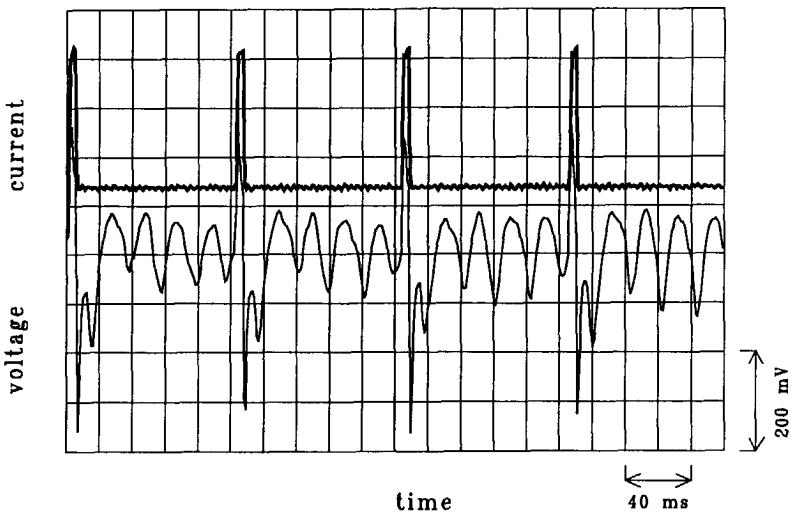

Fig. 6.18 Arc current signal (upper line) and arc voltage signal (lower line) obtained under pulsed current conditions (peak current 200 A, base current 65 A, pulse frequency 10 Hz, peak current duration 4 ms, travel speed 18.6 cm/min, arc length 1 mm, helium as shielding gas and argon as backing gas).

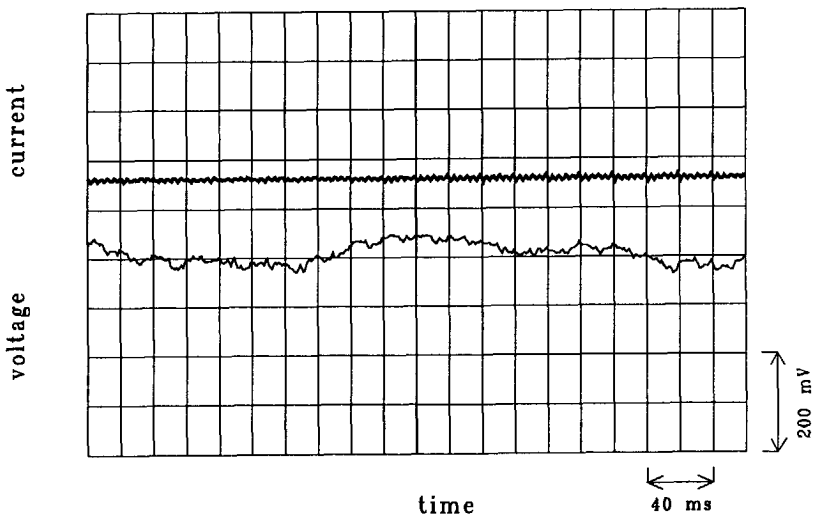

Fig. 6.19 Arc current signal (upper line) and arc voltage signal (lower line) obtained under constant current conditions (arc current 75 A, travel speed 18.6 cm/min, arc length 1 mm, helium as shielding gas and argon as backing gas).

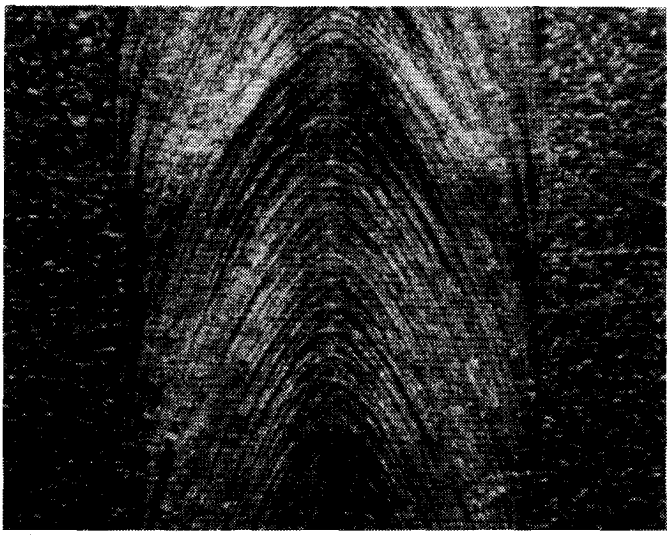

Fig. 6.20 Photograph of the back side surface of the weld bead produced under pulsed arc current conditions (12.5 x).

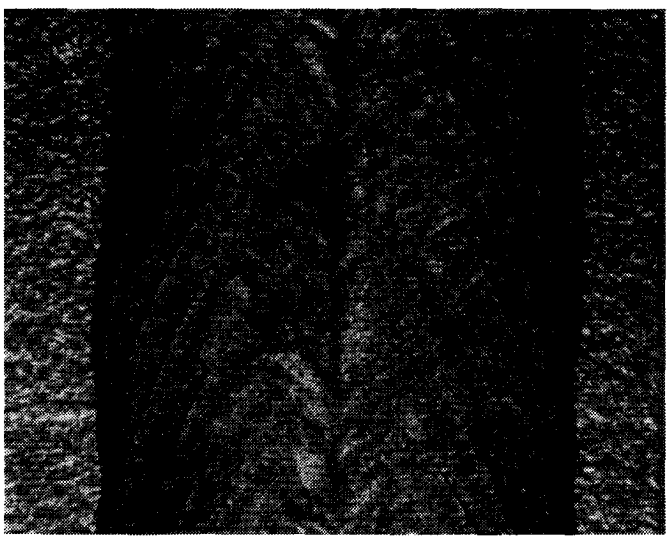

Fig. 6.21 Photograph of the back side surface of the weld bead produced under constant arc current conditions (12.5 x).

6.4 Conclusions

On the basis of the results presented in this chapter, the following conclusions can be drawn.

- During GTA welding under travelling arc conditions the frequency and the amplitude of the weld pool oscillation can be measured by monitoring the arc voltage variation.
- In the case of the partially penetrated weld pool two different oscillation modes can occur, depending on the welding conditions.
- The oscillation of the fully penetrated weld pool is governed by an oscillation mode, which differs significantly from those occurring in the partially penetrated weld pool.
- The observed oscillation behaviour of both the partially penetrated weld pool and the fully penetrated weld pool can be satisfactorily explained in terms of classical hydrodynamics, taking into account the pressure balance on the weld pool surface.
- The abrupt change in oscillation frequency, accompanying the transition from partial penetration to full penetration can be used as a means for in-process control of weld penetration.
- Oscillations in the weld pool are responsible for the formation of ripples on the surface of the weld bead.

References

6.1 M.L. Lin and T.W. Eagar, "Pressures produced by gas tungsten arcs", Metallurgical Transactions, Vol.17B, (1986), p. 601-607.

6.2 D. Rosenthal, "Mathematical theory of heat distribution during welding and cutting", Welding Journal, Vol.20, no.5 (1941), p. 220s-234s.

6.3 T.W. Eagar and N.S. Tsai, "Temperature fields produced by travelling distributed heat sources", Welding Journal, Vol.62, no.12 (1983), p. 346s-355s.

6.4 N.S. Tsai and T.W. Eagar, "Changes of weld pool shape by variations in the distribution of heat source in arc welding", Proceedings of 2nd International Conference on Modeling of Casting and Welding Processes, 31 July - 5 August, 1983, Henniker, New Hampshire, USA, p. 317-328.

6.5 American Society for Metals, Metal Handbook, 9th edition, USA, Vol.1, 1978, p. 145-149.

6.6 M. Ushio, T. Ishimura, F. Matsuda and Y. Arata, "Theoretical calculation on shape of fusion boundary and temperature distribution around moving heat source (Report I)", Transactions of JWRI, Vol.6, no.1 (1977), p. 1-6.

6.7 W.F. Savage, E.F. Nippes and K. Agusa, "Effect of arc force on defect formation in GTA welding", Welding Journal, Vol.58, no.7, (1979), p. 212s-224s.

6.8 N. Yamauchi and T. Taka, "Bead formation in TIG welding", International Institute of Welding Document 212-437-78, p. 1-13.

6.9 M.L. Lin and T.W. Eagar, "Influence of arc pressure on weld pool geometry", Welding Journal, Vol.64, no.6 (1985), p. 163s-169s.

6.10 R.B. Madigan, R.J. Renwick, D.F. Farson and R.W. Richardson, "Computer control of full penetration GTA welds using pool oscillation sensing", Proceedings of 1st Conference on Computer Technology in Welding, The Welding Institute, London, UK, 1986, p. 165-174.

6.11 A.T.D. D'Annessa, "Characteristics redistribution of solute in fusion welding", Welding Journal, Vol.47, no.12 (1968), p. 569s-576s.

6.12 D.L. Cheever and D.G. Howden, "Technical note: natural of weld surface

ripples", Welding Journal, Vol.48, no.4 (1969), p. 179s-180s.

6.13 A.T.D. D'Annessa, "Sources and effects of growth rate fluctuations during weld pool solidification", Welding Journal, Vol.49, no.2 (1970), p. 41s-45s.

6.14 J.G. Garland and G.J. Davies, "Surface rippling and growth perturbations during weld pool solidification", Metal Construction and British Welding Journal, May, 1970, p. 171-175.

6.15 D.J. Kotecki, D.L. Cheever and D.G. Howden, "Mechanism of ripple formation during weld solidification", Welding Journal, Vol.51, no.8 (1972), p. 386s-391s.

6.16 G.M. Ecer, A. Tzavaras, A. Gokhale and H.D. Brody, "Weld pool fluid motion and ripple formation in pulsed current GTAW", Proceedings of Conference on Trends in Welding Research in The United States, New Orleans, Louisiana, USA, 16-18 Nov. 1981, p. 419-442.

Chapter 7

Weld Pool Oscillation during GTA Welding of Austenitic Stainless Steel

7.1 Introduction

In Chapter 6 it was shown that in the case of mild steel Fe 360 under travelling arc conditions, a partially penetrated weld pool can oscillate in two different oscillation modes (mode 1 and mode 2) depending on the welding conditions, whereas a fully penetrated weld pool oscillates in a third oscillation mode (mode 3). Furthermore, it was shown that the transition from partial penetration to full penetration can be detected by monitoring the oscillation behaviour (in particular the transition between mode 1 and mode 3) under controlled welding conditions and that this transition can be used as a possible tool for in-process control of weld pool penetration. This is especially important in the case of welding of austenitic stainless steel, since in that case so-called cast-to-cast variation in weld penetration can occur. The occurrence of this phenomenon is a serious obstacle in GTA welding of austenitic stainless steel, in spite of the use of well controlled welding procedures [7.1-7.7]. Considerable problems may result from this type of behaviour, especially in applications where high standard welds are required, such as in the nuclear and petrochemical industry.

In this chapter the results are presented of an investigation dealing with the oscillation behaviour of both partially penetrated and fully penetrated weld pools during GTA welding of austenitic stainless steel AISI 304, which is one of the most widely used types of stainless steel. Again, special attention is given to the transition from partial penetration to full penetration and also to the possibility

to use the change in oscillation behaviour accompanying the transition, for in-process control of weld penetration.

7.2 Experimental procedure

Weld pools were produced in plates of 10 mm thick (partial penetration) and 4 mm thick (full penetration) austenitic stainless steel AISI 304 using GTA welding under travelling arc conditions. The preparation of the test plates was described in section 5.2. The chemical composition of the plate material is given in Table 5.2. Helium and argon were used as shielding gas, whereas in the case of fully penetrated weld pools argon was used as backing gas to prevent the back side from oxidation and to obtain a smooth back surface. The welding setup, which included two steel hold-down plates, a backing groove and a steel clamping fixture, is shown in Fig. 7.1. The other parts of the experimental equipment were the same as those used in the experiments carried out with mild steel (see Chapter 6). The weld geometry was obtained from the cross-section of the welds after welding.

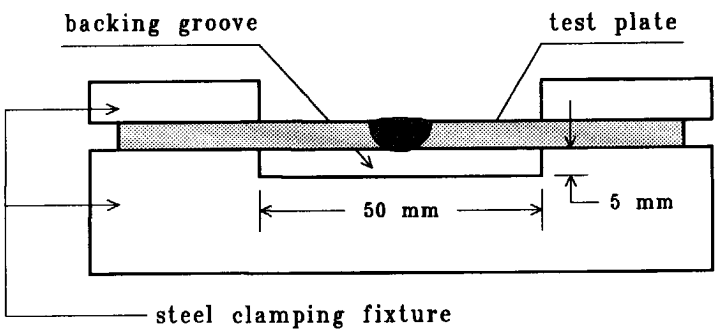

Fig. 7.1 Schematic illustration of test plate clamping unit.

7.3 Results and discussion

7.3.1 Oscillation behaviour of partially penetrated weld pools

As was shown in the previous chapter the oscillation behaviour of a partially penetrated weld pool depends strongly on the welding parameters, such as the magnitude and duration of the peak current, the arc length, the travel speed and the shielding gas. For in-process control of weld pool penetration by monitoring the weld pool oscillation behaviour, it is essential that only mode 1 oscillation occurs in a partially penetrated weld pool. The details about the course of events taking place during the transition from mode 1 to mode 2 were presented in Chapter 5, showing that the decisive factor, which determines the oscillation behaviour of the partially penetrated weld pool, is the pressure pulse duration, i.e. the peak current duration t_p. The oscillation behaviour can be characterized by a critical peak current duration t_{pc} which is defined as follows: when $t_p < t_{pc}$ the weld pool oscillates in mode 1, whereas when $t_p > t_{pc}$ the weld pool oscillates in mode 2. It has been found that, in the case of mild steel Fe 360, the value of t_{pc} depends on the front-to-back flow of the liquid metal in the weld pool. It is evident that the welding conditions play an important role in this front-to-back flow. The value of t_{pc} was found to decrease with increasing peak current, increasing arc length and increasing travel speed. In the case of argon shielding the value of t_{pc} is considerably shorter than that in the case of helium shielding.

To develop a better understanding of the influence of the welding conditions on the value of the critical peak current duration t_{pc} in the case of austenitic stainless steel AISI 304, a large number of experiments was carried out under various welding conditions. To make a comparison possible between the results obtained with austenitic stainless steel and those obtained with mild steel, the effective current was chosen in such a way that the weld pool produced, in all cases, has the same width as that produced in mild steel under otherwise equal welding conditions.

detectability of weld pool oscillation

During the course of the experiments, it was noticed that the amplitude of the arc voltage variation due to the weld pool oscillation in the case of austenitic stainless steel is somewhat lower than that in the case of mild steel and that the oscillation of the weld pool tends to be less detectable by monitoring the arc voltage variation when the arc length is longer than 2.5 mm. It was also found to be difficult to measure the oscillation frequency when argon was used as shielding gas.

The relatively poor detectability of the weld pool oscillation in the case of austenitic stainless steel may be attributed to the shape of the weld pool, which in turn depends on the thermal conductivity and the thermal diffusivity of the material welded. As was dicussed in Chapter 6 the detectability of the weld pool oscillation depends on the position of the arc with respect to the weld pool. The more the arc deviates from the geometrical centre of the weld pool, the smaller the detectability. The thermal conductivity and the thermal diffusivity of austenitic stainless steel are much lower than that of mild steel, as appears from the values listed in Table 7.1. These differences in physical properties will change the weld pool profile and, hence, change the arc position with respect to the weld pool, as will be shown in the following.

To calculate the dimensions of the weld pool, the heat conduction equation of a distributed moving heat source (see Chapter 6) can be used:

$$T - T_0 = \int_0^t dt'' \frac{Q}{\pi \rho_s (4\pi\alpha)^{1/2}} \frac{t''^{-1/2}}{2\alpha t'' + \sigma^2} e^{\left(-\frac{w^2 + y^2 + 2wvt'' + v^2 t''^2}{4\alpha t'' + 2\sigma^2} - \frac{z^2}{4\alpha t''} \right)} \qquad (7.1)$$

in which T, T_0, Q, ρ_s, v, σ and α represent the actual temperature, the temperature before welding, the heat input to the workpiece, the density of the solid material, the travel speed, the distribution parameter of the heat source and the thermal diffusivity of the solid material respectively, $w = x - vt$ (with x the distance from the origin in the arc travelling direction), y the distance from the

origin in the direction vertical to the arc travelling direction and t'' = t - t' (with t' a specific time related to the location of the moving heat source).

Table 7.1 Physical properties of mild steel Fe 360 and austenitic stainless steel AISI 304 [7.8 and 7.9]

material	melting temperature T_m (K)	density of solid* ρ_s (kg/m^3)	thermal conductivity* k_s (J/m.s.K)	specific heat* C_s (J/kg.K)	thermal diffusivity* α (m^2/s)
Fe 360	1800	$7.9 \cdot 10^3$	41.0	662	$7.8 \cdot 10^{-6}$
AISI 304	1673-1723	$8.0 \cdot 10^3$	21.5	500	$5.3 \cdot 10^{-6}$

*) at 500 ^{0}C

By substituting appropriate values of Q, ρ_s, v, σ and α into equation (7.1) and taking T_m for T, the weld pool surface boundary can be calculated. The results of these calculation show that the values of a and b (see Fig. 6.5) depend on the welding parameters and the thermal properties of the material welded. The dependence of the weld pool parameters a and b on the thermal conductivity k_s for a given density ρ_s and specific heat of the solid material C_s (see Table 7.1), weld pool width (6.5 mm) and travel speed (10 cm/min) is shown in Fig. 7.2. It can be seen from this figure that with decreasing thermal conductivity, the value of a decreases, whereas the value of b increases, implying that the lower the thermal conductivity, the longer the trailing part and the shorter the leading part of the weld pool. In other words, the arc moves closer to the front edge of the weld pool and further away from the geometrical centre of the weld pool.

The weld pool top surface profiles of mild steel Fe 360 and austenitic stainless steel AISI 304, calculated using equation (7.1), are shown in Fig. 7.3. It can be seen in this figure that the trailing part of the weld pool is longer but the leading part of the weld pool is shorter in stainless steel than in mild steel, implying that the arc in the case of stainless steel is closer to the front edge of the weld pool and further away from the geometrical centre of the weld pool.

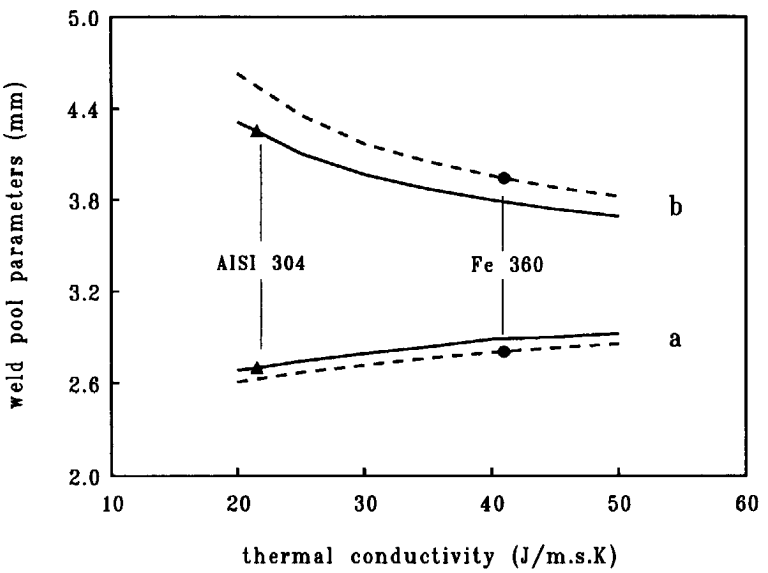

Fig. 7.2 Influence of thermal conductivity on weld pool parameters caculated using equation (7.1) for a weld pool width of 6.5 mm.

As was discussed in Chapter 5, the oscillation amplitude is maximum in the geometrical centre of the weld pool. The more the arc drifts away from the geometrical centre, the lower the oscillation amplitude, as measured by monitoring the arc voltage variation. This is the reason why the weld pool oscillation in the case of austenitic stainless steel is less easily detectable than in the case of mild steel.

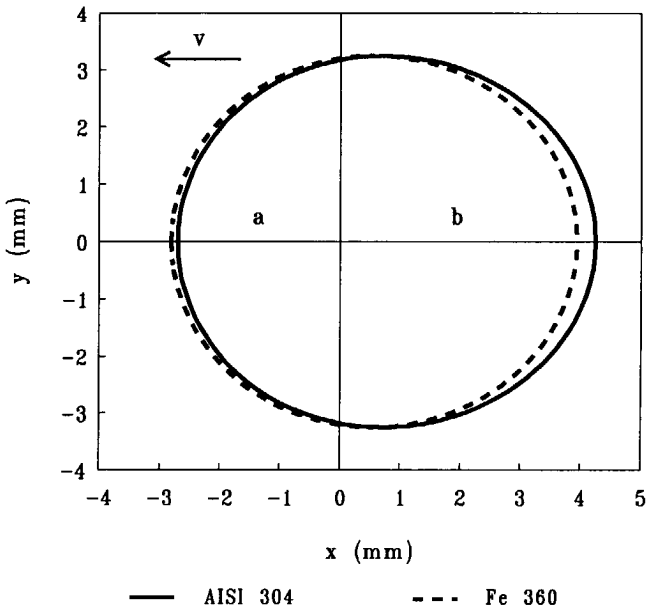

Fig. 7.3 Weld pool surface shape in mild steel Fe 360 and in austenitic stainless steel AISI 304 calculated using equation (7.1) for a travel speed of 10 cm/min and a weld pool width of 6.5 mm.

influence of peak current

As peak current is a dominating factor in affecting the weld pool oscillation behaviour, its influence on the weld pool oscillation behaviour was first investigated. Similarly as in the case of mild steel, five series of experiments were performed under different peak current levels. The welding conditions used are given in Table 7.2.

Table 7.2 Welding conditions used in testing the influence of peak current on critical peak current duration

peak current	250 - 350 A
effective current	100 - 105 A
arc length	1.5 mm
travel speed	10 cm/min
shielding gas	helium; 24 l/min

The results of these experiments together with those of mild steel are shown in Fig. 7.4. It appears that the value of the critical peak current duration t_{pc} in the case of austenitic stainless steel decreases with increasing peak current, which is in accordance with the results obtained in mild steel. However, the values of t_{pc} obtained in the case of austenitic stainless steel are somewhat lower than those obtained in the case of mild steel under the same conditions.

The fact that the values of t_{pc} obtained in the case of austenitic stainless steel are lower than those obtained in the case of mild steel at a given peak current level as depicted in Fig. 7.4, is attributed to the difference in the position of the arc with respect to the weld pool as a result of the difference in weld pool shape, as explained in the foregoing.

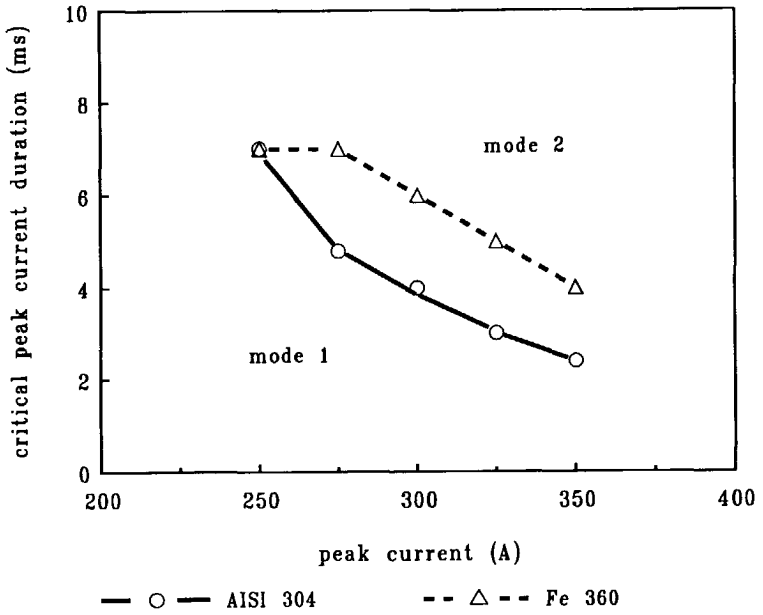

Fig. 7.4 Influence of peak current on critical peak current duration (arc length 1.5 mm, travel speed 10 cm/min and helium as shielding gas).

influence of travel speed

To determine the influence of travel speed on the value of the critical peak current duration t_{pc}, five different values of travel speed were applied in a series of experiments under the conditions listed in Table 7.3. To keep the weld pool width unchanged, the effective current was adjusted to the different travel speeds used. The results of the experiments are presented in Fig. 7.5 together with the results obtained in the case of mild steel. This figure shows that the value of t_{pc} decreases with increasing travel speed and that the difference in the value of t_{pc} for these two materials at a given travel speed is rather small. No mode 2 oscillation occurs at sufficiently low travel speed, even when a relatively long peak

current duration is applied. Further increasing the peak current duration was found to be experimentally impossible, since in that case a very low base current should be applied to keep the effective current unchanged. At a base current lower than 30 A the arc becomes less stable and, hence, the measurement is unreliable.

Table 7.3 Welding conditions used in testing the influence of travel speed on critical peak current duration

peak current	300 A
effective current	80 - 100 A
arc length	1.5 mm
travel speed	5 - 15 cm/min
shielding gas	helium; 24 l/min

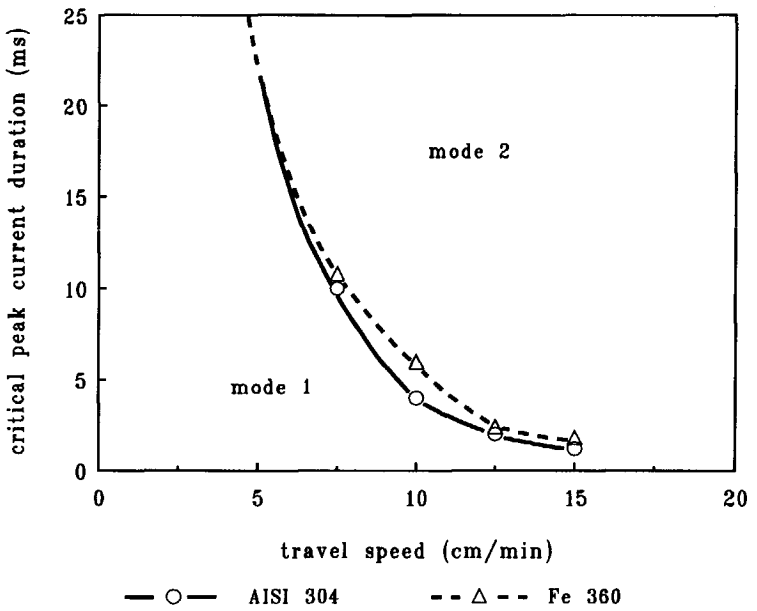

Fig. 7.5 Influence of travel speed on critical peak current duration (peak current 300 A and arc length 1.5 mm and helium as shielding gas).

Figure 7.6 shows the influence of travel speed on the weld pool parameters of the two materials calculated using equation (7.1) for a given weld pool width (6.5 mm). It appears that at a given travel speed, the position of the arc deviates more from the geometrical centre of the weld pool in the case of austenitic stainless steel than in the case of mild steel. Under low travel speed conditions, the deviation of the position of the arc from the geometrical centre is so small that mode 2 oscillation can not occur, neither in the case of austenitic stainless steel nor in the case of mild steel. With increasing travel speed, the probability of mode 2 oscillation increases until mode 1 oscillation is precluded. In the case of austenitic stainless steel the transition to mode 2 oscillation occurs at a lower value of the travel speed than in the case of mild steel. This is due to the more pronounced asymmetry of the weld pool in the case of austenitic stainless steel.

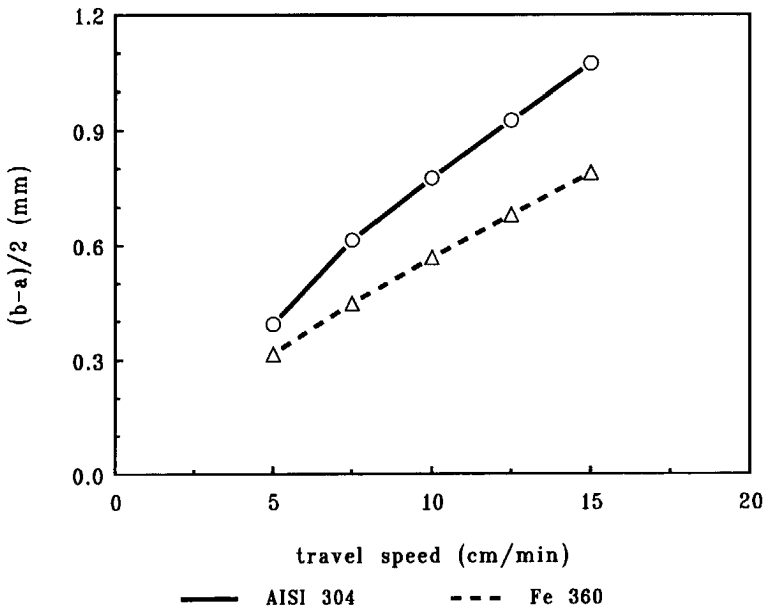

Fig. 7.6 Influence of travel speed on weld pool parameters calculated using equation (7.1) for a weld pool width of 6.5 mm.

influence of arc length

To explore the influence of arc length on the value of the critical peak current duration t_{pc}, a series of experiments was carried out with different arc lengths. The welding parameters used are listed in Table 7.4. The results of the experiments are presented in Fig. 7.7 and show that with increasing arc length the value of t_{pc} decreases. It can be seen in this figure that the results obtained for austenitic stainless steel are similar to those obtained in mild steel. However, the line representing austenitic stainless steel is shifted downwards with respect to the line representing mild steel. This shift is not difficult to understand by taking into account the effect of arc length on the arc position with respect to the weld pool for these two materials as illustrated in Fig. 7.8.

Table 7.4 Welding conditions used in testing the influence of arc length on the critical peak current duration

peak current	300 A
effective current	100 A
arc length	1, 1.5, 2, 2.5 mm
travel speed	10 cm/min
shielding gas	helium; 24 l/min

Summarising the influence of the welding parameters on the oscillation behaviour as discussed in the foregoing, it can be concluded that the value of the critical peak current duration t_{pc} obtained in austenitic stainless steel AISI 304 is lower than that obtained under identical circumstances in mild steel Fe 360. Furthermore, it appears that to maintain mode 1 oscillation in a partially penetrated weld pool it is necessary to use short peak current duration, short arc length, low travel speed and helium as shielding gas. This is consistent with the results obtained in mild steel.

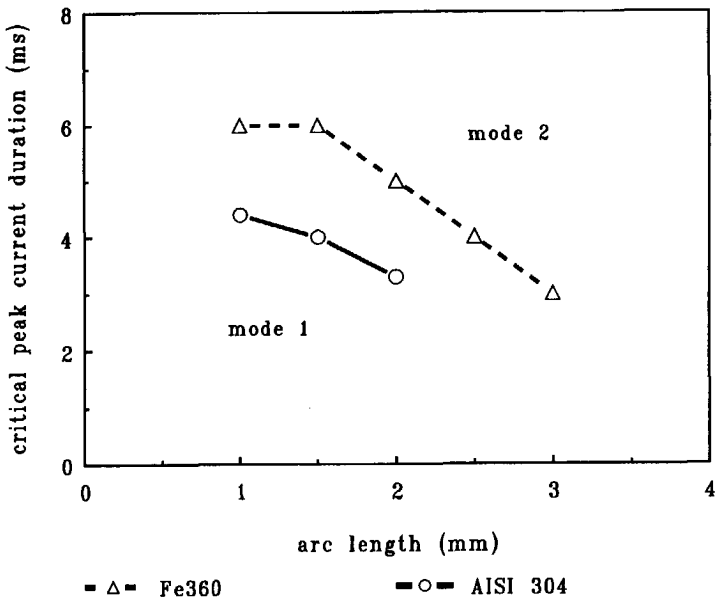

Fig. 7.7 Influence of arc length on critical peak current duration (peak current 300 A and travel speed 10 cm/min and helium as shielding gas).

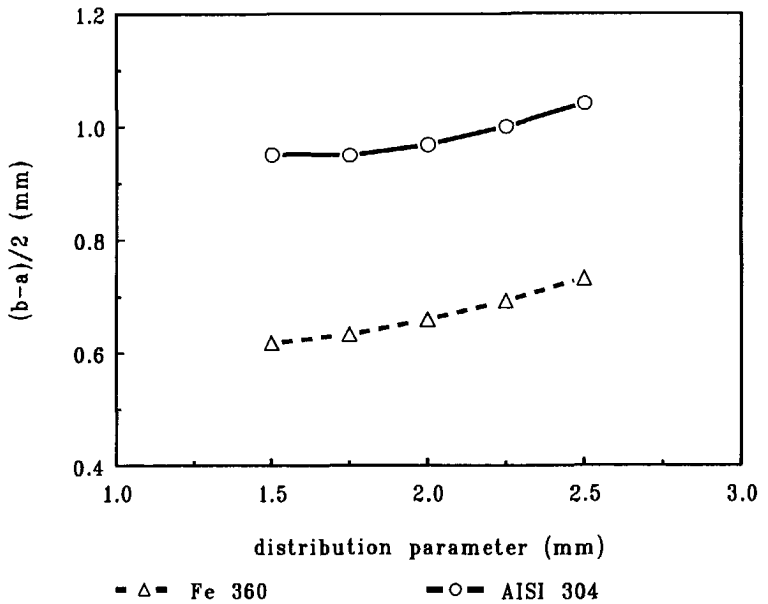

Fig. 7.8 Influence of distribution parameter (proportional to arc length) on weld pool parameters calculated using equation (7.1) for a weld pool width of 6.5 mm.

influence of weld pool geometry on oscillation frequency

It may be expected that, as in the case of mild steel (see previous chapter), also in the case of austenitic stainless steel a relation exists between the weld pool geometry and the oscillation frequency. In order to determine this relationship for mode 1 oscillation as well as for mode 2 oscillation, experiments were carried out under different welding conditions (see Table 7.5). The results of these experiments are given in Fig. 7.9 and in Fig. 7.10 for mode 1 oscillation and for mode 2 oscillation respectively. It appears that in the case of mode 1 oscillation the oscillation frequency lies in the range between 110 and 160 Hz and decreases with increasing weld pool width, whereas in the case of mode 2 oscillation, the oscillation frequency is much lower (between 45 and 60 Hz) and also decreases, albeit very slowly, with increasing weld pool width. These findings are in excellent agreement with those obtained in the case of mild steel (see Chapter 6).

Table 7.5 Welding conditions used in testing the influence of weld pool geometry on oscillation frequency

peak current	250, 300 A
peak current duration	2.4 - 10 ms
base current	80 - 100 A
pulse frequency	5 - 12.5 Hz
arc length	1.5 mm
travel speed	10 cm/min
shielding gas	helium; 24 l/min

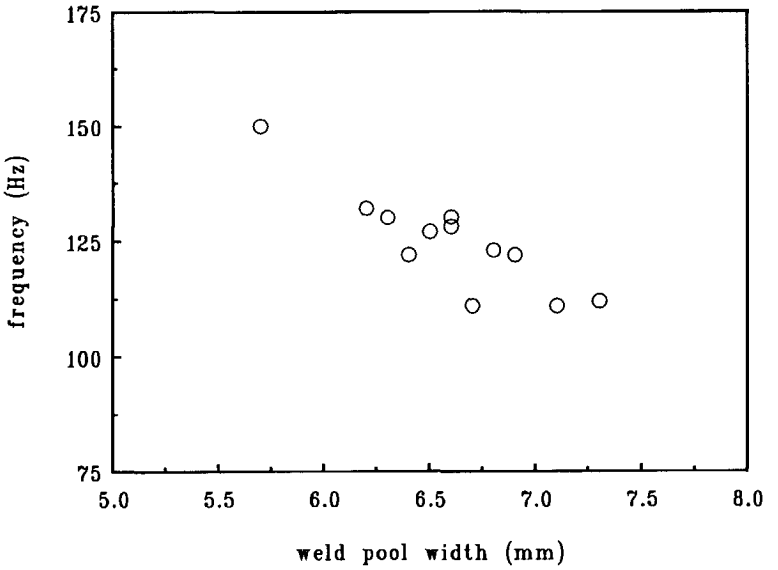

Fig. 7.9 Oscillation frequency of mode 1 oscillation as a function of weld pool width under travelling arc conditions.

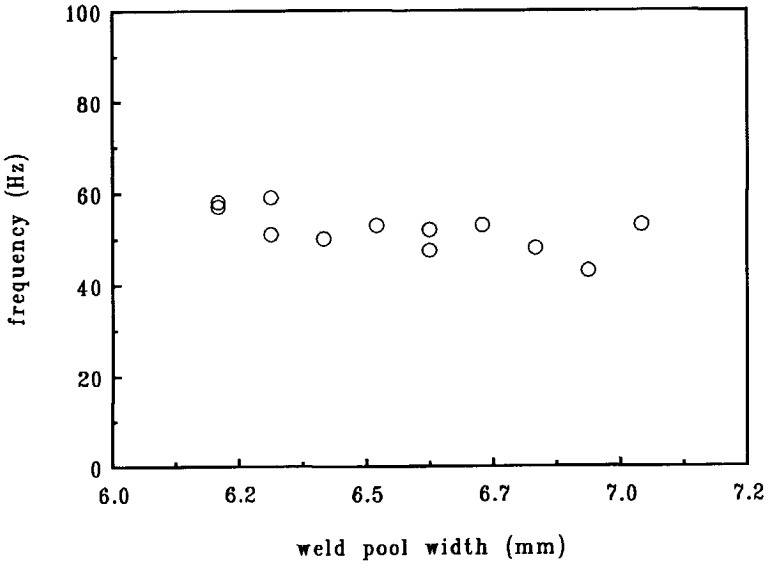

Fig. 7.10 Oscillation frequency of mode 2 oscillation as a function of weld pool width under travelling arc conditions.

It was shown in Chapter 2 that the oscillation frequency of the two oscillation modes which can occur in the partially penetrated weld pool, can be expressed by the following equations:

$$\text{mode 1 :} \qquad f = 5.84\left(\frac{\gamma}{\rho_l}\right)^{1/2} D_1^{-3/2} \tag{7.2}$$

$$\text{mode 2 :} \qquad f = 3.37\left(\frac{\gamma}{\rho_l}\right)^{1/2} D_1^{-3/2} \tag{7.3}$$

with D_1 the diameter of the equivalent circle having a surface area equal to the surface area of the elongated weld pool, γ the surface tension of the liquid metal and ρ_l the density of the liquid metal. As an approximation D_1 can be taken as the weld pool width in the case of travelling arc welding.

To test the validity of equations (7.2) and (7.3) in the case of austenitic stainless steel AISI 304, the measured oscillation frequency is plotted as a function of $D_1^{-3/2}$ for the two oscillation modes in Fig. 7.11, taking for D_1 the average weld bead width as measured after welding. The straight lines in the figure represent equations (7.2) and (7.3) respectively. It can be seen that the measured points fall into two definite groups, one group close to the line representing mode 1 and the other group close to the line representing mode 2. The difference in oscillation frequency between the theoretical prediction and the experimental measurements in this case is somewhat larger than that observed in the case of mild steel. This can be explained by the fact that the weld pool in the case of austenitic stainless steel is more elongated than that in the case of mild steel, resulting in a larger difference between the weld pool width and D_1. Taking this effect into account, it can be concluded that the experimental results are consistent with theory.

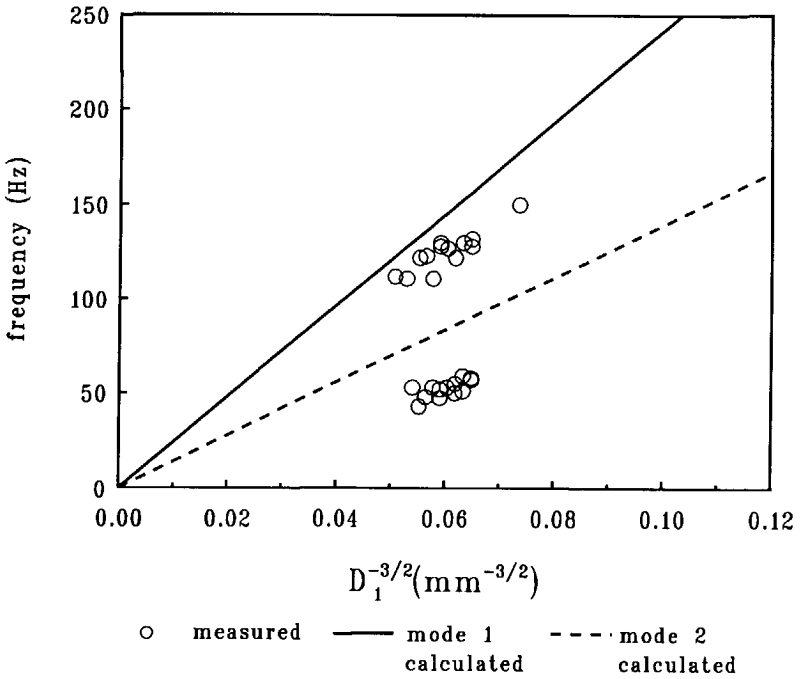

Fig. 7.11 Comparison of measured oscillation frequency with theoretical prediction in the case of partial penetration under travelling arc conditions.

7.3.2 Oscillation behaviour of fully penetrated weld pools

It was shown in the previous chapter that the oscillation behaviour of fully penetrated weld pools in mild steel under travelling arc conditions is similar to that under stationary arc conditions. In fact, it was found that fully penetrated weld pools oscillate in a mode (mode 3) which is considerably different from that of a partially penetrated weld pool. It was also found that a relation exists between the weld pool size and the oscillation frequency. In order to determine the relationship between the weld pool size and the oscillation frequency for austenitic stainless steel, a number of experiments was carried out with 4 mm thick plates

under the conditions listed in Table 7.6. The experimental results are given in Fig. 7.12. In this figure the oscillation frequency is plotted as a function of the weld pool top width. The figure shows that the fully penetrated weld pool oscillates at relatively low frequency, which slowly decreases with increasing weld pool size.

Table 7.6 Welding conditions used in full penetration experiments

peak current	250, 300 A
peak current duration	2.4 - 4 ms
base current	30 - 60 A
pulse frequency	10, 12.5 Hz
arc length	1.5 mm
travel speed	10 cm/min
shielding gas	helium; 24 l/min
backing gas	argon; 5 l/min

The frequency f of the full penetration oscillation mode (mode 3) is given by the equation (see Chapter 6):

$$f = 1.08\left(\frac{\gamma}{H\rho_s}\right)^{1/2} D_2^{-1} \qquad (7.4)$$

with γ the surface tension of the liquid metal, ρ_s the density of the solid metal, H the plate thickness and D_2 the diameter of the equivalent cylinder having a volume equal to the volume of the fully penetrated weld pool. As the same as in the case of mild steel, the value of D_2 can be approached by the relation:

$$D_2^2 = \frac{1}{3}\left(W_t^2 + W_t W_b + W_b^2\right) \qquad (7.5)$$

where W_t and W_b are the top width and the bottom width of the weld pool respectively.

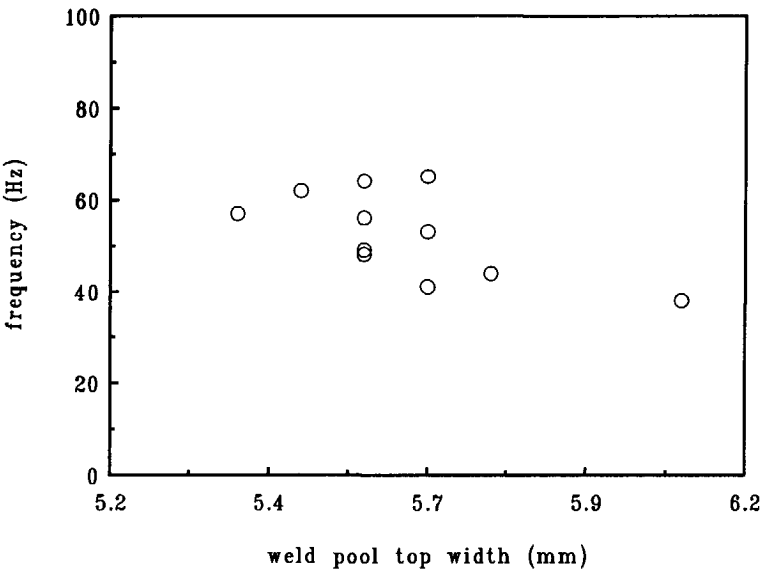

Fig. 7.12 Oscillation frequency of fully penetrated weld pool under travelling arc conditions as a function of weld pool top width.

By substituting for γ, ρ_s and H the values 1.2 N/m, $7.8 \cdot 10^3$ kg/m^3 (see Table 5.3) and 4 mm respectively, the following simple equation can be obtained for the oscillation frequency of the fully penetrated weld pool:

$$f = 0.21\ D_2^{-1} \qquad (7.6)$$

Although equations (7.4) and (7.6) were developed for fully penetrated weld pools under stationary arc conditions, it was found that they are also approximately valid for travelling weld pools in the case of mild steel. To find out whether these equations are also valid in the case of travelling weld pools in austenitic stainless steel, the measured oscillation frequency was plotted as a function of D_2^{-1}. The results are shown in Fig. 7.13. The straight line in this figure represents equation (7.6). It can be seen in this figure that, although some scatter appears in the measured data, reasonable agreement exists between the calculated results and the experimental data.

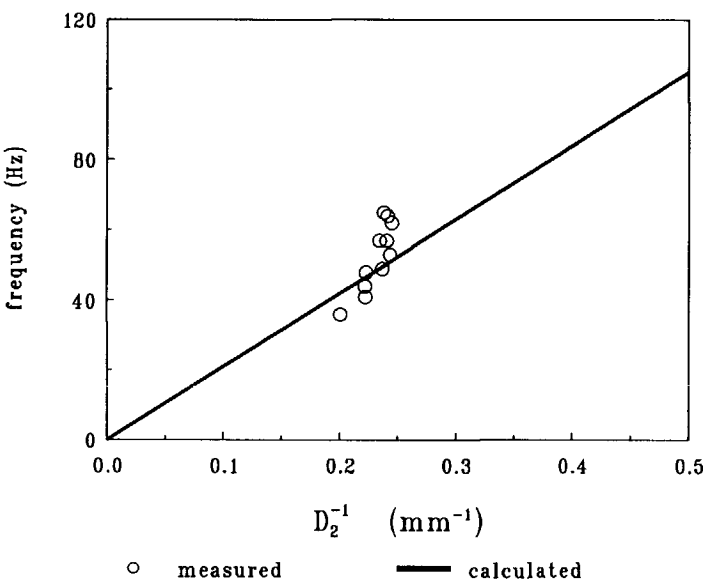

Fig. 7.13 Comparison of measured oscillation frequency with theoretical prediction for fully penetrated weld pools under travelling arc conditions.

Unlike in the case of mild steel, where the measured points lie above the calculated line, in this case some points lie below the line in the range where the value of D_2 is relatively large. The shift of the measured points towards a lower level in austenitic stainless steel compared with that of mild steel, can again be explained by the difference in weld pool geometry, the weld pool being more elongated in the case of austenitic stainless steel (see Fig. 7.3). If the real equivalent diameter of the weld pool would be used in stead of the weld pool width, the results for these two materials would be more in line with each other.

The results presented in Fig. 7.13 clearly show that the oscillation model of the stretched membrane is also valid for fully penetrated weld pools in austenitic stainless steel under travelling arc conditions, at least under the present welding circumstances.

7.3.3 Transition from partial penetration to full penetration

Control of weld penetration by means of monitoring the oscillation behaviour of the weld pool is of particular importance for one-pass GTA welding of thin plate and root-pass GTA welding of thick plate of austenitic stainless steel. For this reason, special attention was given to the transition from partial penetration to full penetration.

To study the transition from partial penetration to full penetration in more detail, a series of welding experiments was carried out in 4 mm thick plate using the welding conditions under which the generation of mode 2 oscillation in a partially penetrated weld pool can be precluded. To gain insight into the details of the transition from partial penetration to full penetration, the size of the weld pool was increased gradually by increasing the base current in small steps. The welding conditions used in these experiments are listed in Table 7.7.

Table 7.7 Welding conditions used in the transition experiments

peak current	300 A
peak current duration	2.4 ms
base current	30 - 50 A
pulse frequency	12.5 Hz
arc length	1.5 mm
travel speed	10 cm/min
shielding gas	helium; 24 l/min
backing gas	argon; 5 l/min

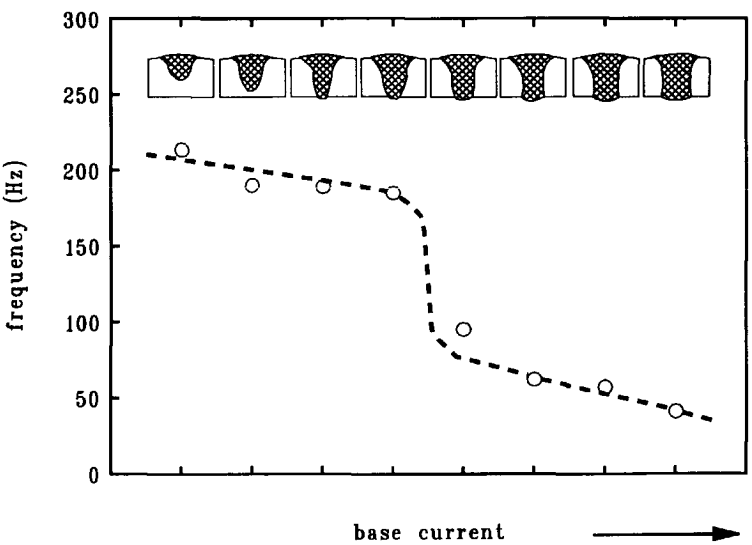

Fig. 7.14 Oscillation frequency and weld pool geometry as a function of base current.

It was found that simultaneously with the growth of the weld pool the oscillation frequency decreases gradually from 277 to 180 Hz at first. At a certain degree of penetration the oscillation frequency drops abruptly, after which it decreases again slowly from 95 to 36 Hz. These findings are entirely consistent with those obtained in the case of mild steel. Some of the results of these experiments are shown in Fig. 7.14. In this figure the weld pool geometry and corresponding oscillation frequency near the transition are given as a function of base current.

As in the case of mild steel, the fast drop in oscillation frequency observed does not exactly coincide with the transition from partial penetration to full penetration. This is more clearly shown in Fig. 7.15, in which the oscillation frequency is plotted as a function of the weld pool bottom width W_b of the fully penetrated weld pool. The results presented in Fig. 7.15 indicate that when W_b is small, the weld pool oscillates still in mode 1. At a certain value of W_b (W_b ~ 2.2 mm), the oscillation of the weld pool transfers to mode 3. This transition is accompanied by a large change in oscillation frequency and oscillatin amplitude. The observed delay in transition between mode 1 and mode 3 is due to the fact that at small value of W_b (~ 2.2) mm the weld pool is still partly supported by the solid material, which hampers the vertical movement of the liquid metal required for mode 3 oscillation (see section 6.3.3).

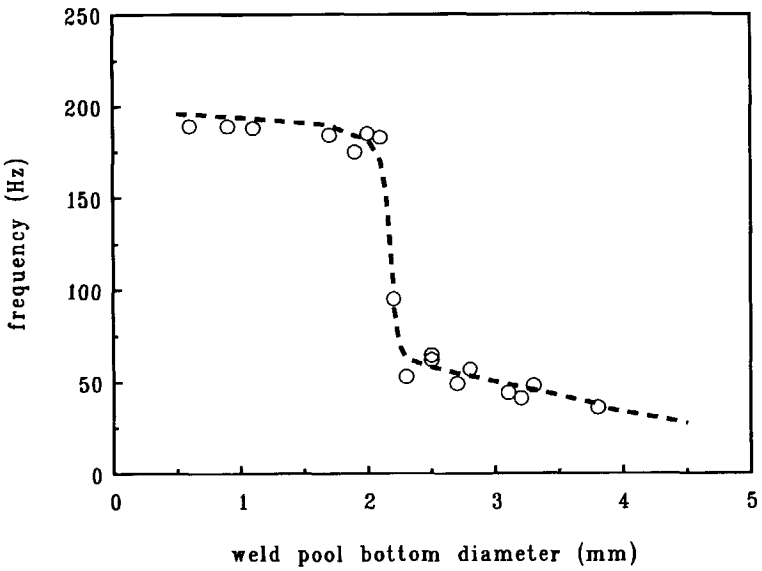

Fig. 7.15 Oscillation frequency of fully penetrated weld pool as a function of the weld pool bottom width.

7.4 Conclusions

Based on the experimental results presented above, the following conclusions can be drawn.

- During travelling GTA welding of austenitic stainless steel AISI 304, it is possible to detect the oscillation frequency of the weld pool by monitoring the arc voltage variation.
- The amplitude in arc voltage variation due to weld pool oscillations in austenitic stainless steel is somewhat lower than that in mild steel under the same welding conditions.
- Oscillation of the partially penetrated weld pool in austenitic stainless steel under travelling arc conditions is dominated by one of two different oscillation modes. The transition between the two modes is characterised by a critical peak current duration t_{pc} which is dependent on the welding conditions.
- The values of t_{pc} in the case of austenitic stainless steel are lower than those obtained in the case of mild steel under the same welding conditions.
- The oscillation of the fully penetrated weld pool is governed by an oscillation mode, which differs significantly from those occurring in the partially penetrated weld pool.
- The observed oscillation behaviour of both the partially penetrated weld pool and the fully penetrated weld pool can be satisfactorily explained in terms of classical hydrodynamics, taking into account the pressure balance on the weld pool surface.
- The transition from partial penetration to full penetration can be detected by monitoring the arc variation under controlled welding conditions.

References

7.1 C.R. Heiple and J.R. Roper, "Mechanism for minor element effect on GTA fusion zone geometry", Welding Journal, Vol.61, no.4 (1982), p. 97s-102s.

7.2 J. Leinonen and L.P. Karjalainen, "The effect of composition and inclusion on penetration in TIG-welding of austenitic stainless steel", Proceedings of International Conference on The Effect of Residual, Impurities, and Microalloying Elements on Weldability and Weld Properties, 5-17 Nov. 1983, London, UK, paper 4.

7.3 J. Leinonen, "Cast-to-cast-variations in GTA weld penetration of austenitic stainless steel", Proceedings of JDC University Research Symposium 1985 International Welding Congress, Toronto, Ontario, Canada, 15-17 Oct.1985, p. 165-169.

7.4 J.L. Robinson and T.G. Gooch, "Effect of composition and physical properties on GTA weld penetration of austenitic stainless and low alloy steels", Proceedings of 2nd International Conference on Trends in Welding Research, Gatlinburg, Tennessee, USA, 14-18 May 1989, p. 403-409.

7.5 H.D. Steffens, H. Thier, R. Killing, E.R. Sievers and Z. Li, "Effect of iron minor elements on the fusion geometry in fully mechanized tungsten gas arc welding of austenitic steels", Welding and Cutting, No.7, 1990, p. E109-E111.

7.6 K.C. Mills and B.J. Keene, "Factors affecting variable weld penetration", International Materials Reviews, Vol.35, no.4 (1990), p. 185-216.

7.7 J.F. Lancaster and K.C. Mills, "Recommendation for the avoidance of variable penetration in gas tungsten arc welding", Document of Internation Institute of Welding: 212-796-91, p. 1-42.

7.8 American Society for Metals, Metal Handbook, 9th edition, USA, Vol.1, 1978, p. 145-149.

7.9 American Society for Metals, Metal Handbook, 9th edition, USA, Vol.3, 1978, p. 33-35.

Chapter 8

Monitoring Weld Pool Geometry by Arc Voltage Signal Processing

8.1 Introduction

In recent years the trend in high productivity and high quality welding has been particularly directed towards process automation. This has led to an increased use of robotics and associated systems. In the course of further development of automated welding systems, there has been an increasing demand for sensors which are able to monitor the welding process in real-time. A number of sensors has so far been developed for seam tracking during automated welding [8.1-8.5]. However, sensors which can be used to monitor the weld pool geometry are still in the development stage.

In the previous chapters the results were presented of experiments which show that a partially penetrated weld pool can oscillate in a mode as depicted in Fig. 8.1a (mode 1) having a frequency ranging from 200 to 350 Hz depending on the weld pool width, while a fully penetrated weld pool oscillates in another mode, depicted in Fig. 8.1b (mode 3), having a much lower frequency (between 25 to 100 Hz) depending on the bottom width of the weld pool. These results suggest that it is possible to sense and control the weld pool width and weld pool penetration by monitoring the weld pool oscillation during welding.

Only few papers have so far been published about the possibility of monitoring the weld pool oscillation as a tool to control weld pool geometry. Madigan et al. [8.6] used the arc voltage signal to monitor the frequency of the weld pool oscillation in the case of fully penetrated weld pools and in this way

these authors were able to regulate the variation in weld bead width. Deam et al. [8.7] demonstrated how the transition between partial penetration and full penetration could be monitored and further controlled by means of measuring the oscillation frequency with the help of an optical system.

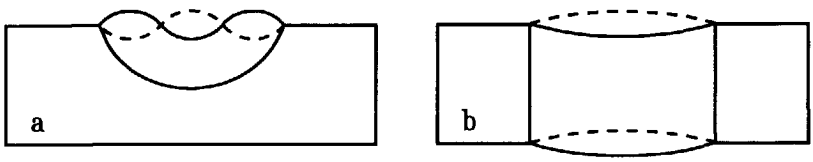

Fig. 8.1 Schematic illustration of oscillation modes 1 and 3.

This chapter deals with attempts to further evaluate the feasibility of sensing and controlling the weld pool geometry (weld pool width and penetration) by means of monitoring the oscillation of the weld pool, making use of the results presented in Chapters 5, 6 and 7. Two cases were considered: the variation in width of a partially penetrated weld pool and the transition from partial penetration to full penetration.

8.2 Experimental conditions

8.2.1 Workpiece design

The material used in the experiments was mild steel Fe 360 in the form of plates. These plates were welded using the GTA welding process under various welding conditions.

In case of travelling arc welding there are two ways to vary the size and/or penetration of the weld bead (weld pool): varying the heat input to the workpiece or changing the heat sink conditions of the workpiece. In this study, the latter approach was chosen and the heat sink conditions were varied by changing the plate shape and/or plate thickness as shown in Fig. 8.2. The design depicted in Fig. 8.2a was used to achieve partially penetrated weld pools of variable width, whereas the design depicted in Fig. 8.2b was used to obtain weld pools of varying degree of penetration. In this way, variation in weld pool size as well as transition from partial penetration to full penetration could be obtained.

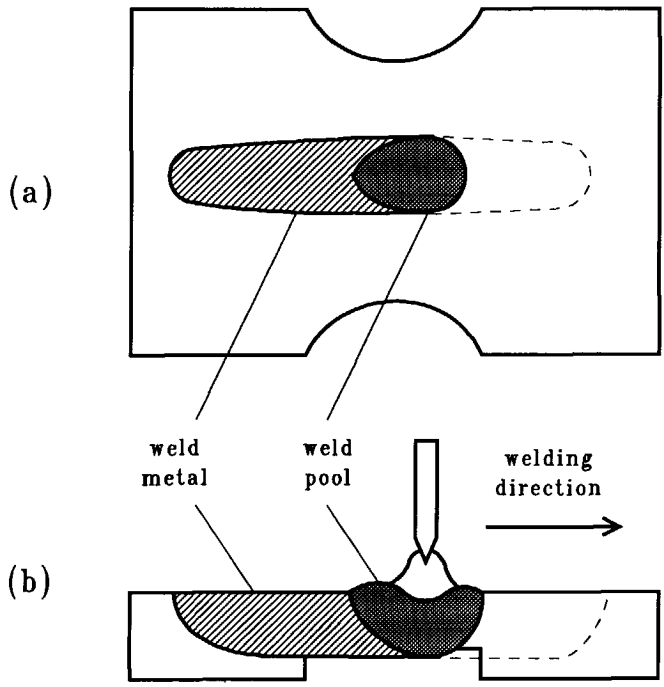

Fig. 8.2 Workpiece design for:
(a) obtaining varying weld pool width;
(b) obtaining a transition between partial penetration and full penetration and vice versa.

8.2.2 Data processing

The weld pool oscillation was sensed in the same way as in the experiments described in the previous chapters, i.e. by monitoring the arc voltage variation during the welding process. In the experiments described in Chapters 5, 6 and 7 the oscillation frequency of the weld pool was determined after welding from the arc voltage variation recorded by a transient waveform recorder. It is evident that for a real-time sensing system an immediate in-process determination of the oscillation frequency is required. This can be accomplished by a computer, provided with a Fast Fourier Transform (FFT) program [8.8]. In the present experiments the arc voltage signals were collected by a computer based data acquisition system of the type described in section 3.3.1. The oscillation frequency of the weld pools was determined by analysing the voltage signal after welding with an FFT program.

An example of the measured data is presented in Fig. 8.3. Figure 8.3a gives the current waveform and the arc voltage variation of a partially penetrated weld pool and Fig. 8.3b gives the current waveform and the arc voltage variation of a fully penetrated weld pool. These figures show that the oscillation amplitude damps out with time in both cases because of the dissipation of oscillation energy. The figures also clearly demonstrate the difference in oscillation frequency and oscillation amplitude between the partially penetrated weld pool and the fully penetrated weld pool.

To extract the oscillation frequency using the FFT program, the original measured voltage data must be pre-processed because of the fact that the signals caused by the arc current pulse, having a much higher amplitude and a much lower frequency, obscure the oscillation frequency in the FFT spectrum as illustrated in Fig. 8.4. According to the FFT theory, the frequency spectrum is dominated by the low frequency part of the signal. This means that the contribution of the arc current pulse, which has a low frequency but a high amplitude, is much stronger than the contribution of the weld pool oscillation, which is high in frequency but low in amplitude. To minimise the influence of the low frequency arc current pulse on the frequency extraction, the original measured

data were first processed in such a way that the value of the data points collected during and immediately after the current pulse, is set to be equal to the average value of the arc voltage. Figure 8.5 shows the treated data of Fig. 8.3. The frequency spectrum obtained after this data processing is presented in Fig. 8.6. The oscillation frequency can now easily be distinguished in the FFT spectrum. The accuracy of the oscillation frequency obtained in this way is about 1 Hz (sample speed/data points, i.e 1000/1024 in the present case). The low frequency peaks in the figures represent the frequency of the current pulse (5 Hz) and the high frequency peaks represent the oscillation frequency of the weld pool. The low frequency noise in the FFT spectrum caused by the current pulse peaks can be avoided by choosing the data block length shorter than the period of the current pulse.

As can be seen in Fig. 8.6, the obtained frequency peaks are somewhat broadened, especially in the case of partial penetration. This broadening of the frequency peaks can be understood by realising that the weld pool size and the temperature change periodically in step with the arc current pulse. During the arc current pulse, the weld pool size and the surface temperature both increase, and hence the weld pool oscillates with decreased frequency. After the arc current pulse the weld pool size and the surface temperature decrease gradually, resulting in a gradually increase in oscillation frequency. In the present case, the frequency with highest FFT amplitude was taken as the mean frequency of the weld pool oscillation.

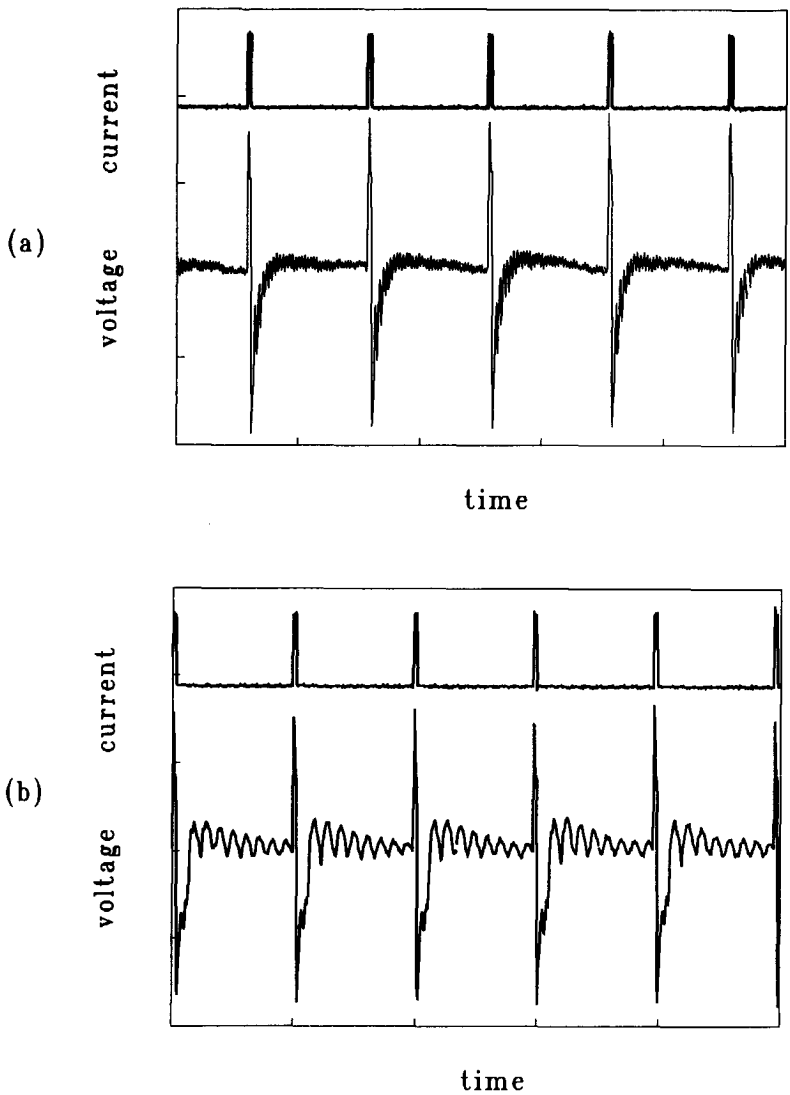

Fig. 8.3 Measured arc current and arc voltage data (peak current 300 A, arc length 1.5 mm and helium as shielding gas): (a) partial penetration; (b) full penetration.

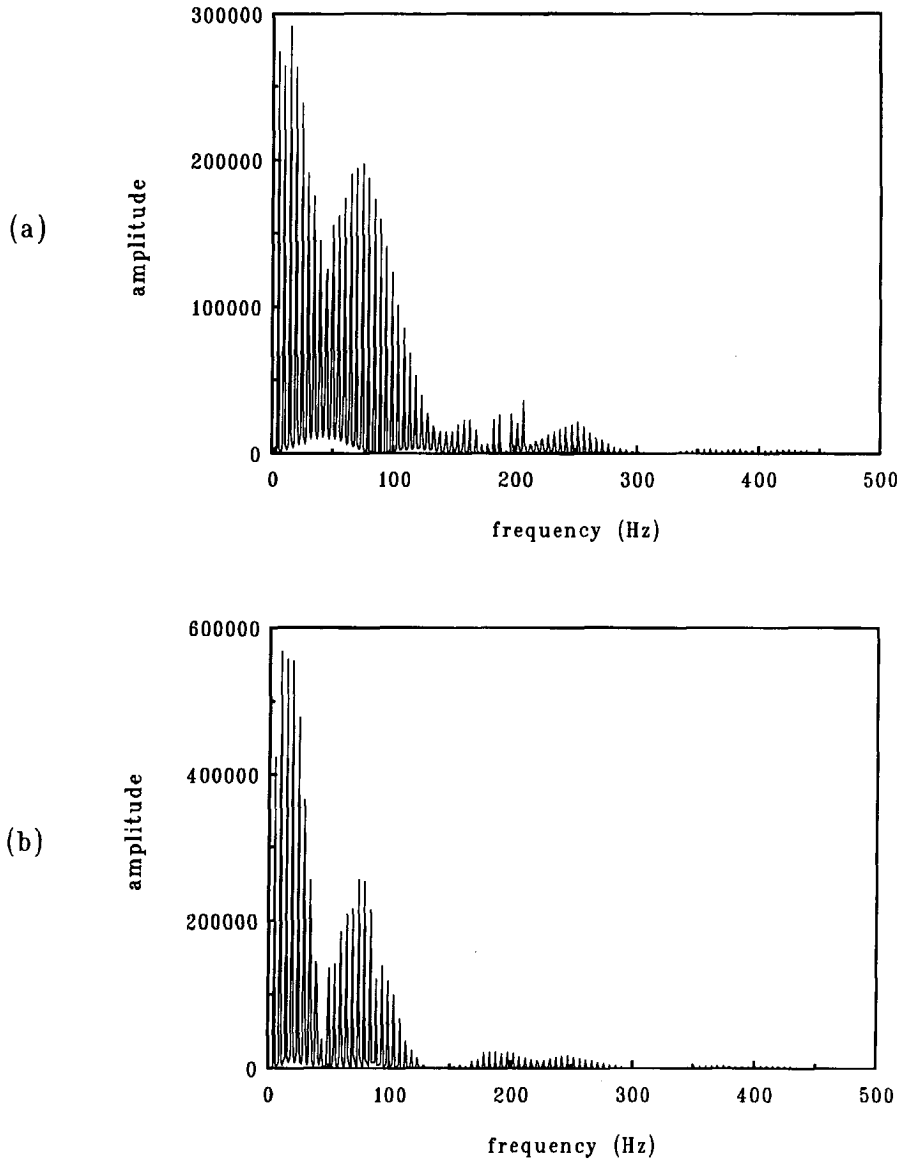

Fig. 8.4 Frequency spectrum obtained by FFT without data processing: (a) partial penetration; (b) full penetration.

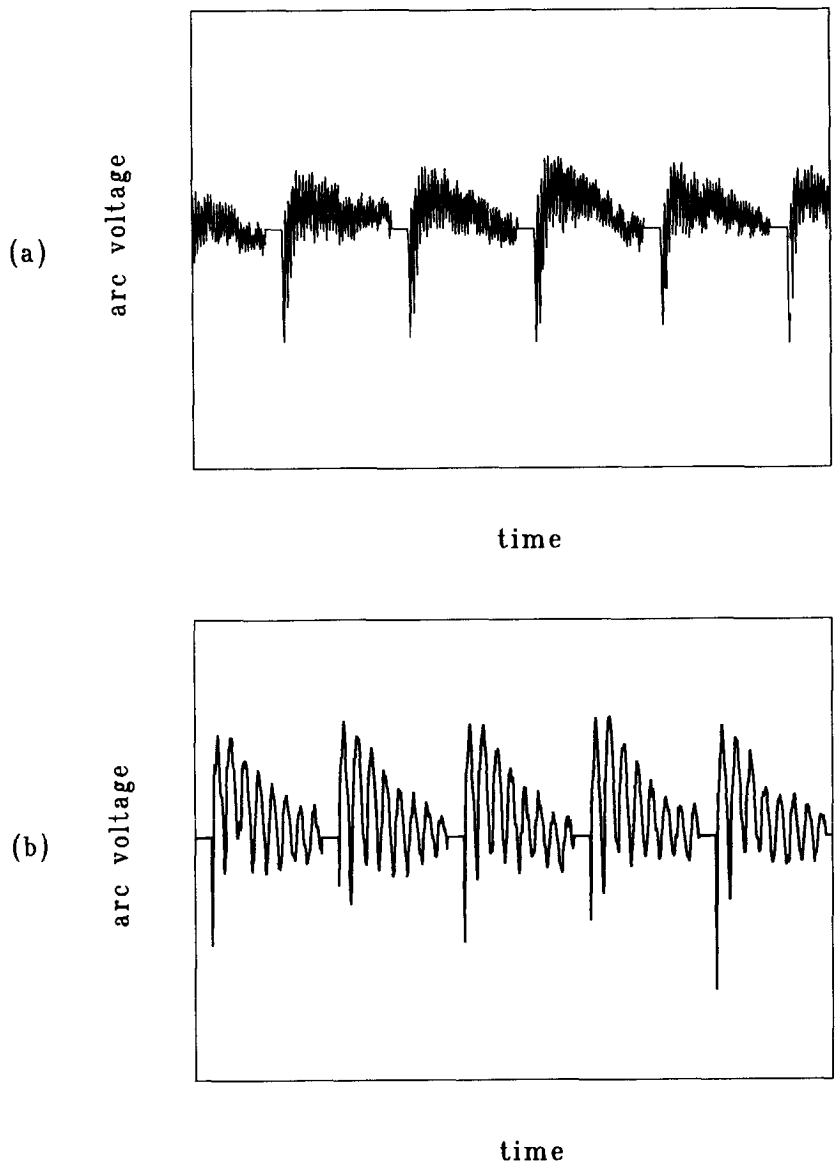

Fig. 8.5 Processed arc voltage data:
(a) partial penetration; (b) full penetration.

(a)

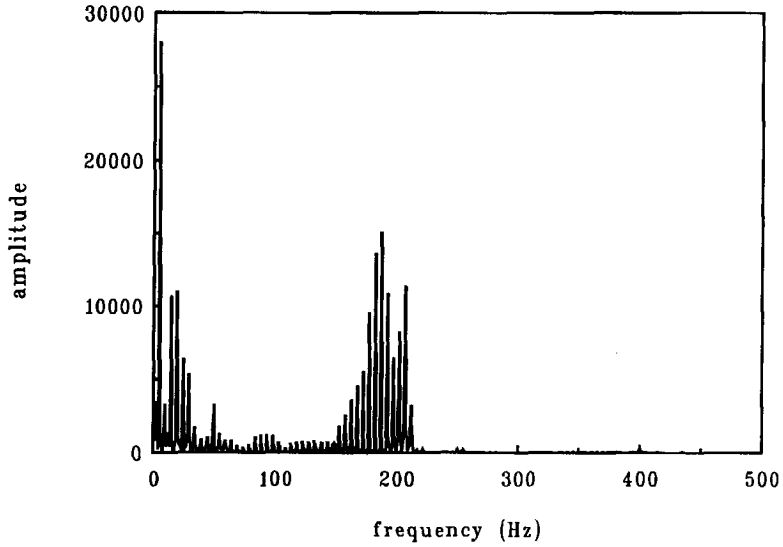

(b)

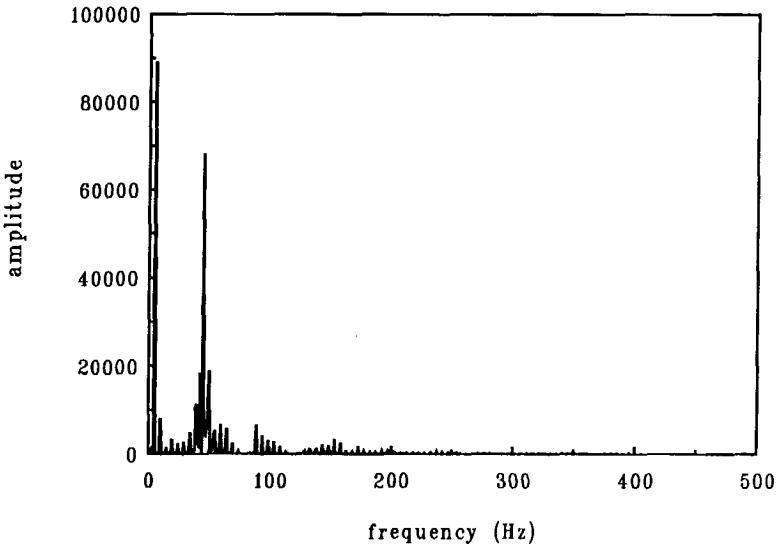

Fig. 8.6 Frequency spectrum obtained by FFT after data processing: (a) partial penetration; (b) full penetration.

8.3 Results and discussion

8.3.1 Monitoring weld pool width variation in case of partial penetration

To demonstrate how the variation in weld pool size in the case of partial penetration can be monitored by continuously measuring the variation in oscillation frequency, bead-on-plate welds were made in 10 mm thick plates having a shape as shown in Fig. 8.2a. The welding conditions used are listed in Table 8.1. They were chosen in such a way that the occurrence of mode 2 oscillation during welding was precluded.

Table 8.1 Welding conditions used in monitoring weld pool width variation in the case of partial penetration

peak current	300 A
peak current duration	6 ms
base current	100 A
pulse frequency	5 Hz
arc length	1.5 mm
travel speed	6.5 - 8 cm/min
shielding gas	helium; 24 l/min

The results of the experiments are presented in Fig. 8.7. It appears that when the arc approaches the narrowed section of the plate, the weld pool width (as measured after welding) increases. This is evidently due to the fact that less heat is conducted away to the surrounding metal, so that more heat is available for melting. The oscillation frequency was observed to decrease simultaneously. As the arc progresses out of the narrow section, the weld pool width decreases gradually

and the oscillation frequency simultaneously increases. The observed change in oscillation frequency with the change in weld bead width is fully consistent with the results presented in the previous chapters and shows that it is indeed possible to sense the variation in weld pool width by monitoring the weld pool oscillation frequency in case of partial penetration.

8.3.2 Monitoring the transition between partial penetration and full penetration

In order to explore the possibility of sensing the transition from partial penetration to full penetration by monitoring the oscillation frequency of the weld pool, welding experiments were carried out in plates of the shape depicted in Fig. 8.2b, the thicker section having a thickness of 6 mm, the thinner section having a thickness of 4 mm. The welding conditions used are listed in Table 8.2 and were again selected in such a way that mode 2 oscillation could not occur.

As an example of the experimental results obtained, Fig. 8.8 shows the weld pool width and the weld pool penetration along the weld, together with the corresponding oscillation frequency. It can be seen from this figure that in the beginning the weld is partially penetrated and the weld bead width increases gradually from about 5.8 mm to about 6.1 mm, whereas the oscillation frequency decreases from ~ 230 Hz to ~ 175 Hz. As the weld pool reaches the thinner section, full penetration is achieved and the oscillation frequency is observed to decrease abruptly from ~ 175 Hz to ~ 50 Hz. Over the thin section, full penetration is maintained and only small variations in weld bead width and corresponding oscillation frequency are observed. When the weld pool reaches the thick section again, a transition occurs from full penetration to partial penetration and the oscillation frequency rises from ~ 50 Hz to ~ 160 Hz. The large change in oscillation frequency is the result of transition in oscillation mode (from mode 1 to mode 3 and vice versa).

The results obtained are in excellent agreement with those presented in Chapters 5, 6 and 7 and clearly show that it is possible to control the weld pool penetration by monitoring the oscillation frequency.

Table 8.2 Welding conditions used in monitoring the transition between partial penetration and full penetration

peak current	300 A
peak current duration	6 ms
base current	60 A
pulse frequency	5 Hz
arc length	1.5 mm
travel speed	6.5 - 8 cm/min
shielding gas	helium; 24 l/min
backing gas	argon; 5 l/min

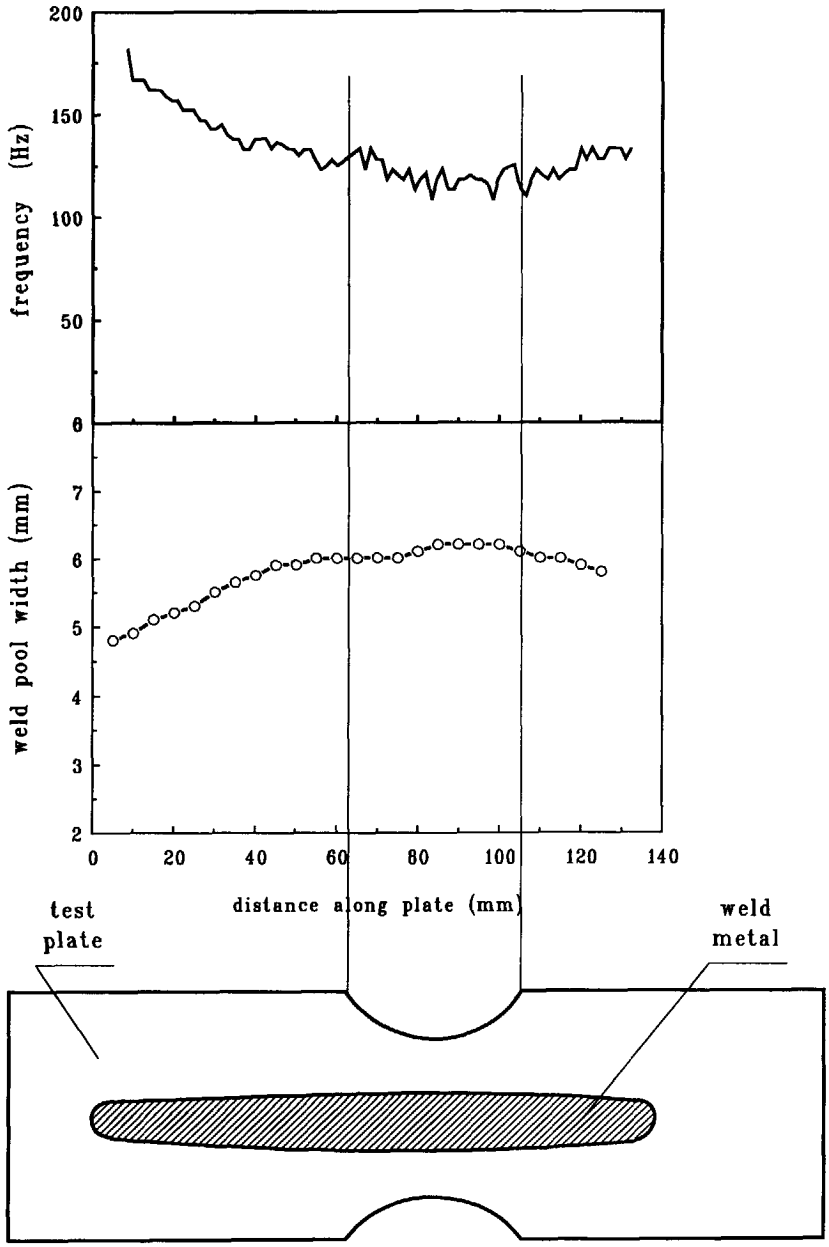

Fig. 8.7 Oscillation frequency and weld pool width of partially penetrated weld pool as a function of position.

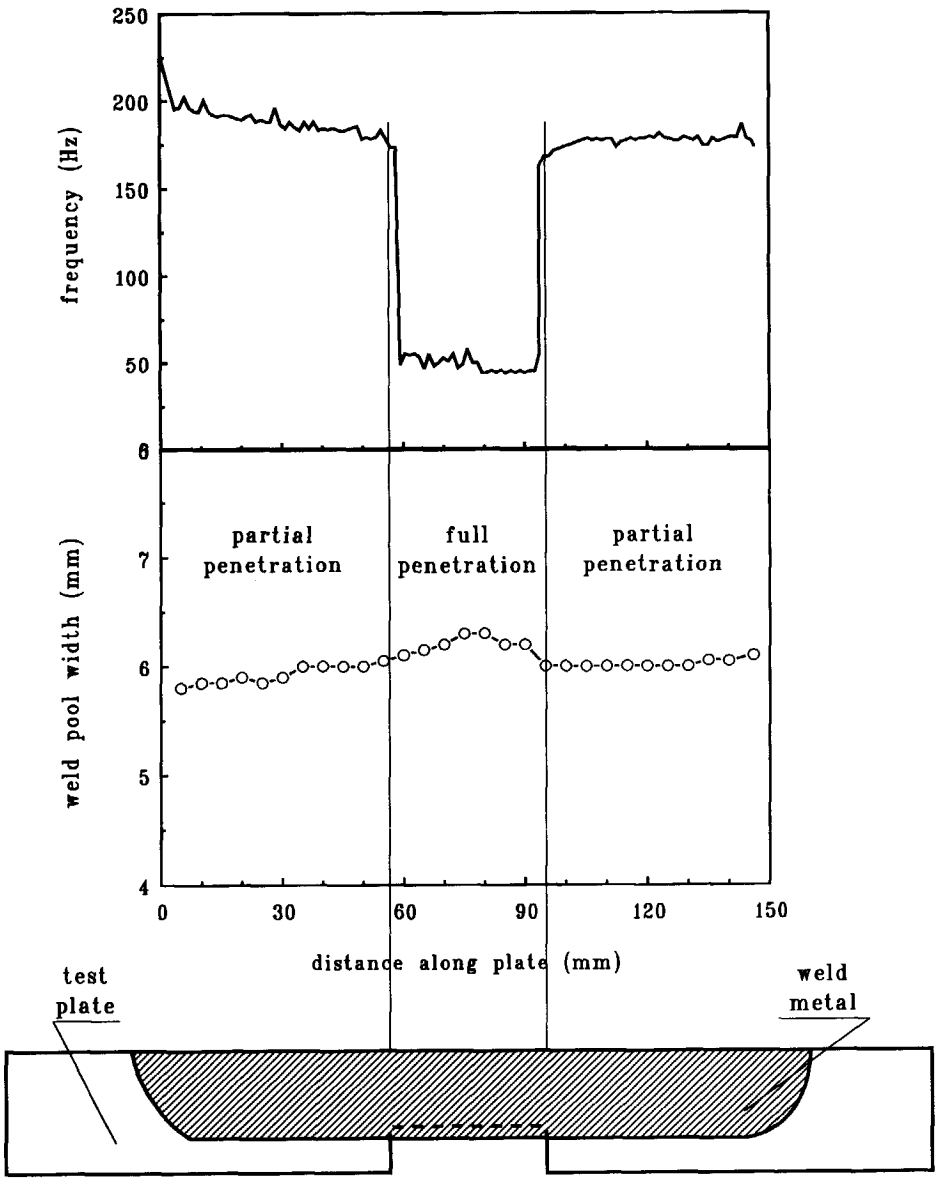

Fig. 8.8 Oscillation frequency and weld pool geometry as a function of position.

8.4 Conclusions

The results presented in this chapter show that it is possible to sense the variation of both weld pool size and weld pool penetration by continuously monitoring the oscillation frequency of the weld pool with the help of a computer based system. Although the results concern on-line sensing in combination with off-line analysing, it is expected that with the help of appropriate computer software and equipment, it is possible to carry out both sensing and analysing on-line. This implies that real-time control of weld pool geometry, width and penetration, can be achieved by monitoring weld pool oscillation.

References

8.1 F.J. King and P. Hirsch, "Seam tracking systems with the arc as sensor", Proceedings of 4th International Conference on Advances in Welding Processes, 9-11 May 1978, Harrogate, UK, p. 193-202.

8.2 R.W. Richardson, "Seam tracking sensors - improving all the time", Welding Design and Fabrication, Sept. 1982, p. 77-82.

8.3 J.S. Smith, A.B. Parker and J. Lucas, "A vision based seam tracking for TIG welding", Proceedings of 1st International Conference on Computer Technology in Welding, TWI, London, England, 3-5 June 1986, p. 61-68.

8.4 J.E. Agapakis, J.M. Katz, M. Koifman, G.N. Epstein, J.M. Friedman, D.O. Eyring and H.J. Ruishauser, "Joint tracking and adaptive robotic welding using vision sensing of the weld joint geometry", Welding Journal, Vol.61, no.11 (1986), p. 33-41.

8.5 F. Eichorn and J. Borowka, "Adaptive through-the-arc seam tracking system for the narrow gap welding process", Proceedings of 2nd International Conference on Developments in Automated and Robotic Welding, 17-18 Nov. 1987, London, UK, p. 125-132.

8.6 R.B. Madigan and R.J. Renwick, "Computer based control of full penetration GTA welds using pool oscillation sensing", Proceedings of 1st International Conference on Computer Technology in Welding, The Welding Institute, London, UK, 1986, p. 165-174.

8.7 R.T. Deam, "Weld pool frequency: A new way to define a weld procedure", Proceedings of 2nd International Conference on Trends of Welding Research, Gatlinburg, Tennessee, USA, 14-18 May 1989, p. 967-971.

8.8 E. Oran Brigham, The Fast Fourier Transform and Its Applications, Prentice-Hall, Englewood Cliffs, 1988.

Summary

This thesis deals with a study of the oscillation behaviour of gas tungsten arc (GTA) weld pools in mild steel Fe 360 and in austenitic stainless steel AISI 304. Special attention is given to the possibility to use the weld pool oscillation behaviour as a sensor of weld pool geometry during welding, which is one of the objectives in adaptive control of the welding process.

The topics discussed include the theoretical background of the oscillation phenomenon, the direct observation of weld pool oscillation, the experimental determination of the relation between the weld pool geometry and the oscillation frequency both under stationary arc conditions and under travelling arc conditions and the possibility of sensing the weld pool geometry, especially the weld pool penetration, by monitoring the oscillation frequency.

In Chapter 2 the theoretical background of weld pool oscillation is given and a model of weld pool oscillation is proposed, taking into account the situation occurring during practical arc welding. This model predicts that different oscillation modes may occur in the weld pool depending on the welding conditions (mode 1 and mode 2 in partially penetrated weld pools and mode 3 in fully penetrated weld pools) and that the oscillation frequency for each of these oscillation modes is related to the weld pool geometry and the physical properties of the liquid metal. It appears that a large difference in oscillation frequency exists between the three oscillation modes, forming the base of controlling weld pool penetration by monitoring the oscillation frequency of the weld pool.

In order to obtain a fundamental understanding of the weld pool oscillation phenomenon and to confirm the existence of the oscillation modes predicted by theory, weld pool oscillation, triggered by short arc current pulses, is studied by means of high-speed filming (Chapter 4). Thus it is possible to directly observe in

what way the weld pool surface is depressed during the pressure pulse and in what way the oscillation of the weld pool develops after the pressure pulse. All three oscillation modes predicted by theory, are observed under different welding conditions.

The oscillation behaviour of the weld pool in mild steel Fe 360 and in austenitic stainless steel AISI 304 is studied under stationary arc conditions by measuring the arc voltage variation after triggering the weld pool by means of short arc current pulses of rectangular shape (Chapter 5). The sensitivity of the measurement is tested and it is found that the smallest detectable oscillation amplitude is ~ 0.05 mm in argon shielding and ~ 0.03 mm in helium shielding. The influence of welding conditions on the oscillation amplitude is also evaluated. It is shown that in order to obtain reliable results, short arc length and helium as shielding gas should be applied. Both in the case of partial penetration and in the case of full penetration a relation is found to exist between the oscillation frequency and the weld pool geometry. It appears that partially penetrated weld pools oscillate in mode 1, while fully penetrated weld pools oscillate in mode 3. The oscillation frequency of a partially penetrated weld pool is considerably higher than the oscillation frequency of a fully penetrated weld pool. As a consequence of this, an abrupt drop in oscillation frequency occurs when the weld pool transfers from partial penetration to full penetration.

To develop a better understanding of the oscillation behaviour under more realistic conditions, experiments are carried out under travelling arc conditions with mild steel Fe 360 (Chapter 6) and with austenitic stainless steel AISI 304 (Chapter 7). It is found that the oscillation of the partially penetrated weld pool is dominated by one of two different oscillation modes (mode 1 and mode 2) depending on the welding conditions, whereas the oscillation of a fully penetrated weld pool is characterised by a third oscillation mode (mode 3). It is possible to maintain mode 1 oscillation in a partially penetrated weld pool by choosing proper welding conditions such as short arc current pulse duration, low travel speed, short arc length and helium as shielding gas. Under these welding conditions, an

abrupt decrease in oscillation frequency can be observed when the weld pool transfers from partial penetration to full penetration.

It is also found that a relation exists between the oscillation of the weld pool and the formation of surface ripples on the weld bead, indicating that the formation of surface ripples is due to weld pool oscillation.

Finally, attempts are made to use the obtained relations between the oscillation frequency and the geometry of the weld pool for in-process control of weld pool geometry with the help of a computer aided sensing system (Chapter 8). The results show that with this sensing system it is possible to monitor the variations in weld pool size and also to detect the transition between partial penetration and full penetration in real-time.

Samenvatting

In dit proefschrift worden de resultaten beschreven van een onderzoek naar het oscillatiegedrag van het lasbad bij het TIG-lassen van ongelegeerd staal Fe 360 en austenitisch roestvast staal AISI 304. Hierbij is speciale aandacht besteed aan de mogelijkheid het oscillatiegedrag van het lasbad toe te passen als sensor ten behoeve van lasbadbeheersing tijdens het lassen.

Achtereenvolgens komen aan de orde: de theoretische achtergrond van het oscillatieverschijnsel, de directe waarneming van oscillaties in het lasbad, de experimentele bepaling van de relatie tussen de lasbadgeometrie en de oscillatiefrequentie, zowel in het geval van een stationaire als in het geval van een voortlopende lasboog, en de mogelijkheid tijdens het lassen informatie over de lasbadgeometrie te verkrijgen door middel van het meten van de oscillatiefrequentie.

In Hoofdstuk 2 wordt de theoretische achtergrond van lasbadoscillatie gegeven en wordt een model voor oscillatie van het lasbad ontwikkeld, waarbij rekening gehouden wordt met praktische lasomstandigheden. Dit model voorspelt dat afhankelijk van de lasomstandigheden verschillende oscillatiemodes in het lasbad kunnen optreden (mode 1 en mode 2 bij onvolledige doorlassing en mode 3 bij volledige doorlassing), en dat de oscillatiefrequentie van elk van deze oscillatiemodes gerelateerd is aan de lasbadgeometrie en de fysische eigenschappen van het vloeibare metaal. Het blijkt dat er een groot verschil bestaat tussen de frequentie van de verschillende oscillatiemodes. Dit vormt de basis voor de mogelijke beheersing van lasbadpenetratie door middel van meting van de oscillatiefrequentie van het lasbad.

Om een fundamenteel begrip van het oscillatieverschijnsel te verkrijgen en om het bestaan van de voorspelde oscillatiemodes te bevestigen, zijn oscillerende lasbaden, gegeneerd door korte stroompulsen, bestudeerd met behulp van snelle-

film opnamen (Hoofdstuk 4). Door middel van deze films is het mogelijk direct vast te stellen op welke wijze het lasbadoppervlak wordt ingedrukt tijdens de drukpuls en hoe de lasbadoscillatie zich ontwikkelt na de drukpuls. De drie oscillatiemodes, voorspeld door de theorie, kunnen onder verschillende lasomstandigheden worden waargenomen.

Het oscillatiegedrag van het lasbad in ongeleerd staal Fe 360 en in austenitisch roestvast staal AISI 304 is onderzocht onder stationaire lasomstandigheden door de boogspanningsvariaties te meten, nadat het lasbad in oscillatie is gebracht door korte stroompulsen (Hoofdstuk 5). De gevoeligheid van de meting is getoets en het blijkt dat de kleinste detecteerbare oscillatieamplitude ~ 0,05 mm bedraagt bij gebruik van argon als beschermgas en ~ 0,03 mm bij gebruik van helium als beschermgas. Ook is de invloed van de lasomstandigheden op de oscillatieamplitude experimenteel bepaald. Hieruit komt naar voren dat de meest betrouwbare resultaten verkregen worden bij toepassen van een korte booglengte en helium als beschermgas. Zowel bij gedeeltelijke als bij volledige doorlassing is een relatie gevonden tussen de oscillatiefrequentie en de lasbadgeometrie. Het blijkt dat bij gedeeltelijke doorlassing het lasbad in mode 1 oscilleert, terwijl bij volledige doorlassing het lasbad in mode 3 oscilleert. De oscillatiefrequentie van het lasbad bij gedeeltelijke doorlassing is aanzienlijk hoger dan bij volledige doorlassing. Tengevolge hiervan treedt een abrupte daling van de oscillatiefrequentie op bij de overgang van gedeeltelijke naar volledige doorlassing.

Om een beter begrip te krijgen van het oscillatiegedrag onder meer realistische lasomstandigheden, zijn experimenten uitgevoerd met voortlopende boog in ongelegeerd staal Fe 360 (Hoofdstuk 6) en in austenitisch roestvast staal AISI 304 (Hoofdstuk 7). Het blijkt dat bij gedeeltelijke doorlassing de lasbadoscillatie wordt gedomineerd door mode 1 of mode 2, afhankelijk van de lasomstandigheden, terwijl bij volledige doorlassing de lasbadoscillatie wordt gedomineerd door mode 3. Het is mogelijk om oscillatie in mode 1 te handhaven bij gedeeltelijke doorlassing door de juiste lasomstandigheden te kiezen, zoals

korte stroompulstijd, lage voortloopsnelheid, korte booglengte en helium als beschermgas. Onder deze lasomstandigheden kan een abrupte daling van de oscillatiefrequentie worden waargenomen bij de overgang van gedeeltelijke naar volledige doorlassing.

Voorts is gevonden dat er een relatie bestaat tussen de lasbadoscillatie en de vorming van rimpels op het lasoppervlak, waaruit blijkt dat de rimpels worden gevormd door lasbadoscillaties.

Tenslotte zijn er pogingen gedaan om het verband tussen de oscillatiefrequentie en de lasbadgeometrie te gebruiken voor beheersing van de lasbadgeometrie tijdens het lassen met behulp van een computergestuurd meetsysteem (Hoofdstuk 8). Uit de resultaten blijkt dat het met behulp van dit meetsysteem mogelijk is variaties in lasbadafmetingen en ook de overgang van gedeeltelijke naar volledige doorlassing tijdens het lassen continu te registreren.

ACKNOWLEDGEMENT

I am sincerely grateful to my promotor Prof. Dr. Gert den Ouden for his consistent encouragement, support and guidance during this research. His understanding and flexibility are very much appreciated.

Special thanks are due to Willem Brabander for his indispensable help in building the experimental equipment and solving technical problems, no matter small or large. Thanks are extended to Frans Bosman, Gijs Kerkhof and Joop de Snoo who were always willing to help me during the experiments.

I am obliged to Johan Zijp for his kind help in computer programming and for many constructive discussions. I am indebted to Ben Stoop, Theo Luijendijk, Marcel Hermans, Wim Vink, Jan-Paul Krugers, Jaap Hooijmans and Erik Peekstok for many simulating discussions on scientific and other topics.

It pleases me very much to thank Anneke van Veen for her enthusiastic help and her friendship during the whole period I stay here.

I wish to thank all colleagues in the laboratory who helped me in one way or another during the work, although it may not be possible to name all here.

I would like to thank Jaap Meijer for his good service in literature.

Thanks are due to Mr. H. van Baarle and his workshop colleagues in the laboratory for their technical assistance in preparing test plates. Thanks are also due to Mr. H.L.M. Klijnhout, Mr. J. Pehlemann, Mr. P.F. Colijn and Mr. A.M.J.W. Bakker for their help in chemical analysis, in figures reproduction, microscope and photography respectively.

Finally, many thanks are due to Yingkai for his consistent support, his understanding and his special contribution to this work.

Youhong Xiao
February 1992

CURRICULUM VITAE

The author was born on 15 august 1958 in Hubei, China. She graduated at the 10th High School of Wuhan, Hubei, China in July 1975.

After two and half years work in a Hydraulic Engineering and Electric Power company, she began to study in the Second Department of Mechanical Engineering, Huazhong University of Technology, Wuhan, China, where she obtained the B. Eng. degree in January 1982. Then she continued her study in the Institute of Metal Research, Chinese Acadamy of Science, Shengyang, China and obtained the M. Sc degree in December 1984.

From December 1984 to June 1988 she worked in the Laboratory of Welding Processes and Technology, the Second Department of Mechanical Engineering, South China University of Technology, Guangzhou, China.

Since June 1988 she worked for her doctor degree as a research assistant in the group Welding Technology and Non-Destructive Testing, the Department of Chemical Engineering and Materials Science, Delft University of Technology, Delft, The Netherlands. This work was carried out under the supervision of Prof. Dr. G. den Ouden.

Notes:

Notes: